The feasibility of using EM waves in determining the moisture content and factors effecting measurements in building fabrics

Patryk Kot

A thesis submitted in partial fulfilment of the requirements of Liverpool John Moores University for the degree of Doctor of Philosophy

December 2016

Dedicated to my daughter Aleksandra, wife Monika and parents Malgorzata and Ryszard.

Acknowledgments

I would like to express my greatest thanks to my director of study Professor Andy Shaw for his advice, guidance, and encouragement during the research. I would like to thank my second supervisor Dr Karl O. Jones for his support and guidance during the research especially in the area of data analysis. I would also like to thank my third supervisor Professor A. Al-Shamma'a for his invaluable support and guidance.

I would like to thank Dr Alex Mason for his advice, support and help in many aspects during the research. Dr Jeff Cullen who was always available when I required the benefit of his knowledge and experience in the area of electrical engineering. Magomed Muradov for his help and support during experiments as also during all those years at university.

Also, I would like to say a huge thanks to my colleagues in the Built Environment and Sustainable Technology (BEST) group for their help and continued support, particularly, Dr Olga Korostynska, Dr Steve Wylie, Dr Ateeq Muhammad, Dr Mamadou Diallo, Dr Ahmed Abdou.

I would like to also thanks Elizabeth Hoare for her hard work on the admin side of things, allowing the process to run smooth and efficiently.

I also wish to take the opportunity to thank all the technicians for their technical support.

Finally, my sincere thanks go to my mother for all her support during my studies. I know that without her support it would have been harder to be at the place where I am now.

Abstract

This work addresses the use of an electromagnetic wave sensor to determine moisture content within building fabrics. Building materials that require a special mixing ratio such as concrete, mortar and membrane layers will be subject to significant effects when exposed to unpredictable weather changes owing to the excess of the acceptable moisture content. The acceptable moisture content level varies with various building fabrics and exceeding this level will affect the overall performance of building constructions. The project proposes using a novel electromagnetic (EM) sensor to monitor, in a non-destructive manner, the signal reflected from building structures in real time to determine exceeded moisture content level. This project involves the design and construction of an EM sensor operating at two frequency ranges: 2GHz to 6GHz and 6GHz to 12GHz at a power of 0dBm. This research is a new approach for monitoring moisture in buildings which has not been investigated before. The simulation software High Frequency Structure Simulator (HFSS) was used to model the microwave sensor. The pyramidal horn antenna was chosen as the preferred antenna for this work owing to higher gain, directivity and overall performance. Different building materials and structures have been made in a laboratory environment to determine the levels of moisture content, as well as to determine the modes of building fabrics failures owing to membrane failure, a pipe burst and ground source. Finally, a graphical user interface was developed and used to control the sensor parameters as well as frequency sweep, to capture the data from the sensor. Based on the findings of this project, the EM wave sensor could be used to determine the moisture content of building fabrics in a non-destructive manner.

Table of Contents

List of Figures

List of Tables

List of Equations

List of Acronyms

AAC/ Aircrete	Autoclaved Aerated concrete
Arx	Auto regressive
EM	Electromagnetic
FNBW	First Null Beamwidth
GHz	Gigahertz
GPR	Ground Penetrating Radar
HFSS	High Frequency Structure Simulator
HPGe	High-Purity Germanium
ISM	Industrial Scientific Medical
LabVIEW	Laboratory Virtual Instrument Engineering Workbench
LC	Inductor- capacitor
LTCC	Low Temperature Co-Fired Ceramic
MHz	Megahertz
NMR	Nuclear Magnetic Resonance
PCA	Principal Component Analysis
PLS	Partial Least Squares Regression
SIP	Structurally Insulated Panels
TDR	Time Domain Reflectometry
UV	Ultraviolet
VNA	Vector Network Analyser
VSWR	Voltage Standing Wave Ratio

Chapter 1 Introduction

Building construction represents one of the largest, single investment of national resources. The success of such economies is therefore heavily dependent upon the satisfactory performance of its constructions (Moore 1992). Building materials are the material foundation for all construction engineering. Various buildings and structures are constructed by all kinds of building materials on the basis of a reasonable design. The varieties, specifications and qualities of building material are directly related to the applicability, artistry and durability of buildings and also the cost of projects (Zhang 2011). Failures in the built environment occur for a variety of reasons and on a variety of scales. An excess of the acceptable moisture content in building materials is the primary factor of deterioration and, combined with diurnal temperature variation, has the greatest influence upon the overall performance of building materials. Moisture can influence external walling in all its states, i.e. as a solid (ice, snow); liquid (wind-driven rain) and gas (water vapour). Most constructional defects, e.g. movement, cracking, fungal attack, chemical reaction, are initiated and aggravated by the presence of moisture (Stirling 2011).

1.1 Problem Statement

In recent years there was an increase in the need to implement sustainable solutions in building fabrics and structures. To achieve the optimum life span of these structures it is important to monitor parameters such as moisture content, indoor temperature profiles, influence of vibration and material fatigue. This is especially important for construction forms that are sensitive to environmental influences. Inconsistent performance of building materials that cannot withstand changing conditions and activities around them, will result in the building not functioning as intended (Phillipson *et al.* 2008). Building materials that require a special mixing ratio such as concrete, mortar and membrane layers will be subject to significant effects when exposed to a variety of weather changes. Bailey and Bradford (2005), through their study regarding defects in roofs, highlighted that moisture and water penetration was due to factors other than environmental problems. Moisture from the air permeates porous building materials such as bricks, concrete, wood, mortar and rock wool insulation. One of the most important performance parameters is the moisture content of building materials. It is necessary to investigate the moisture content because moisture and

water penetration has a negative influence on the physical, chemical and biological corrosion processes taking place inside these materials (Gromicko & Shepard 2013; Maksimović *et al*. 2012).

Currently, moisture content is being measured by surveyors using commercially available devices. However, the techniques require drilling into building materials (Davies & Ye 2009) for further analysis. Another disadvantage of these techniques is the requirement of taking a long time to conduct the measurements. Therefore, approaches have been investigated by McCann and Forde (2001) to use non-destructive techniques to measure moisture content although, these methods provided unsatisfactory results.

1.2 Novelty

This thesis describes a novel approach to develop a non-destructive electromagnetic wave (EM) sensor to determine the moisture content of bulk building materials in real time (data obtained from the sensor will be analysed during the measurement and the result will be instantly displayed on graphical user interface (GUI)). This research will undertake experimental work to demonstrate the potential use of EM waves to provide surveyors time efficient and accurate measurements in a non-destructive manner. Limitations of commercially available devices are destructive/require contact with a material, low penetration capability and unable to identify a source of the excess moisture. Additionally, some of the devices are limited to a specific building fabric. Thus, the novelty of this investigation is to develop a contactless method for instant determination of an excess moisture content level in various building fabrics. In addition, proposed method will allow to penetrate through a building material in order to identify the source of the excess moisture.

1.3 Aim and Objectives

The aim of this PhD is to develop a novel non-destructive electromagnetic wave sensor to determine the excess moisture content and the factors effecting measurements in various building fabrics.

The objectives of this project are:

- To investigate the current common problems and sensing methods in determining moisture content in building fabrics
- To design a simulation model of EM sensor
- To identify potential factors effecting EM measurement, namely foreign objects and various building materials
- To develop an EM wave sensor to determine excess moisture content of building fabrics
- To determine the waterproof membrane failure in a concrete flat roof structure based on the case study
- To develop a prediction model to identify the excess moisture content of building fabrics

1.4 Overview of thesis

Chapter 2 is the review of the literature that consists of four sections namely built environment, current methods to determine moisture content of building fabrics, commercially available devices and the EM measurement approach. In the built environment section, moisture content of building fabrics, different building fabrics, types of wall structures and concrete flat roof structure will be discussed. The current methods to determine the moisture content of building fabrics will discuss different non-destructive and destructive measurement techniques. All the methods will be explained and analysed. The commercially available devices section shows devices that are currently used by surveyors. EM measurement approach shows the different research undertaken in microwave spectroscopy field to determine moisture content of different material which could be potentially used to monitor the moisture content in building fabrics. Chapter 3 is the EM

approach and Theoretical modelling. First section of that chapter will explain the EM spectrum, different types of antennas and dielectric properties. The second section of that chapter presents theoretical modelling in High Frequency Structure Simulator (HFSS) software where the theoretical model of developed sensor will be discussed. The third section presents the preliminary experiment which was undertaken to show the potential of microwave spectroscopy to non-destructive measurements of building fabrics. Chapter 4 is devoted to experimental methodology for identification of building materials and foreign objects. In this chapter laboratory experimental setups will be presented, and achieved results will be explained. Data analysis techniques will be presented to achieve accurate measurements. Undertaken experiments will be discussed. In chapter 5, an experimental methodology for monitoring moisture content of building fabrics will be presented. This chapter will demonstrate the experimental setups and the obtained results will be explained. In addition, the prediction models for an excess moisture determination will be presented. Chapter 6 is devoted to experimental methodology for detection of defects in concrete flat roof structure. In this chapter laboratory experimental setups will be presented, achieved results will be explained. Data analysis techniques will be presented to achieve accurate measurements. Chapter 7 consists of three sections namely conclusions, limitations and future work. In conclusions section the whole thesis will be summarised. The future work section shows recommendations that could be implemented to improve novel technology.

Chapter 2 Review of the Literature

It is important to improve the overall performance of building structures to avoid large refurbishment costs as well as an increased risk of building collapse, which may cause injury or even death to occupants (Brimblecombe *et al.* 2006). Algo Centre Mall, a retail hub for Elliot Lake, Ontario, was constructed in 1980. The two stores structure had 190,000 square feet of floor space occupied by commercial units as well as a hotel. A prominent feature of the complex was a roof top parking deck (Figure 2.1). Throughout the life of the mall there had been reports of water leaking into the occupied units. This water presence and damage had been so severe that drip tarps were put up in plain sight of the customers. This water infiltration led to a variety of serviceability problems and, eventually, to businesses leaving the mall. The collapse occurred on June 23, 2012. The chemical process of corrosion has several parts. In this case a metallic surface was exposed to an electrolyte. The de-icing salts acted as the electrolytes, and had been dissolved into solution with the presence of water. The solution then migrated through the roof top parking deck and settled on a connection of the frame. After a lengthy exposure time, the chemical process degraded the frame connection and led to collapse. The water presence below was an indication of the water movement through the structure's skin (McDonald 2013).

Figure 2.1. Algo Mall Collapse. [Adopted from (McDonald 2013).]

This chapter is devoted to a literature review. Section 2.1 consists of background knowledge of built environment, whilst section 2.2 illustrates current methods to determine moisture content in building fabrics. Section 2.3 considers commercial devices used by surveyors while undertaking measurements. Section 2.4 consists of electromagnetic (EM) wave approach where microwave radiation is explored in different research fields. Section 2.5 concludes the literature review.

2.1 Built Environment

2.1.1 Moisture Content of Building Fabrics

Moisture is involved in most building problems. The most serious tend to be structural damage owing to wood deterioration, unhealthy fungal growth, corrosion and damage to moisture sensitive interior finishes (Singh *et al.* 2010). Avoiding these problems requires an understanding of moisture, the nature of materials, and how moisture interacts with materials (Straube 2002).

2.1.1a The Science of Dampness

It is significant to understand the physical (Halim *et al.* 2012) and chemical processes (Young 2007) that are the root cause of dampness. Water, in liquid or vapour is all around us. One of the physical properties of water is that it expands rather than contracts when freezes.

Moisture in buildings cause a problem because:

- It will expand and contract as the temperature fluctuates, possibly causing cracks, and degradation of material over time.

- It enables the house dust mite population to rise, and moulds to grow which is detrimental to human health.

- Damp timber can be subjected to dry or wet rot.

Most construction materials such as plasters, bricks, concrete, timber or insulants are porous, with their relative porosity being related more or less to their density. Those materials function well within their own particular safe range of moisture content, depending on the

location of the material in the construction and the function it is required to carry out (Ong *et al.* 2008). Damp in a material usually refers to its content of free moisture i.e. H_2O that is not chemically bound to the material. A small amount of moisture in a material should not be a concern. However, when porous materials are subject to persistent high humidity or when moisture has arrived from an outside source by soaking through, the material may be damp enough to suffer a problem (Burkinshaw & Parrett 2004).

2.1.1b Moisture Movement through Materials

Traditional masonry structures take in and give out moisture. Some building elements, for example masonry external walls, are designed to take in moisture during rain and give it out again later by evaporation (Lourenço *et al.* 2014). This cycle of change in moisture content can be harmless, but it can be problematic if high or low levels of moisture are allowed to persist for too long. In the UK, no porous material will be completely dry because the air always contains some moisture, and the porous material will take in some of it via various physical or chemical processes such as: Vapour pressure diffusion, Capillary attraction, Hygroscopicity, Diffusion, Osmotic pressure, Wind pressure and Gravity (Burkinshaw & Parrett 2004).

2.1.1c Acceptable Moisture Level

A brick at the wall face obtains 10% actual moisture content after rain; in this case there may be no problem for a building to then dry out later. However, if a similar brick located in the inner thickness of the wall were to achieve persistent moisture content of above 3%, problems could result in damp plaster, damaged decoration or damp timbers which could lead to timber rot. Dampness exists where there is sufficient moisture in a material to cause problems for that material, adjacent materials, the building or the users of the building (Burkinshaw & Parrett 2004). It is important that materials do not become visibly damp, and do not feel damp to the touch, until they are quite dangerously damp. Wood, for example, does not feel damp below 30% moisture content (at around 97% or 98% relative humidity), although rot will develop at 20% moisture content and above (PCWI International Pty 2000).

2.1.1d Sources of Moisture

It is significant to identify the source of the moisture in order to terminate the source and solve dampness problems (Sanders & Phillipson 2003). The source is responsible for the

greatest amount of the moisture present which can be identified by an elimination process or by a monitoring process. Sources of moisture in buildings can be various, and some examples are given in Table 2.1 (Burkinshaw & Parrett 2004).

Table 2.1. Source of moisture in buildings. Adopted from (Burkinshaw & Parrett 2004).

Moisture source	**Typical examples**
Air moisture condensation	Cooking
	Heating
Penetrating dampness	Rainwater, snow
	Leaking external rainwater goods
Internal plumbing leaks	Long-term breakdown of plumbing joints
	Burst pipes
Below-ground moisture	Underground plumbing leaks
	Leaking ponds

2.1.2 Building Fabrics

Materials fall into three categories natural, manufactured and new. Natural materials such as stone and timber have been used for centuries as building materials. However, because they are natural materials, they are of variable quality and often contain significant defects. Secondly, manufactured materials such as steel and aluminium alloy are produced under carefully controlled factory conditions, with frequent testing and monitoring throughout the manufacturing process. The third category is new materials, such as fibre reinforcement composites. These are highly manufactured materials, but unlike steel, have not been in existence long enough to be fully understood (Seward 2009). Same types of building fabrics are presented in the following sections.

2.1.2a Brick

Bricks, in one form or another, have been in use for thousands of years for constructing different types of buildings. At first, bricks were sun-dried but after further investigation it was found that firing them considerably increased their strength (Raut *et al.* 2011). Clay is a natural material formed due to the weathering of rocks and consists mainly of two minerals: silica (SiO_2) and alumina (Al_2O_3). The usual size of the clay brick is 215 x 102.5 x 65 mm. Clay usually shrinks on drying and firing, therefore brick manufacturers allow for shrinkage by making the bricks originally bigger than the final product (Virdi 2012). The properties of clay bricks are variable, although good bricks are generally free from cracks, have a good texture and are well burnt. The strength of clay bricks can be up to 180N/mm^2, but

considerably lower strengths are adequate for the loads that are usual in small buildings. The Building Regulations (Gwynne 2010) require only 2.8N/mm^2 for inner walls of two-storey houses. The compressive strengths of engineering bricks are at least 70.0 and 50.0N/mm^2. The durability of bricks can by affected by the absorption of the water. The limits for water absorption for engineering bricks are 4.5% and 7% (Seward 2009). Clay bricks can contain salts like sulphates of sodium and calcium. Porous bricks absorb water through their surfaces and the water dissolves these soluble salts. During the drying off process in the warmer season the salt solution moves to the surface of the brick. The water evaporates leaving a white powder on the surface, as shown in Figure 2.2. This effect is known as efflorescence. The salt deposit on the surface does not cause any damage and it can be removed by brushing the surface of the brickwork. If the efflorescence is heavy and occurs below surfaces, it could result as crumbling of under-fired bricks.

Figure 2.2. Efflorescence effect on red brick.

2.1.2b Autoclaved Aerated Block

Autoclaved Aerated concrete (AAC), also known as Aircrete, is a versatile lightweight construction material. Compared with normal concrete, aircrete has a low density and excellent insulation properties. The density of aerated concrete is achieved by the formation of air voids to produce a cellular structure. Voids typically are between 1mm and 5mm across and give the material its characteristic appearance. This type of concrete contains 80% air. Aerated concrete blocks have strengths between 3 to 9 Nmm^2. This type of building material is a great thermal insulator and is often used to form the inner leaf of a cavity wall. Another common use of aerated concrete is structures' foundations. Autoclaved aerated concrete is cured in a large pressure vessel (Hamad 2014). It can be produced using a wide range of

cement materials such as Portland cement, lime and pulverised fuel ash or lime and fine silica sand. Most of the time a small amount of gypsum is added. Aerated concrete does not contain any aggregate and all the main components are reactive (Fischer Innovative Solutions 2012).

2.1.2c Timber

Timber is one of the main materials used in the construction of low-rise domestic buildings (Kadir *et al.* 2015). Timber is an organic material obtained from mature trunk trees cut to suitable sizes. The moisture content of the raw wood is reduced by the seasoning process. Seasoned timber is lighter, stronger, easier to work with and easier to finish with paint/varnish. Seasoning may be natural (air seasoning) or artificial (kiln seasoning). After this process wood is known as timber and it is ready to use as a construction material. There are two types of timber: softwood and hardwood. Softwood is obtained from evergreen trees, whereas hardwood is obtained from deciduous trees (Virdi 2012).

Timber is a light material with the density of different species ranging from 160 to 1250kg/m^3. Although all species of timber are composed of the same substances, the differences in their microstructure affect the values of density. The densities of the most commonly used softwoods in the UK range from 380 to 550 kg/m^3.

Timber is a lightweight but strong material with a high strength–weight ratio both in tension and compression. There is a large variation in the strength as there are so many different species of timber. Generally, the strength of timber is directly proportional to its density, and inversely proportional to its moisture content. Defects such as knots can also affect timber strength. The tensile strength of timber ranges between 2.5 and 13.8N/mm^2. The modulus of elasticity of timber ranges between 4600 and 18000N/mm^2 (BS 5268-2:1996) (Seward 2009).

2.1.2d Cement

Cement is one of the most important construction materials and is used in the production of concrete and mortar. The most commonly used type of cement is known as Portland cement because the colour of solid cement resembles natural Portland stone. Portland cement is made from two raw materials: chalk and limestone. Both are natural materials: chalk occurs as a soft rock whereas limestone occurs as a hard rock. Cement may be manufactured either

by a wet process or by a dry process. The wet process requires a large volume of water to make the clay–chalk slurry, which in turn consumes more energy than that of the dry process in evaporating the water. The dry process is therefore the preferred method where feasible (Seward 2009; Virdi 2012).

2.1.2e Concrete

Concrete is used in the construction of many building elements. It can be found in housing, industrial and commercial buildings, bridges, roads, airport runways, foundations, tunnels and drainage systems (Domone & Illston 2010). It is a composite material made by mixing together cement, aggregates (sand and/or gravel) and water. The proportion of these ingredients affects not just the strength but also the ease with which concrete can be placed and compacted. Cement is responsible for the strength of concrete, but it is not used without the aggregates because it is the most expensive ingredient of concrete. Its volume in concrete is kept to a minimum, as per the mix design, because cement shrinks after setting and hardening. This may happen in concretes in which the amount of cement used is far more than what is required. Aggregates help to reduce the cracking in concrete. Concrete is likely to be stronger than neat cement if is properly made. The raw materials of concrete are cement, fine aggregate, coarse aggregate and water (Seward 2009).

Concrete is made by mixing the raw materials in correct proportions. A chemical reaction is initiated when cement comes into contact with water. This is known as hydration, and is responsible for the setting and hardening of cement. Cement needs water for setting and hardening, therefore concrete is never allowed to dry out during the first 2 to 3 weeks. This is known as “curing of concrete” (Virdi 2012).

The proportions of aggregates, cement and water for a particular mix depend on the part of the building where it is to be used. It is therefore important to mix the constituents of concrete in the correct proportions so that the final product has the required workability and strength. A typical concrete mix for a strip foundation of a two-storey house is 1:3:6.

The quantity of water used in making a concrete mix is perhaps the most important factor in influencing the workability of fresh concrete and the strength of matured concrete. The amount of water in a mix is expressed as the w/c ratio according to Equation 1 (Seward 2009).

$$\text{w/c ratio} = \frac{\textbf{Amount of water}}{\textbf{Amount of cement}} \qquad \textbf{(1)}$$

The density of concrete depends on the type of aggregate used. Aggregates with a higher density improve the density of concrete to 2400 kg/m^3, lightweight aggregate produces concrete with a density less than 2000kg/m^3.

Concrete is very strong in compression but weak in tension. The strength of concrete is affected by several factors such as voids, water-cement ratio, fine aggregate or shape and texture of aggregates. Voids are the spaces occupied by coarse aggregate which is the sum of the volume of solids and the volume of air voids. To obtain dense concrete, the voids must be filled with fine aggregate, which is possible by compaction. The most important factor that affects the strength of concrete is its w/c ratio. If the volume of water used is more than the optimum requirement, then the excess water remains free while the concrete is still in a semi-fluid state. As the concrete becomes solid, the excess water evaporates leaving voids which make the concrete weaker. Therefore, there must be an adequate quantity of fine aggregate in the mix to fill the voids between the coarse aggregate. The shape and texture of aggregates also affect the strength of concrete. The crushed aggregates interlock into one another and produce a higher strength than uncrushed aggregates (Seward 2009).

2.1.2f Reinforce bar (steel)

Reinforced concrete structures are made of steel strengthening bars and concrete. Concrete has a very high compressive strength but has low tensile stress and is also brittle, whereas steel has a high tensile strength and is malleable but has a low compressive strength therefore the combination of concrete and steel creates a strong composite material. The steel reinforcement is fabricated out of steel bars or mesh sheets (Karayannis *et al.* 2016). The reinforcement structure is designed to satisfy the requirements set in Eurocode 2 (European Union 2004). The main bar carries the tensile load to each support where the load is then transferred into the columns these bars are the largest bars ranging from 8mm up to 40mm in diameter. The link bars run perpendicular to the main bars in order to tie them together. The other main reason for the link bars is to resist shear stress therefore making the concrete less brittle. Link bars are generally smaller in diameter than the main bar ranging from 8mm to 25mm. Additional Steel reinforcement is also used locally around connections where beams, columns or slabs meet (Bond *et al.* 2006).

2.1.3 Types of Wall Structure

Building structures are built from different fabrics owing to building design, functionality, performance as well as climate influence. Types of wall also depends from their functionality in the structure such as inner walls or outer walls. This section consists of different types of wall for further investigation of building materials' influence on the electromagnetic (EM) sensor.

2.1.3a Brick Wall

Masonry bricks is a construction in which uniform unit bricks, are laid on top of one another to build up a structure such as a brick wall. Bricks are joined by mortar layers. Brick is a popular medium for constructing buildings, bricks can be laid in different bond patterns. Brick walls are commonly used as an outer wall of cavity walls. Figure 2.3 presents a solid (i.e. not cavity) brick wall structure built in the English bond pattern (Brick Southeast 2006).

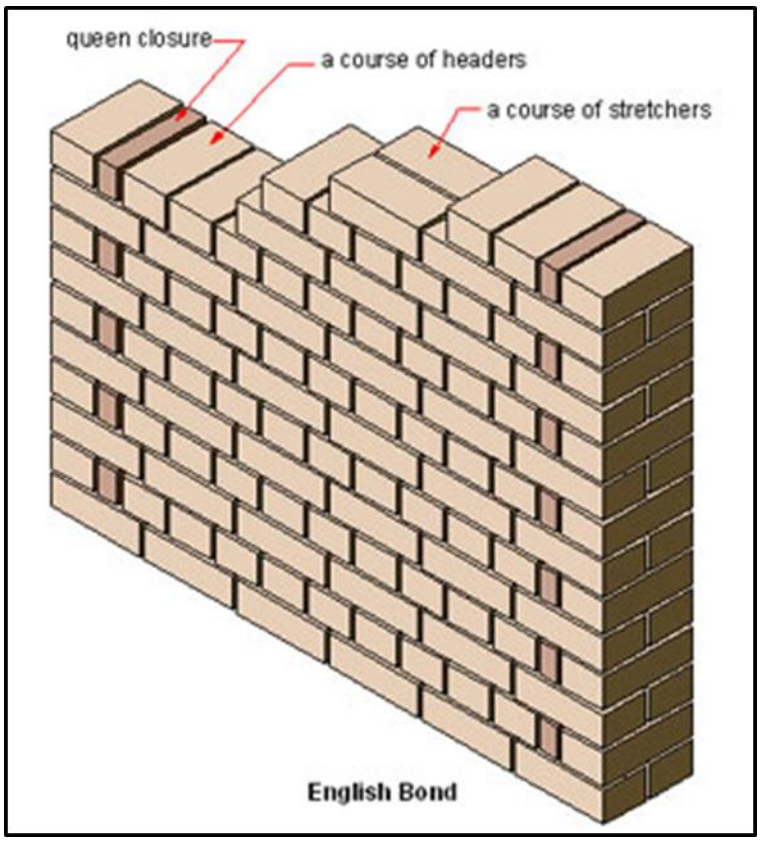

Figure 2.3. Brick wall structure. [Adopted from (Interior Shapes & Designs 2013).]

Brick walls have some limitations. Bricks absorb water easily, therefore, it causes fluorescence when not exposed to air, also rough surfaces of bricks may cause mold growth if not properly cleaned.

2.1.3b Aerated Wall

Aerated block walls are created from aerated blocks that are joined with thin bed mortar. Components can be used for walls, floors and roofs. Often aerated walls are used as the inner part of cavity walls (Kus *et al.* 2004). Figure 2.4 illustrates an example of the aerated wall in a real environment.

Figure 2.4. Aerated wall structure. [Adopted from (Thomas Armstrong LTD 2016).]

Aerated blocks have some limitations, such as lower strength than most concrete products in load- bearing applications and require reinforcement. Also aerated blocks require a protective finish as the material is porous and would deteriorate if left exposed (Virdi 2012; Domone & Illston 2010).

2.1.3c Plasterboard Wall (Dot and Dab technique)

Dot and Dab is a technique that was developed to replace traditional wet plastering. This method has low cost, fast installation, quick drying time and ease of finishing. The dabs of plasterboard adhesive should never be more than 25mm thick. Each dab should be approximately 250mm in length and 50 mm wide Figure 2.5a presents the dot and dab installation technique, while Figure 2.5b presents a complete section of the wall.

(a) (b)

Figure 2.5. (a) Dot and Dab installation technique **(b)** Dot and Dab completed wall section. [Adopted from (HubPages 2015).]

Plasterboard is pressed onto the adhesive until the spirit level indicates that the wall is straight. It is required to leave for 24 hours for the plasterboard adhesive to set fully before attempting to skim the wall with finishing plaster. The disadvantages of using the dot and dab method is the thermal bypass created between plasterboard and wall. All the cracks in the wall allow outside air to flow around behind the linings, cooling them and the home (Virdi 2012).

2.1.3d Block and Brick cavity wall

A cavity wall is essentially made of two walls separated by a continuous hollow space (cavity) and anchored together with metal ties for strength. Cavity walls are lighter and have higher thermal resistance than solid masonry walls. They also protect against rain penetration in wet climates. Insulation materials are usually added inside the cavity to further increase its thermal resistance. This is done by either filling the whole existing cavity by, for example, injecting polyurethane foam; or partially by installing a board of insulation material during the construction stage. Without insulation, the whole cavity becomes essentially an air space of finite thickness across which heat is transferred by conduction, convection and radiation

(Al-Sanea *et al.* 2003). The walls are commonly masonry such as bricks or concrete blocks. Figure 2.6 illustrates a block and brick cavity wall diagram.

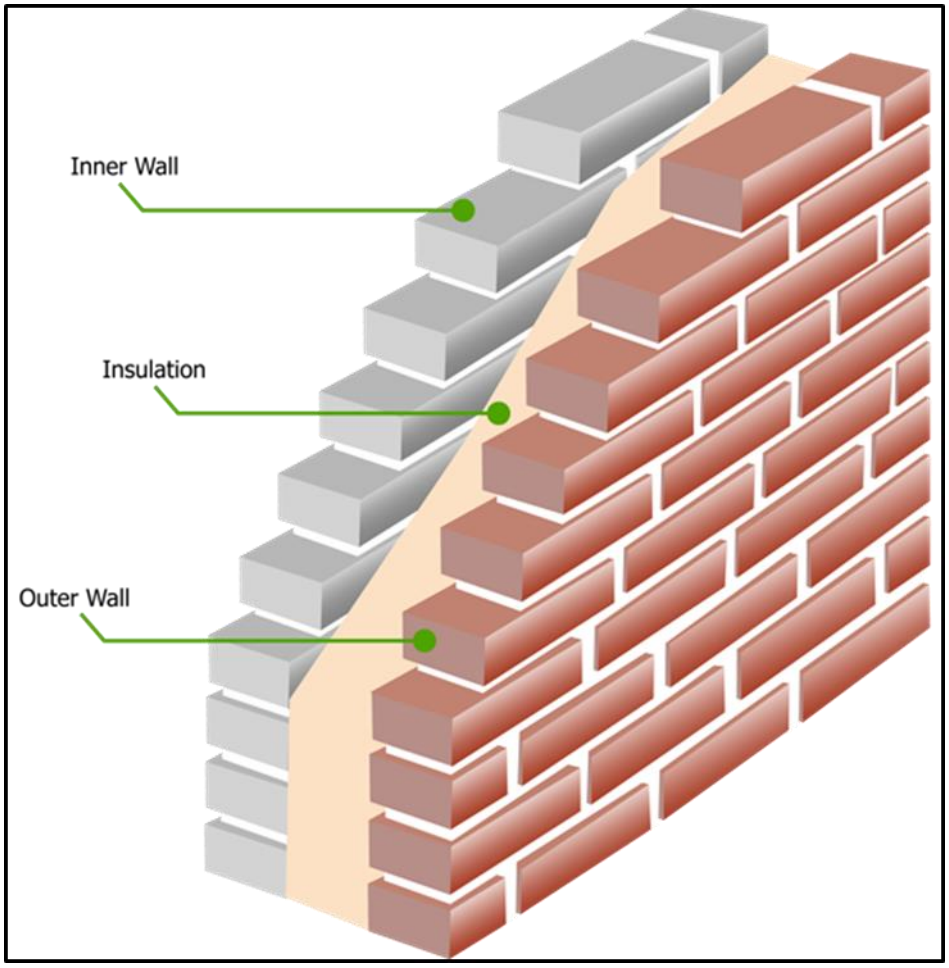

Figure 2.6. Block and brick cavity wall. [Adopted from (Firstcall 2014).]

A cavity wall is designed and built as a moisture-deterrent system. This system takes into account the possible moisture penetration through the outer wall. Moisture will penetrate a masonry wall where hairline cracks exist between the masonry unit and mortar. Water which runs down the exterior wall surface will be drawn towards the inner cavity due to wind pressure exerted on the exterior of the wall and the negative pressure present within the cavity (Hens *et al.* 2007). Providing a clean air space will allow this moisture to flow unobstructed down the cavity face of the outer wall. Flashing installed at recommended locations will then divert this moisture back to the building's exterior through weep holes. Proper drainage of moisture will reduce the chance of efflorescence and freeze-thaw damage (Masonry Advisory Council 2002).

2.1.3e EcoMech Insulation Wall

EcoMech insulation wall is a new industrial wall designed and supplied by EcoMech Structurally Insulated Panels Ltd Company for investigation of the waterproofness of their outer wall design. EcoMech uses traditional Structurally Insulated Panel (SIP) techniques, enhancing structural strength and thermal efficiency by use of precision engineered steel, magnesium oxide board, and structural polyurethane. This type of structure enables the reduction of the overall time and costs of the building development process. Figure 2.7 illustrates an EcoMech wall sample (EcoMech 2014).

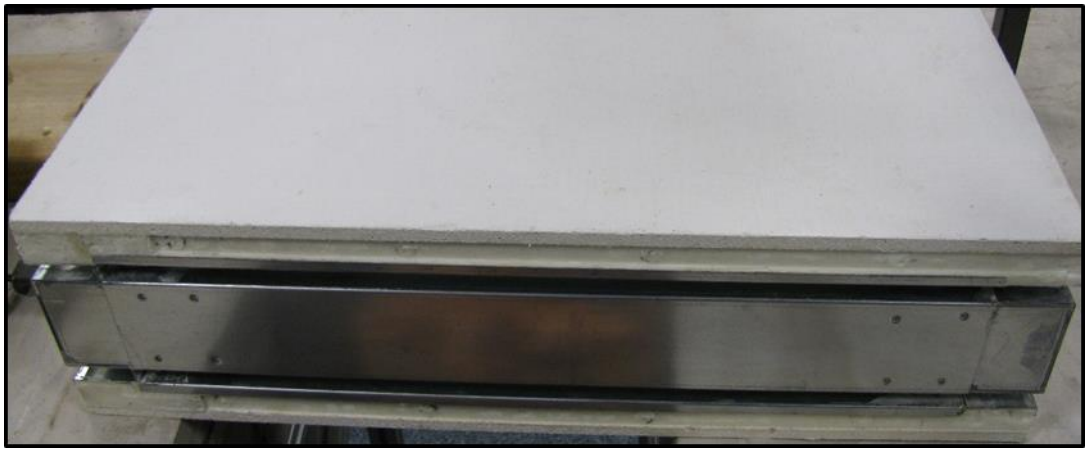

Figure 2.7. EcoMech wall sample.

2.1.4 Concrete Flat Roof Structure

A flat roof is one which is almost level in contrast to the many types of sloped roofs. Any sheet of material used to cover a flat roof is known as a membrane and the primary purpose of these membranes is to waterproof the roof area (CIB & RILEM 1987). Figure 2.8 illustrates a concrete flat roof structure.

Figure 2.8. Concrete flat roof structure. [Adopted from (Chelas Roofing 2007).]

Cracks in the roof parapet wall, and damage to the waterproofing membrane are the common defects of roof construction that require frequent maintenance (Bailey & Bradford 2005; Lo *et al.* 2005). De Silva and Ranasinghe (Ranasinghe 2010) investigated maintainability of concrete flat roofs and found that the causes of defects for concrete flat roofs were design, construction, maintenance and environment, as shown in Table 2.2. About 50 multi-storey buildings were randomly selected to identify maintainability problems of their flat roofs, which comprised residential buildings (46%), commercial buildings (30%) and office buildings (24%). The ages of the building sample spanned from 5 to 25 years. A condition survey was carried out to explore the existing defects and their extent (Ranasinghe 2010).

Table 2.2. Causes of defects for concrete flat roofs. [Adopted from (Ranasinghe 2010).]

No	Defects	Design	Construction	Maintenance	Material/ Environment	No. of defects
1	Splitting	*	*		*	64
2	Blistering of waterproofing membrane system		*			34
3	Joint failure	*	*	*	*	43
4	Crack on roof slab	*	*	*	*	66
5	Crack at roof drainage		*	*	*	38
6	Water leakage through the slab	*	*			38
7	Mechanical damage			*		33

Membrane layers that had been installed on a flat concrete roof revealed durability problems in the long term. Durability of membrane layers will be affected by environmental conditions such as extreme heat, biological agents, Ultraviolet radiation, chemical reactions and material compatibility to roof construction (CIB & RILEM 1987). Thus, the choice of a suitable damp proof membranes and regular monitoring are required to mitigate problems of damage to the membrane. Building defect investigations tend to commence when there are signs of damage that directly or indirectly interfere with the function of the building and the activities within it. For instance, buildings using composite materials exposed to sulphur and salt content will give a reaction when in the presence of tricalcium aluminate and high moisture content over time. Less flexible composite materials require plasticizer to react with other substances. This plasticizer may not be permanent and will disappear in the long term owing to changes of temperature and surrounding weather (Allen 1995). The surrounding environment and weather characteristics such as acidic rain and extreme heat cause reaction to the composite material. This reaction will lead to increased expansion and shrinkage, which result in cracks on the surface of concrete structures.

2.2 Current Methods to Determine Moisture Content of Building Fabrics

Measurements of the moisture content are very important to extend the lifespan of the building. There is a lot of research undertaken in this area owing to the high cost to refurbish buildings. The current methods to determine moisture content of building fabrics will be presented and reviewed. Section 2.2.1 considers radiological measurements, section 2.2.2 illustrates ultrasonic measurements, section 2.2.3 considers ground penetrating radar, section 2.2.4 presents electrical measurements, while section 2.2.5 describes physical property measurements.

2.2.1 Radiological Measurements

2.2.1a Neutron Method

Neutrons interact mainly with the hydrogen nuclei and give a direct measurement of water content by volume. Higher energy neutrons emitted from a radioactive substance such as a radium beryllium source are slowed and changed in direction by elastic collisions with atomic nuclei. The process in which the high energy neutrons lose energy by kinetic

collisions with surrounding nuclei is called thermalisation, the neutrons being reduced in energy to the thermal energy of atoms in a substance at room temperature. Hydrogen having a nucleus of similar size and mass as the neutron has a much greater thermalising effect than any other element. A measurement of the thermal neutron density in the vicinity of a neutron source will be a measure of the concentration of hydrogen nuclei on a volume basis (Wittmann *et al.* 2008), and thus a measure of the water concentration (Phillipson *et al.* 2007). The source and detector are placed in a probe. The neutron source is mounted in a lead shield at the bottom of the gas filled detector tube. The unit is constructed to be set over an access hole in the porous material, and the probe lowered through the bottom of the shield into the hole. The resolution of the probe is non-sufficient; it is impossible to measure accurately the water content within 6 in. of the surface. Deficiency of high resolution makes the measurement of water content distribution with depth in a soil inaccurate in detail, it being impossible to detect accurately any sudden change in the profile (Wormald & Britch 1969; Imal 2002).

2.2.1b Gamma Ray Method

Gamma rays interact with the orbital electrons of matter in three ways. Firstly, the photoelectric effect, in which the whole of the energy of gamma rays is absorbed where this occurs at low energies. The Compton Effect, which is the scattering of gamma rays by electrons at medium energies, and finally the creation of positron- electron pairs, becomes important at high energies. Measuring the attenuation of gamma radiation enables us to determine the density of material. The essential components of that system are a source of gamma rays, a detector, an amplifier, a discriminator and a device to record the pulses from the detector. The gamma ray method offers high accuracy in the determination of moisture content at ±1.0%. Therefore, there is no effect of temperature change or of dissolved conducting materials. Unfortunately, there are high capital costs and precautions are necessary with radioactive equipment. The gamma scattering method determines the moisture content of concrete by measuring the intensity of scattered radiation in limestone concrete using an ingeniously built goniometer and an HPGe spectrometer (Vijayakumar *et al.* 2002; Bucurescu & Bucurescu 2011).

2.2.2 Ultrasonic Measurements

Non-destructive sonic and ultrasonic testing methods are non-invasive and have been used in recent years in the assessment of civil engineering structures and materials. Sonic methods refer to the transmission and reflection of a mechanical stress wave through a medium at sonic and ultrasonic frequencies. The most commonly used sonic methods are: Sonic transmission method, Sonic/seismic tomography, Sonic/ seismic reflection method, Ultrasonic reflection method and sonic resonance method. The detection of flaws by the sonic transmission method is possible owing to the fact that sonic waves cannot transmit across an air gap, which could be owing to a crack, void or delamination at the interface between brick or stone and mortar. A propagating wave must find a path around the void, resulting in attenuation and an increase in the transit time of the signal. Data scatter from sonic tomography has the effect of increasing the residual of tomographic velocity reconstruction and may lead to identification of false anomalies. The accuracy of the velocity reconstruction can be improved by a better understanding of the input signals, by a carefully planned choice of position and number of the readings stations (McCann & Forde 2001). Sonic reflection method is not a method currently recommended since the resolution achievable with the low frequency energy is poor and it is often difficult to distinguish reflections from surface waves and refracted arrivals (McCann & Forde 2001; Vun et al. 2007).

2.2.3 Ground Penetrating radar

Ground Penetrating Radar (GPR)is a technique that uses electromagnetic waves to obtain three-dimensional images of natural or manmade structures and subsoil. GPR in civil engineering is well established, it is used to locate buried services, detect voids or cavities as well as location steel reinforcement in concrete (Manacorda *et al.* 2015). Reci (2016) investigate the GPR for the non-destructive evaluation of moisture content in wood material by using direct wave method in wide angle radar reflection configuration, where one GPR antenna is moved while the other is kept in a fixed position. The reflected signal is recorded for different separations between transmitting and receiving antennas. Direct waves are compared to reflected waves. It is observed that they show a different behaviour when the moisture content varies, due to their different propagation paths. The relative dielectric permittivity was measured by using the resonance technique at 1.26 GHz, and results were

compared to GPR measurements carried out with a 1.5 GHz ground-coupled antenna. The results show that the reflected waves has good agreement with results available in the literature. direct waves, the measured values of the relative permittivity turn out to be weakly affected by the polarisation of the electromagnetic field.

2.2.4 Electrical Measurements

2.2.4a Electrical resistance measurement

Electrical resistance measurement is based on the fact that each material possesses electrical resistance, and that water content has a direct impact on the electrical resistance of the material, more water means less resistance (Maksimović *et al.* 2012). Measurement of the electrical resistance is usually carried out using needle-shaped electrodes. Two measuring detectors are placed by driving or drilling into a building element and electrical resistance as a function of the electrical conductivity is measured. Wet materials have higher conductivity and lower electrical resistance. The measuring device indicates the results according to different construction materials which can be converted into percentages of moisture. (Wormald & Britch 1969; Maksimović *et al.* 2012).

2.2.4b LTCC sensor

Low Temperature Co-Fired Ceramic (LTCC) sensor with design and fabrication of an inductor-capacitor (LC) planar sensor have been made to monitor moisture content of the most often used buildings materials (Radosavljevic 2012). The sensor can be used in the following ways: it can be put into the building material through a small cut for already built walls or it can be buried in the plaster during the building wall process. Variation of the water content in the tested specimens is measured wirelessly, with an antenna coil, tracking changes in the sensor resonance frequency (Maksimović *et al.* 2012). This sensor consists of two dielectric layers. The first layer has a screen printed LC structure and the second layer has a window over the capacitor's electrodes. Through this window the sensor is exposed to moisture, which will then cause change of its dielectric constant and total capacitance and consequently the resonant frequency of the LC sensor. The sensor exhibits from 0% to 70% wide detection range of water absorption with high linearity and fast response (Maksimović *et al.* 2012).

2.2.5c Time Domain Reflectometry (TDR)

The principle of TDR used for the measurement of moisture is to transmit an electromagnetic signal down the parallel electrodes of a waveguide inserted into the dielectric material under investigation. The time taken for the signal to return after reflecting from the end of the waveguide is measured. This gives a direct measure of the permittivity of the surrounding material along the length of the waveguide (Wormald & Britch 1969). Current state of research of common applications of TDR technique for monitoring moisture content in all porous materials, regardless of their type, are not possible yet. The method requires further investigation particularly in the data acquisition process. General formulas for determination of moisture content from measured relative permittivity are not yet available (Černý 2009).

2.2.5 Physical Property Measurements

2.2.5a Thermal method

The thermal conductivity of a material increases with increasing the moisture content. One of the methods used to determine the thermal conductivity is to supply a probe in the material with a known heat input, and to measure the temperature rise at a fixed distance from the heat source using thermocouples or thermistors. One advantage of thermal conductivity measurements is that they are independent of the salt content of the porous body. However, thermal conductivity does depend on environmental temperature which can be compensated for, and also upon the density of the material, necessitating several calibration curves for different densities of the material measured (Yunus & Mukhopadhyay 2011).

The thermal conductivity method suffers from the difficulty in obtaining reproducible calibration curves, and each calibration curve is only valid for a specific density of the material. IR Thermography can be used to monitor the moisture content of buildings. This method requires scanning all surfaces of a building and comparing it to the image of the interested area. The identification of the damp areas is achieved by the comparison between the temperature of the dry and moist surfaces. One of the thermal techniques is a ‘pad’ sensor (Davies & Ye 2009). The inventors of this sensor demonstrated a non-destructive technique for the measurement of moisture content within a material using thermal diffusion wherein heat is delivered into a surface and the resulting temperature increase is detected at a distance from the injection point. In the ‘pad’ sensor method the heater and temperature sensor are fixed at the surface of a thermal insulation material block (the ‘pad’). The

preliminary results illustrate 0.01kg/kg accuracy. The device offers the benefits of the traditional dual probe which has the accuracy ±2% kg/kg (Ye *et al.* 2007), but with the important advantage that no holes are required to be drilled in the material of interest (Davies & Ye 2009). However, limitations are depending on environmental temperature and the density of the material necessitating several calibration curves for different densities of the materials measured.

2.2.5b Vapour pressure

Measurement of the equilibrium relative humidity of air in contact with a porous body enables us to deduce directly the water tension of the porous body, which can be correlated with the moisture content. The conversion of water tension values to moisture content requires an individual calibration for each type of porous material and is not a reliable procedure. Vapour pressure method requires very accurate measurements of the equilibrium relative humidity between the porous body and the surrounding air (Wormald & Britch 1969).

2.3 Commercially Available Devices

A moisture meter is an essential device used in many industries to detect moisture content in building materials. Home and building inspectors depend on moisture meters to identify potential problems and damage to structures from moisture accumulation. Woodworking industries, such as furniture makers, use wood moisture meters to ensure a quality product. Flooring contractors use moisture meters to determine ideal conditions when installing a floor over a concrete slab or subfloor. Moisture meters can have an analogue or digital scale to display moisture content in percentage (Grainger 2012). Figure 2.9 illustrates measurement methods for different moisture devices.

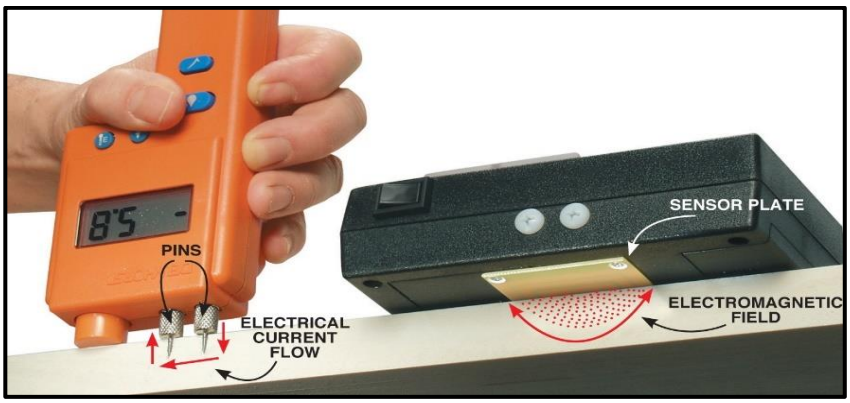

Figure 2.9. Moisture meters and their measurement methods. [Adopted from (Munkittrick 2015).]

There are three types of moisture meters used for the inspection of building and structure materials namely pin-type, pin less and pin/pin less/all-in-one meters. Temperature and wood density affect the readings given by moisture meters. All meters are calibrated to read the moisture content at about 20ºC. Therefore, it is required to apply correction to the meter readings while device is used in different temperature ranges. Manufacturers include charts that adjust for species and temperature variations. More expensive meters have built-in species correction and temperature correction. Pin meters are more sensitive to temperature variations than pin less meters. Pin less meters are more sensitive to differences in density of different species than pin meters (Munkittrick 2015). Summary of factors affecting each type of moisture meter is presented in Table 2.3.

Table 2.3. Comparison of factors affecting each type of moisture meter. [Adopted from (Moisturemeters 2010).]

Factor	Pin less Meter	Pin Meter
Temperature	No	Yes
Chemicals	No	Yes
Wood Orientation	No	Yes
Moisture Gradient	No	Yes
Wet Pockets	No	Yes
Wood Species	Yes	Yes
Wood Density	Yes	No
Surface Texture	Yes	No

2.3.1 Pin-type meter

Pin-type moisture meters' measure percentage of moisture content at the depth of the head of the contact pins. Pin-type moisture meter shown in Figure 2.10 has two pins on the instrument, which are used to penetrate into the test surface at a desired depth. The reading of moisture content is determined by measuring the electrical resistance between the tips of the two pins. This method of inserting pins into a surface is an invasive process for measuring percentage of moisture content. Typically these moisture meters will read up to 5/16" depth which is equal to 0.79375 cm depth (Grainger 2012). Pin-type moisture meters use the principle of electrical resistance to measure the moisture content in materials by measuring the conductivity between the pins. The tips of the pins are relatively sharp, uninsulated and penetrate into the surface for a sub-surface reading. With pin-type meters, you can also obtain a reading by touching the pins to the surface for testing. Most pin-type moisture meters use a scale calibrated to wood, however this does not mean that the meter cannot be used to measure moisture in other substrates and materials. This type of moisture meter can also be used for, but not limited to: concrete, drywall, ceiling tiles and painted surfaces (Smith 2015). When using the wood scale on a pin-type moisture meter, the moisture content percentage reading can range from 5% to 40% in moisture content. The low end of this reading falls into the 5 to 12% range, the moderate range will be 15 to 17%, and the high or saturated range will read above 17%. Scales for moisture percentage ranges are provided in the instrument instructions and should be consulted concerning measuring ranges for particular surface materials. Pin-type meters are the only instruments that allow the inspector to identify exact location of moisture at a given point. Using a pin-type meter is an effective way to determine the difference between shell and core moisture content. In some cases, the depth of the reading exceeds the length of the pin on the meter. Many meters are equipped

with a connection option to add accessory probes that can be inserted further into a substrate for more accurate core or depth detection (Grainger 2012).

Figure 2.10. Pin-type moisture meter. [Adopted from (Grainger 2012).]

2.3.2 Pin less moisture meter

Pin less or non-invasive moisture meter (Figure 2.11) operates on the principle of electrical impedance. This meter provides a non-destructive measurement of moisture in wood and other substrates, such as concrete and gypsum. Scales on these meters are similar to that of pin-type meters, where the wood scale reads moisture content percentage at 5 to 30%, and non-wood materials moisture content percentage is read on a relative scale of 0 to 100%. Pin less moisture meters are capable of reading up to a typical depth of 3/4" (1.91cm) or 1" (2.54cm) into a subsurface. These are useful for detecting problem moisture accumulation where visual indicators are non-existent (Grainger 2012).

Figure 2.11. Pin less moisture meter. [Adopted from (Smith 2015).]

2.3.3 Pin/ Pin less/ All-in-one moisture meter

The Pin/ Pin less/ All-in-one moisture meter illustrated on Figure 2.12 is a type of moisture meter which utilizes both methods for measuring moisture content in surfaces. Since this type of meter offers the option to measure moisture content in substrates using both methods of reading moisture, one meter may be able to identify problem areas and then also be used to pinpoint the exact location where moisture damage or accumulation is occurring. Essentially, this type of meter would utilize the same scales of moisture content for wood and non-wood substrates and allow the end user the versatility necessary for a full inspection in determining areas where moisture is an issue (Grainger 2012).

Figure 2.12. Pin/ Pin less/ All-in-one moisture meter. [Adopted from (Grainger 2012).]

2.4 Electromagnetic (EM) Waves Measurement Approach

Microwave radiation can be used in different fields and within different industries. Currently the most known device that is using microwave radiation is the microwave oven. Microwave radiation can also be used to transmit signals such as mobile phone calls. Microwave transmitters and receivers on buildings and masts communicate with the mobile phones in their range. Certain microwave radiation wavelengths pass through the Earth's atmosphere and can be used to transmit information to and from satellites in orbit. Microwave radiation has interested many researchers, Wendling (Wendling *et al.* 2009) used microwave sensor technology for monitoring and detection of ethanol in water/ethanol mixtures in non-destructive manner. The tests have been realized using samples of water/ethanol mixtures going from 0% ethanol (pure water) until 100% ethanol. Every sample alcohol concentration is determined by its unique frequency, magnitude, and phase. Also, microwave spectroscopy was investigated by Muradov (Muradov *et al.* 2014) to monitor meat drying process in real-time. The results of the research demonstrate a significant linear relationship between the reflection coefficient and weight loss of the meat sample. The weight of the sample drops down dramatically first week and then keeps steadily decreasing. Likewise, an amplitude shift is greater at the beginning of the drying process and then the shift stabilises. In both researches there is an interesting relationship between the water and the microwave spectroscopy which could be explored in building environment for detection of the moisture content in building structures.

2.5 Summary

The literature review started focusing on moisture content of building fabrics to investigate the causes of the dampness, their chemical and physical processes, as well as the movement through building materials. The acceptable moisture level and the most common sources of moisture in building fabrics was studied. Also, different types of building fabrics used in modern building have been reviewed which enabled us to understand concrete flat roof and wall structures and their mechanical and chemical properties. Section 2.2 was devoted to current methods to determine moisture content in building fabrics. Current methods can be organised into categories: Destructive measurements and Non-destructive measurements. The neutron method is destructive measurement with the non-sufficient resolution that makes measurement inaccurate. The advantage of current destructive measurements is the

accuracy of the results. Non-destructive measurements have lower accuracy and repeatability than destructive measurements but they do not damage building material to process with measurements. Another disadvantage of current non- destructive measurements, such as the gamma ray method, is high cost and risk of radiation. The gamma ray method offers high accuracy in the determination of moisture content at ±1.0%. Unfortunately, there are high capital costs and precautions are necessary with radioactive equipment. Sonic measurement methods require further improvement of the accuracy of the velocity reconstruction. Sonic reflection method is not one currently recommended since the resolution achievable with the low frequency energy is non-sufficient and it is often difficult to distinguish reflections from surface waves and refracted arrivals. Ground Penetrating radar shows promising results, this method requires further investigation. Measurement is limited to specific surface namely wood. Electrical resistance measurement provides accurate results but require drilling into material which makes the measurement destructive also the penetration depth of the measurement is limited to the length of the electrodes and further extension equipment has to be used to extend the penetration depth. Low Temperature Co-Fired Ceramic sensor has to be implemented into the measured sample via prepared hole or sensor has to be implemented inside of the measured material during its manufacturing process. Time Domain Reflectometry method requires further investigation particularly in the data acquisition process. General formulas for determination of moisture content from measured relative permittivity are not yet available. The thermal conductivity method requires to supply a probe in the material with a known heat input. Thermal conductivity does depend on environmental temperature and the density of the material necessitating several calibration curves for different densities of the materials measured. A "pad" sensor uses thermal conductivity method. The sensor provides similar results to dual probe technique however the limitation will be the same as the standard thermal conductivity method. Vapour pressure require individual calibration for each type of porous material and is not a reliable procedure. Vapour pressure method requires very accurate measurements of the equilibrium relative humidity between the porous body and the surrounding air. The limitations of the current research methods are listed in Table 2.4.

Table 2.4. Limitations of current research methods to determine moisture content in building fabrics.

Research	Limitations
Neutron Method	Drilling Required, Penetration depth up to 15cm, unable to detect sudden changes
Gamma Ray Method	High capital cost, Radioactive equipment
LTCC Sensor	Put into material through a cut or buried in the material during building process
Time Domain Reflectometry	Drilling Required, this technique requires further investigation
Ultrasonic Method	Cannot transmit across an air gap (Ash block, modern bricks)
Thermal Method	Drilling Required, temperature dependent, calibration required

Section 2.3 illustrated commercially available devices to measure moisture content in building materials. Commercial meters are highly depended on different factors namely, temperature, orientation or material species. Also current moisture meters have limited penetration depth during their measurement. The disadvantages of commercial devices are summarised in Table 2.5.

Table 2.5. Limitations of commercially available devices to determine moisture content in building fabrics.

Device	Limitations
Pin-type moisture meter	Drilling Required
	Measurement limited to length of pins
	Unable to identify source of failure
Pin less moisture meter	Contact Required
	Penetration depth approx. 2.54cm
	Unable to identify source of failure

Section 2.4 illustrated the different research undertaken in microwave spectroscopy filed to determine moisture content of different material which could be potentially used to monitor the moisture content in building fabrics.

Chapter 3 Electromagnetic approach and Theoretical modelling

Currently, microwave spectroscopy is used in multiple industrial projects as discussed earlier in section 2.4. Presented results identify electromagnetic (EM) waves as a potential technique for non-destructive measurement to determine the moisture content of building fabrics in real time. This chapter tells about electromagnetic approach and theoretical modelling. Section 3.1 consists of the electromagnetic spectrum theory. Section 3.2 considers fundamental parameters of antennas namely radiation pattern, gain and directivity. Different types of antennas are illustrated in section 3.3. Sensor design and simulation results are described in section 3.4, while section 3.5 consists of dielectric properties of selected building materials namely sand, water, and cement. Section 3.6 shows the preliminary experiment undertaken to identify different building materials in non-destructive manner. Section 3.7 summarises the electromagnetic approach and theoretical modelling and results from the experiment.

3.1. Electromagnetic Spectrum

The spectrum of electromagnetic waves ranges from the longest radio waves through the infrared and optical regions and on to X-rays and gamma rays (Scott 2005). Microwaves are radio waves with wavelengths ranging from one meter to one millimetre, or equivalently with frequencies between 300 MHz (0.3 GHz) and 300 GHz (Sarwate 1993). Figure 3.1 depicts the full electromagnetic spectrum from long waves up to Gamma Ray (Sorrentino & Bianchi 2010). The electromagnetic wavelength in vacuum is measured by following Equation 2 (Bakshi & Bakshi 2009).

$$\lambda = \frac{c}{f} \qquad \textbf{(2)}$$

where:

c is the velocity of light equal to 3×10^{8} (ms^{-1})
f is the frequency (Hz)

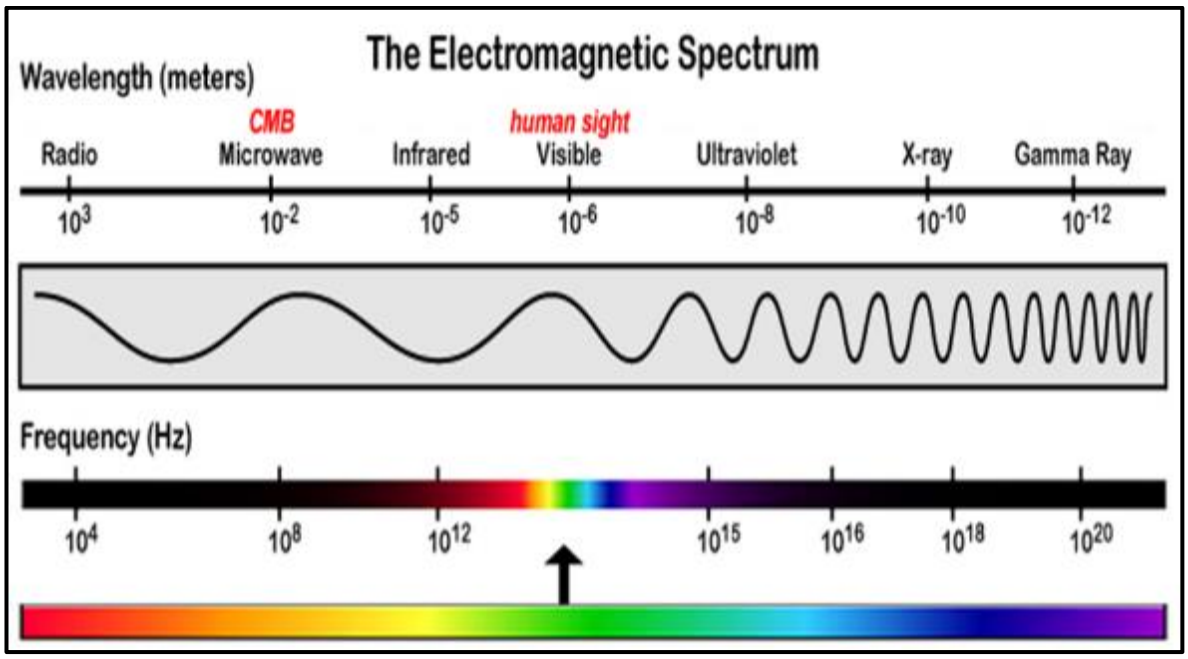

Figure 3.1. The electromagnetic spectrum. [Adopted from (Lawrence *et al.* 2012).]

Table 3.1 presents electromagnetic spectrum and applications which are operating in a specific range of the radio frequency.

Table 3.1. Electromagnetic spectrum and applications by radio regulations. [Adopted from (Sorrentino & Bianchi 2010).]

Frequency	Band	Wavelength	Applications
3-30 kHz	VLF	10-100km	Navigation, sonar, fax
30-300 kHz	LF	1-10 km	Navigation
0.3-3 MHz	MF	0.1-1 km	AM broadcasting
3-30 MHz	HF	10-100 m	Fax, CB, ship communications,
30-300 MHz	VHF	1-10 m	TV, FM broadcasting
0.3-3 GHz	UHF	0.1-1 m	TV, mobile, radar, wireless LAN, microwave devices
3-30 GHz	SHF	10-100 mm	Radar, satellite, mobile,
30-300 GHz	EHF	1-10 mm	Radar, wireless communications, microwave remote sensing
0.3-3 THz	THz	0.1-1 mm	Terahertz imaging

3.2. Fundamental Parameters of Antennas

In order to describe the performance of the antenna it is required to use the fundamental parameters of antennas, namely as radiation pattern, gain and directivity.

3.2.1 Radiation pattern

The radiation pattern of an antenna is defined as a mathematical function or a graphical representation of the radiation properties of the antenna as a function of space coordinates, distribution of the power radiated from the antenna (transmitting antenna), or power received at the antenna (receiving antenna) as a function of direction angles from the antenna (Sadia Khandaker *et al.* 2010).

Radiation pattern lobe is the portion of the radiation pattern bounded by regions of relatively weak radiation intensity. Lobes can be categorised into Main lobe, Minor lobes, side lobes and back lobes as shown in Figure 3.2 (Rodrigo 2010).

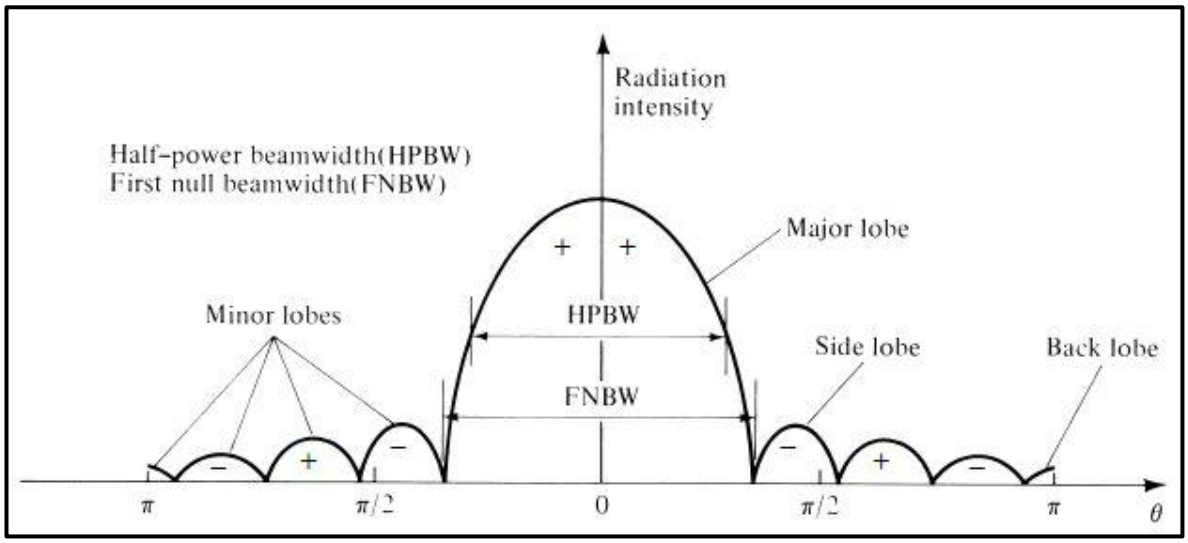

Figure 3.2. Radiation Pattern Lobes. Adopted from (Rodrigo 2010).

A major lobe is a clear peak in the radiation intensity surrounded by regions of weaker radiation intensity. Minor Lobes are any radiation lobes other than the main lobe. A Side lobe is a radiation lobe in any direction other than the direction of intended radiation, while the Back lobe is the radiation lobe opposite to the main lobe. Half-Power Beamwidth (HPBW) is the angular separation in which the magnitude of the radiation pattern decrease by 50% (or -3 dB) from the peak of the main beam. First Null Beamwidth (FNBW) is the

angular separation from which the magnitude of the radiation pattern decreases to zero (negative infinity dB) away from the main beam (Rodrigo 2010).

3.2.2 Gain

Antenna gain relates the intensity of an antenna in a given direction to the intensity that would be produced by a hypothetical ideal antenna that radiates equally in all directions and has no losses. The gain is a measure of how much of the power is concentrated in a particular direction (Roy & Puri 2015).

3.2.3 Directivity

Directivity is a ratio of the radiation intensity in a given direction from the antenna to the radiation intensity averaged over all directions (Sadia Khandaker *et al.* 2010).

3.3. Types of Antennas

Antennas have been around for a long time used in radio systems. An antenna is defined as a transitional structure between free-space and a guiding device. The guiding device or transmission line may take the form of coaxial line or a waveguide, and it is used to transport electromagnetic energy from the transmitting source to the antenna or from the antenna to the receiver. There are different types of antennas which can be used to transmit and receive a microwave signal:

3.3.1 Wire Antennas

Wire Antennas have various shapes such as a straight wire (dipole), loop, or helix. This type of antenna is one of the most common antennas which can be found in lots of applications such as cars, buildings, ships. For example, loop antenna is a directional type antenna which has one or more complete turns of conductors. The loop antenna has a very low radiation resistance (Goh *et al.* 2006).

3.3.2 Aperture Antennas

Aperture antennas are most common at microwave frequencies. There are different types of aperture antennas such as pyramidal horn, conical horn or rectangular waveguide (Balanis

2005). Horn antennas provide high gain, wide bandwidth and low Voltage Standing Wave Ratio (VSWR). There are three types of rectangular horn antennas namely H-plane sectoral horn (Figure 3.3), E-plane sectoral horn (Figure 3.4) and Pyramidal horn (Figure 3.5). A microwave horn antenna produces a uniform phase front with larger aperture than the waveguide, hence greater directivity. A horn antenna consists of a rectangular metal tube closed at one end, flaring into an open-ended pyramidal shaped horn on the other side (Vijayakumar *et al.* 2009). The microwaves are introduced into the waveguide by a coaxial cable attached to the horn antenna. Aperture Antennas are often used for higher frequency applications than wire-type antennas (Huang & Boyle 2008). Pyramidal horns are ideally suited for rectangular waveguide feeders. The head of a horn antenna, acts as a gradual transition from a waveguide mode to a free-space mode of the EM wave (Roy & Puri 2015). The horn antenna diagram is shown in Figure 3.6.

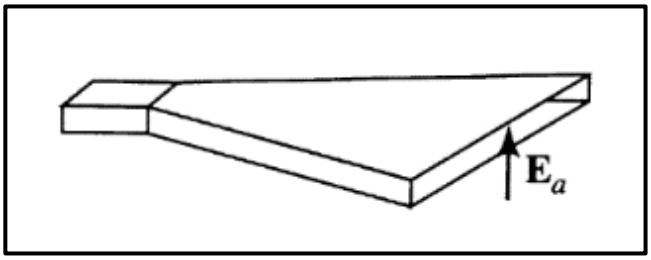

Figure 3.3. H-plane sectoral horn. [Adopted from (Nikolova 2014).]

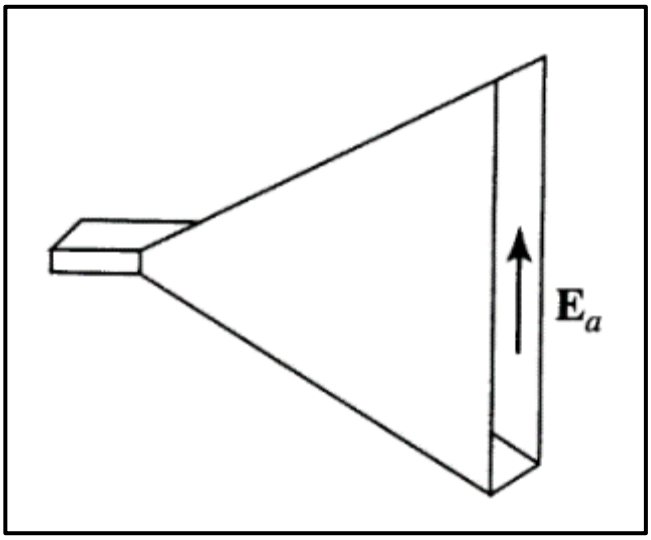

Figure 3.4. E-plane sectoral horn. [Adopted from (Nikolova 2014).]

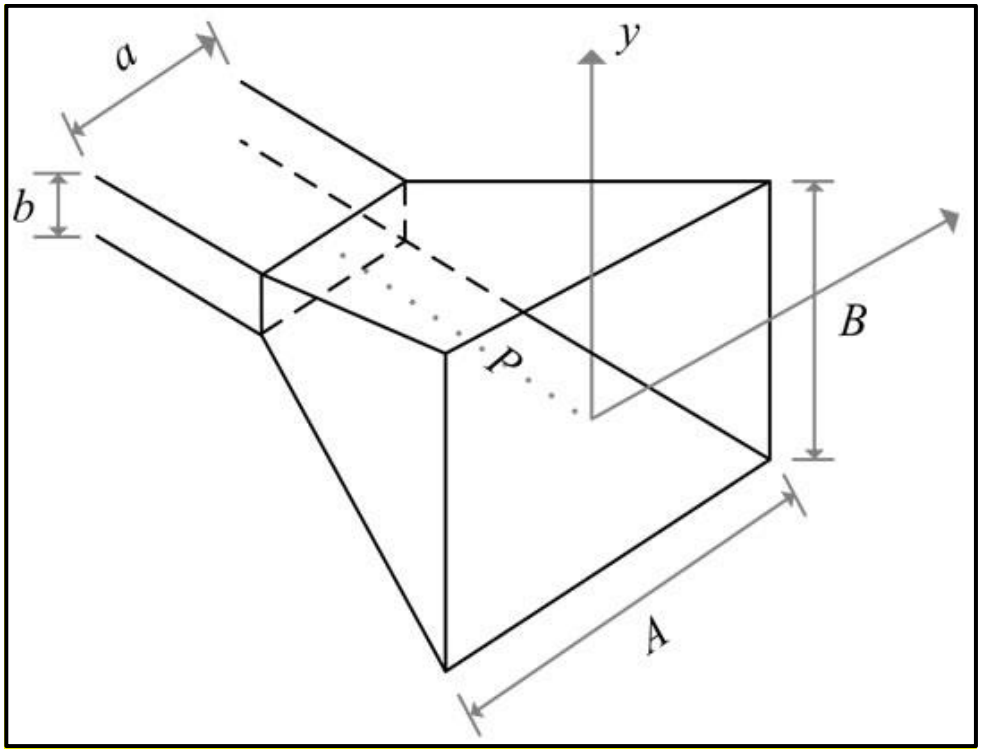

Figure 3.5. Pyramidal horn antenna. [Adopted from (Nikolova 2014).]

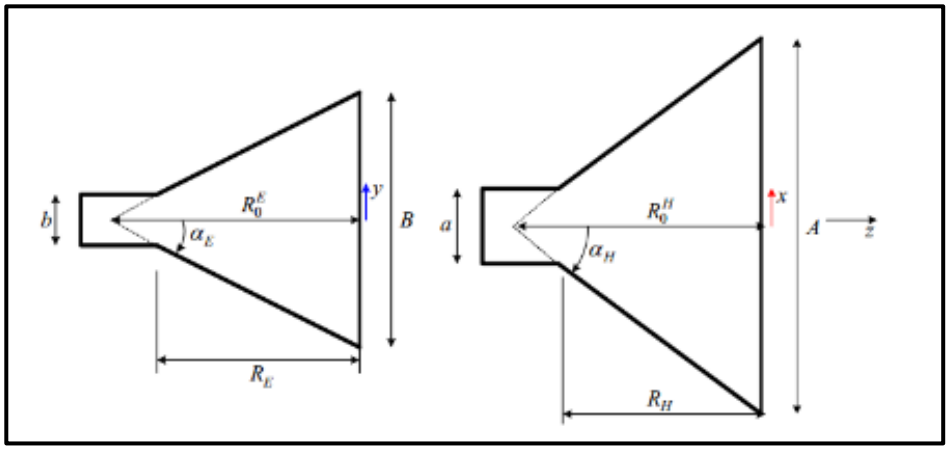

Figure 3.6. Horn Antenna diagram. Adopted from (Roy & Puri 2015).

One of the significant properties of the horn antenna is the angle at which the horn flares out. This affects many areas of the performance including the gain and directivity. The angle of flare is shown in Figure 3.7 and there can be a different angle for both the E-plane (E field) and the H-plane (H field). These are referred to as θ_E and θ_H (Sharma 2014).

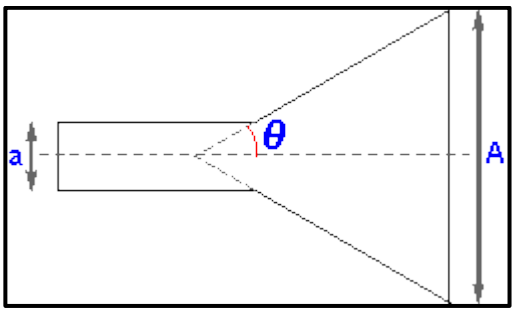

Figure 3.7. Horn antenna flare angle. [Adopted from (Poole 2015).]

As the frequency used by a horn antenna increases, so does the gain and directivity (Beamwidth decreases). The reason for this is that the aperture of the horn remains constant in terms of physical dimensions, but increases in terms of the number of wavelengths. As antennas tend to have higher gain levels as they become larger, so it can intuitively be seen that the gain and directivity of the horn antenna will increase with frequency.

Pyramidal horns are normally constructed to provide optimal gain. The gain of a pyramid horn antenna over an isotropic source, namely one that radiates equally in all direction can be derived from following Equation 3 (Poole 2015).

$$\boldsymbol{Gain = \frac{4\pi A}{\lambda^2} e_A} \qquad \textbf{(3)}$$

where:

A is the physical area of the aperture

λ is the wavelength

e_A is the aperture efficiency and is a figure between 0 and 1

3.3.3 Microstrip Antennas

The Microstrip antenna, sometimes called a patch antenna, is defined as an antenna which consists of a thin metallic conductor bonded to a thin grounded dielectric substrate (Fung 2011). The metallic patch can take different configurations. The Microstrip antennas are low profile, comfortable to planar and nonplanar surfaces, simple and inexpensive to fabricate using printed-circuit technology (Korostynska *et al.* 2014). There are many different variations of shape for patch antenna's radiating element. Some common shapes are square, circle, ellipses, triangle, circular ring, and dipole. To design an antenna to resonate at a desired frequency it is required to follow equations 4-7 (Ramna & Sappal 2012).

Resonant frequency (f_r) of the rectangular Microstrip patch is given by Equation 4 (Chintakindi *et al.* 2007).

$$\boldsymbol{f_r = \frac{c}{2L\sqrt{(e_{reff})}}} \quad \textbf{(4)}$$

The effective refractive index value of a patch is an important parameter in the design procedure of a Microstrip patch antenna. The radiation traveling from the patch towards the ground pass through air and some through the substrate (called fringing). Both the air and the substrates have different dielectric values, therefore in order to account this, it is necessary to find the value of effective dielectric constant. The value of the effective dielectric constant e_{reff} is calculated using Equation 5 (Ramna & Sappal 2012).

$$\boldsymbol{e_{reff} = \frac{\varepsilon_r+1}{2} + \frac{\varepsilon_r-1}{2}\left(1+\frac{12h}{W}\right)^{-0.5}} \quad \textbf{(5)}$$

Equation 6 gives the width of the Microstrip patch (Ramna & Sappal 2012).

$$\boldsymbol{W = \frac{c}{2L_{f_r}}\sqrt{\frac{2}{\varepsilon_r+1}}} \quad \textbf{(6)}$$

where,

W = Width of the patch

C= Speed of light

ε_r= value of the dielectric substrate

The length (L) of the patch is calculated using Equation 7 (Afridi 2015).

$$\boldsymbol{L = \frac{C}{2f_r\sqrt{e_{reff}}} - 2\Delta L} \quad \textbf{(7)}$$

3.4. Sensor Design and simulation results

The HFSS model of the sensors used will be presented and analysed. Quality simulation of sensor designs, which is based on horn antenna, prior to construction not only saves time, but also money. It is possible to derive a mathematical model for the frequency response of a horn antenna. The changes in the building construction material properties in the time domain make a design using a simplified mathematical formula impossible. For this reason, a powerful simulation software package is required to assess possible designs. Modelling the

sensors was carried out using the High Frequency Structure Simulator (HFSS) software (Ansoft 2005)

The ANSYS HFSS software is a high-performance full wave electromagnetic (EM) field simulator for arbitrary 3D volumetric passive device modelling. The HFSS software can be used to calculate parameters such as S- Parameters, Resonant Frequency and Fields (Ansoft 2005; Maragoudakis & Rede 2009)

Figure 3.8 presents the HFSS model of the horn antenna, which operates from 2-18 GHz. The gain (G) of a pyramidal horn antenna is the ratio of the power intensity along its beam axis to the intensity of an isotropic antenna with the same input power. The gain of the horn antenna was calculated using Equation 2. For any waveguide to be operational at an intended frequency, it must, as a critical condition, pass the frequency cut–off tests for it to be operational. The horn low cut-off frequency is the lowest frequency below which the horn should not function, high cut–off frequency is the highest frequency above which the horn would not function. The horn low cut-off frequency can be estimated using Equation 8 (Daniyan *et al.* 2014).

$$\boldsymbol{\lambda_{LC}(mm) = 1.706 \times base\ length\ (mm)} \qquad \textbf{(8)}$$

Using standard wavelength formula, low cut-off frequency is therefore shown in Equation 9 (Daniyan *et al.* 2014):

$$\boldsymbol{F(GHz) = \frac{C}{\lambda} = \frac{300}{\lambda_{LC}}} \qquad \textbf{(9)}$$

The horn high cut-off frequency is given by Equation 10:

$$\boldsymbol{\lambda_{HC} = 1.3065 \times base\ length\ (mm)} \qquad \textbf{(10)}$$

Using standard wavelength formula the high cut-off frequency is (Daniyan *et al.* 2014):

$$\boldsymbol{F(GHz) = \frac{300}{\lambda_{HC}}} \qquad \textbf{(11)}$$

In estimating the overall length of the horn antenna the wavelength inside the waveguide is Wd as shown in Equation 12, the waveguide length is cut to 75% of Wd (Daniyan *et al.* 2014).

$$\boldsymbol{Wd = \frac{1}{\sqrt{(\frac{1}{\lambda})^2 - (\frac{1}{\lambda_{LC}})^2}}} \qquad \textbf{(12)}$$

The length of the waveguide is shown in Figure 3.8 (Daniyan *et al.* 2014).

$$\boldsymbol{Waveguide\ Length = 0.75 \times Wd} \quad \textbf{(13)}$$

It is to calculate the Flare size. The outer length of the hood H2 is 1.5 times the free space wavelength λ as given by Equation 14 (Daniyan *et al.* 2014).

$$\boldsymbol{H2 = 1.5\ \times\ \lambda\ (mm)} \quad \textbf{(14)}$$

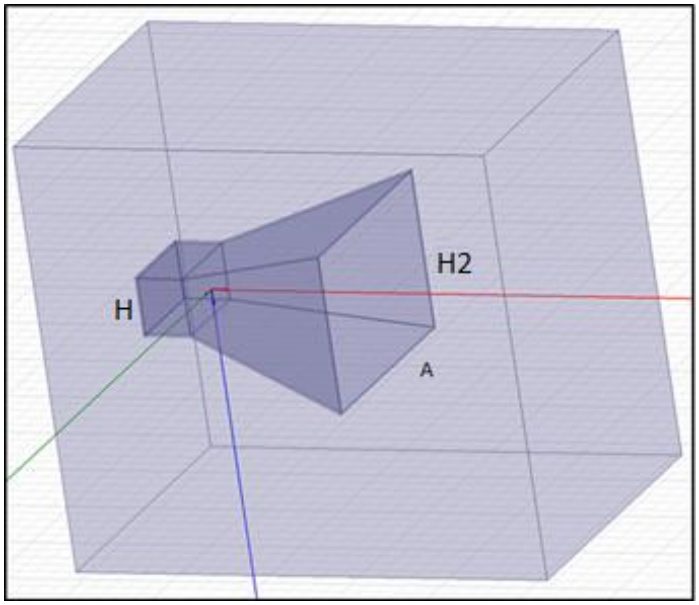

Figure 3.8. HFSS model of a single horn antenna.

The 3D gain plot (Figure 3.9) shows the value of the gain for the designed pyramidal horn antenna. The radiation pattern of the antenna is one of the significant plots that provides knowledge about the Beamwidth angle, and helps in understanding the radiation caused by it. It is a far field radiation plot.

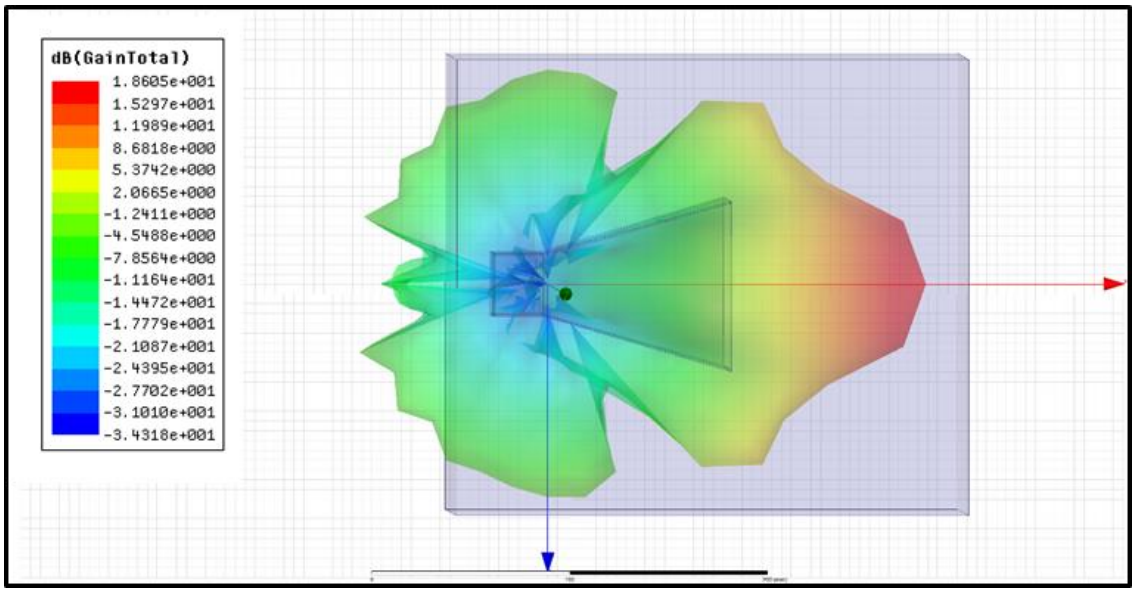

Figure 3.9. 3D Directive Gain Plot for a single horn antenna.

HFSS model of the EM wideband horn antenna and metal plate is shown in Figure 3.10. The metal plate is placed in front of the antenna and it can be seen in this figure that EM radiation is fully reflected from the metal plate.

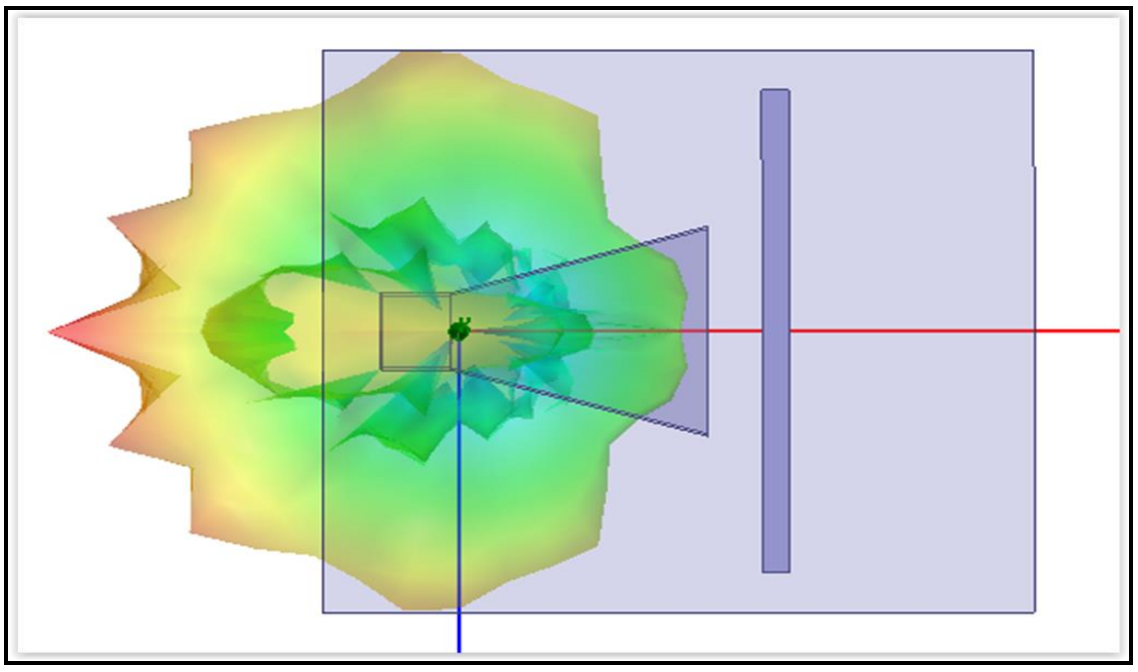

Figure 3.10. HFSS model of a single horn antenna with metal plate in front.

Figure 3.11 (2-6GHz) and Figure 3.12 (6-12GHz) demonstrate the simulation results of the HFSS model, which are provided by S-parameters, namely S_{11} (return loss). The S-parameters are complex scattering parameters, which describe the input-output relationship

between ports (or terminals) in an electrical system. The return loss is a numerical value that indicates how much of the signal is reflected back and is generally calculated in dB. If the power of a reflected signal is close to 0dB, it indicates higher reflection. Therefore, the results in both examples illustrate high signal reflection.

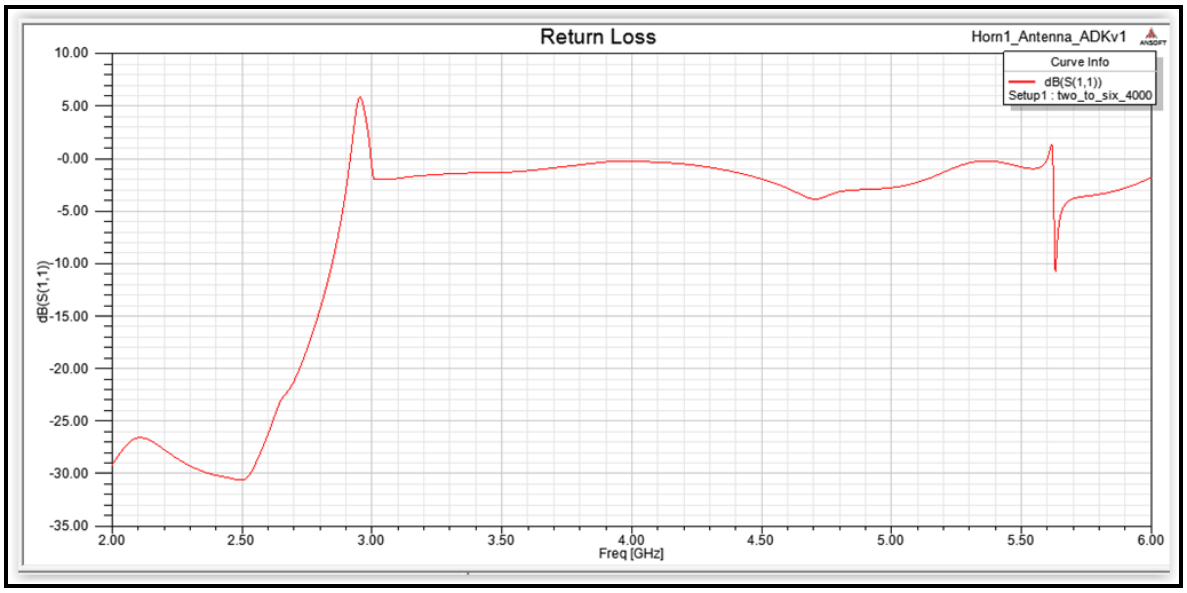

Figure 3.11. HFSS Return loss against Frequency at 2-6 GHz for a single horn antenna with metal plate in front.

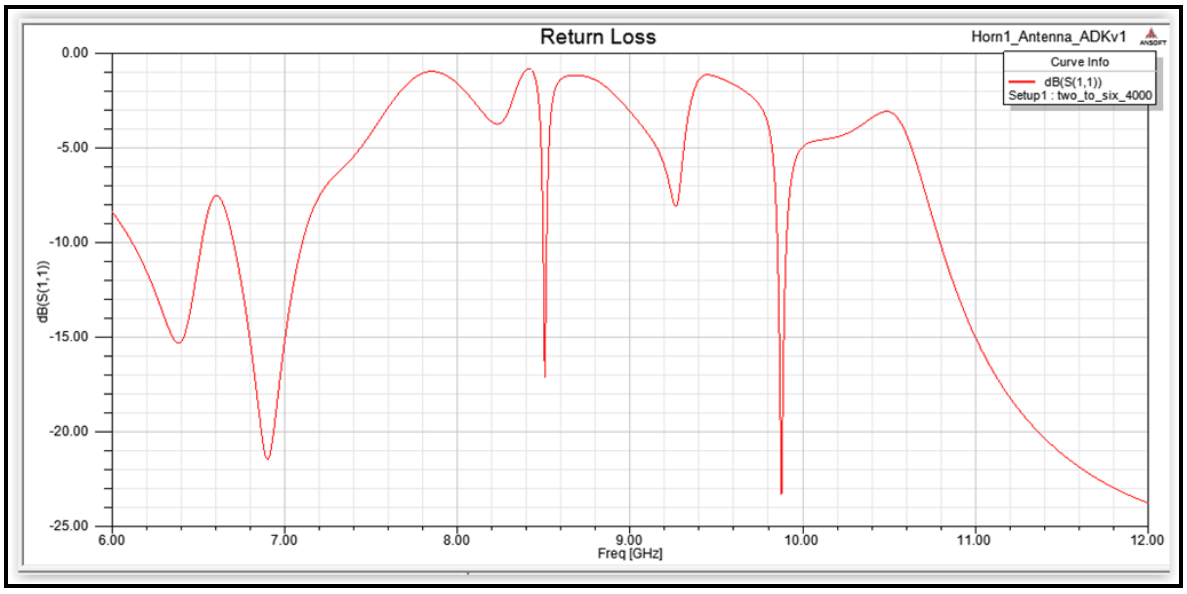

Figure 3.12. HFSS Return loss against Frequency at 6-12 GHz for a single horn antenna with metal plate in front.

Measurement of the distance between the metal plate and horn antenna was simulated in High Frequency Structural Simulation (HFSS). Measurements were provided by S-parameters namely S_{11} i.e. the graph represents reflected power signal from the metal plate.

The purpose of this measurement was to simulate the microwave spectroscopy characterisation while the metal plate is moved away from the horn antenna. There are different distances measured such as 0mm, 15mm, 30mm and 60mm. Results are presented in Figure 3.13. While the metal plate touches the horn antenna (0mm distance) microwave spectroscopy is fully reflected from the metal plate owing to its dielectric properties as a consequence the reflected power level is close to 0 dB. While the metal plate is moved further away from the horn antenna the reflected power decreases as well as there is a microwave frequency shift noticeably. The changes thought to be caused by the increase of a distance between the antenna and the metal plate, which let to change of the wavelength of the signal.

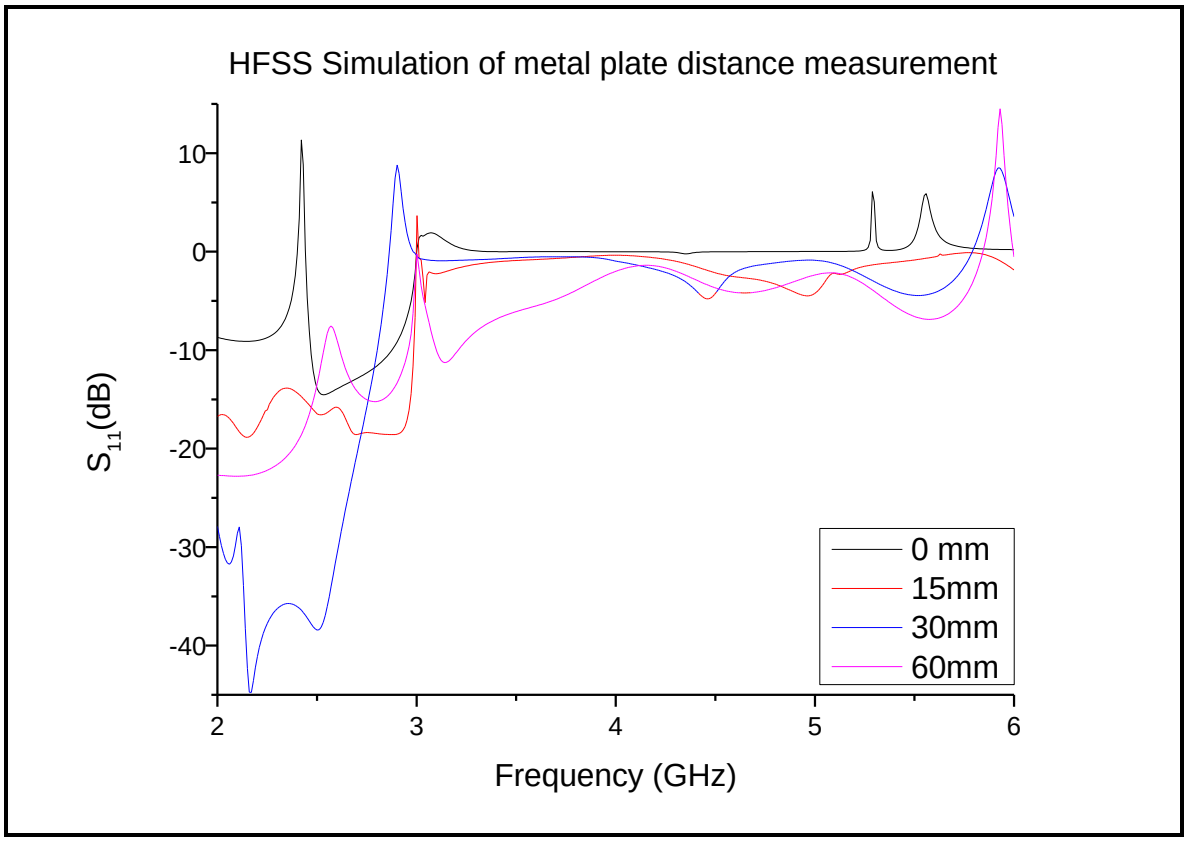

Figure 3.13. HFSS Simulation of a metal plate distance measurement.

Figure 3.14. Experimental setup of a single horn antenna and metal plate.

Experimental setup of the laboratory experiment for metal plate distance measurement is shown in Figure 3.14. Results from the measurement (Figure 3.15) show a good agreement with the simulation results (Figure 3.13), namely decrease of a reflected power and frequency shift owing to increased distance between the horn antenna and the metal plate.

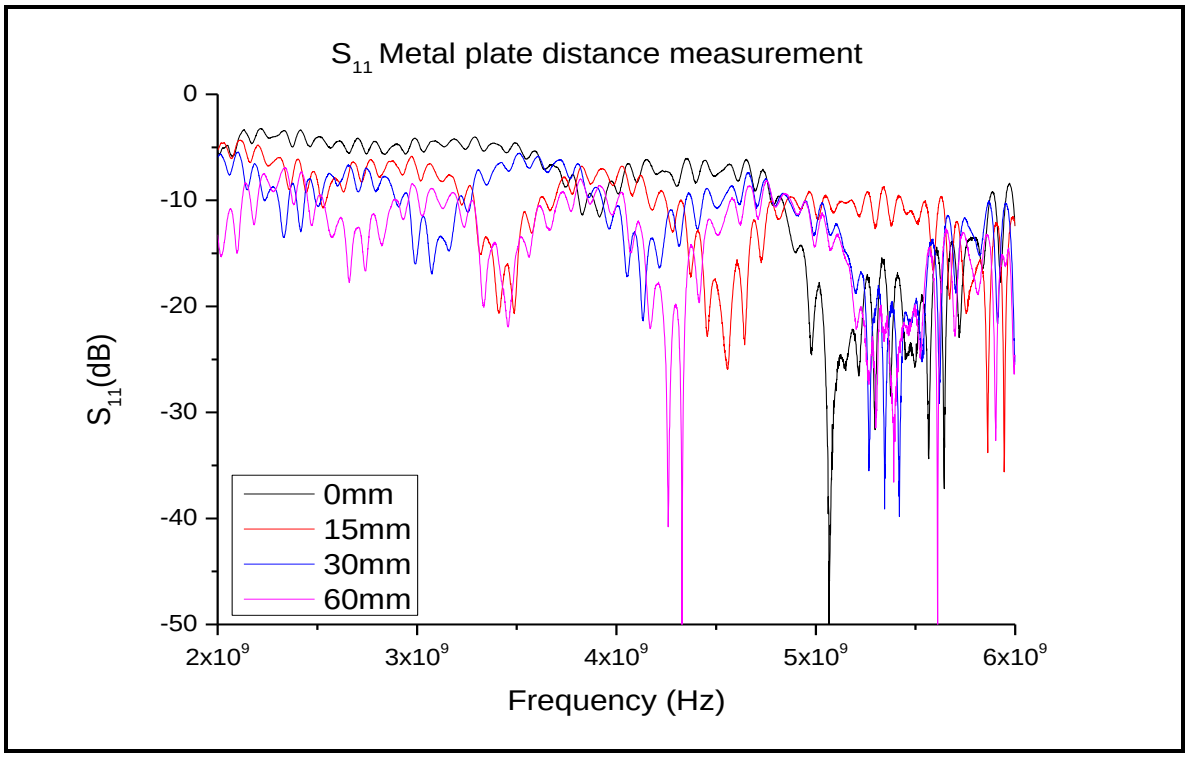

Figure 3.15. S_{11} Metal Plate Distance Measurement.

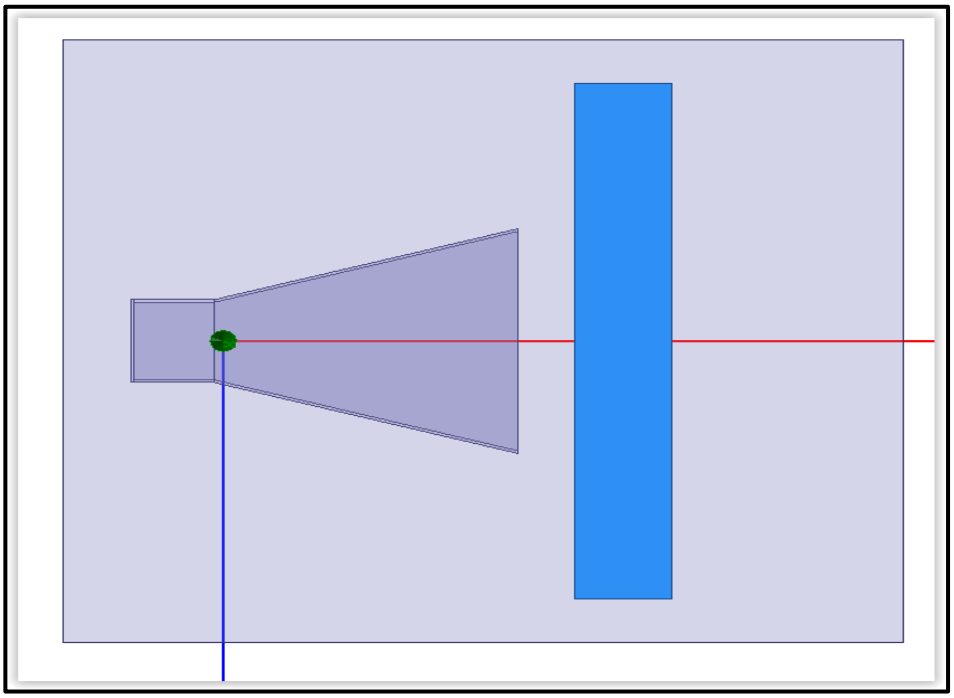

Figure 3.16. HFSS Model of a single horn antenna with water in front.

Measurement of distance between water container and horn antenna was simulated in HFSS (Figure 3.16). The purpose of this measurement was to simulate the microwave spectroscopy characterisation while water container will be moved away from the horn antenna. There are different distances measured such as 0mm, 15mm, 30mm and 60mm. Results are presented in Figure 3.17. While water container touches horn antenna (0mm distance), the microwave spectroscopy is fully absorbed by water owing to its dielectric properties. While the water container is moved further away from the horn antenna, the microwave energy decreases as well as there is a noticeable frequency shift.

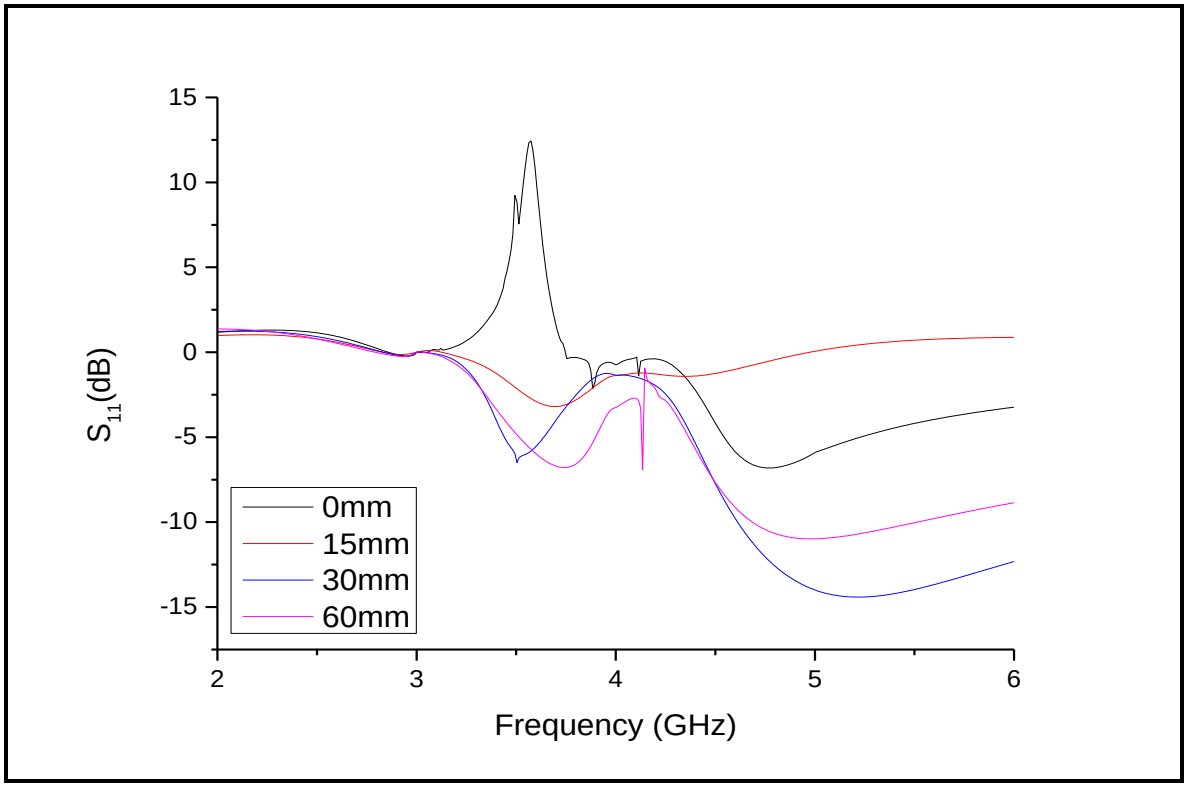

Figure 3.17. HFSS Simulation of water distance measurement.

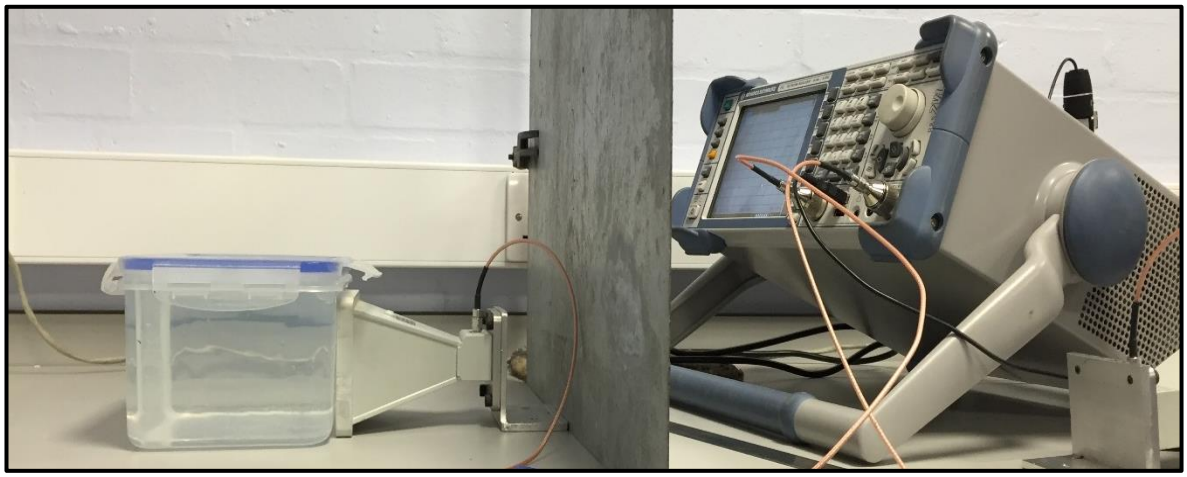

Figure 3.18. Experimental setup of a single horn antenna and water.

Experimental setup of a single horn antenna and water in front is shown in Figure 3.18. Results from laboratory measurement (Figure 3.19) shows the frequency shift between 2GHz and 4GHz. The frequency is decreasing while the distance between the horn antenna and the water container is increasing (0mm, 15mm, 30mm and 60mm). Although these results didn't agree well with the simulation results, it did agree well with the results from Figure 3.15. In both occasions, there is a decrease of a frequency from 5GHz to 2GHz, which is caused by the increase of a distance between the horn antenna and measured object.

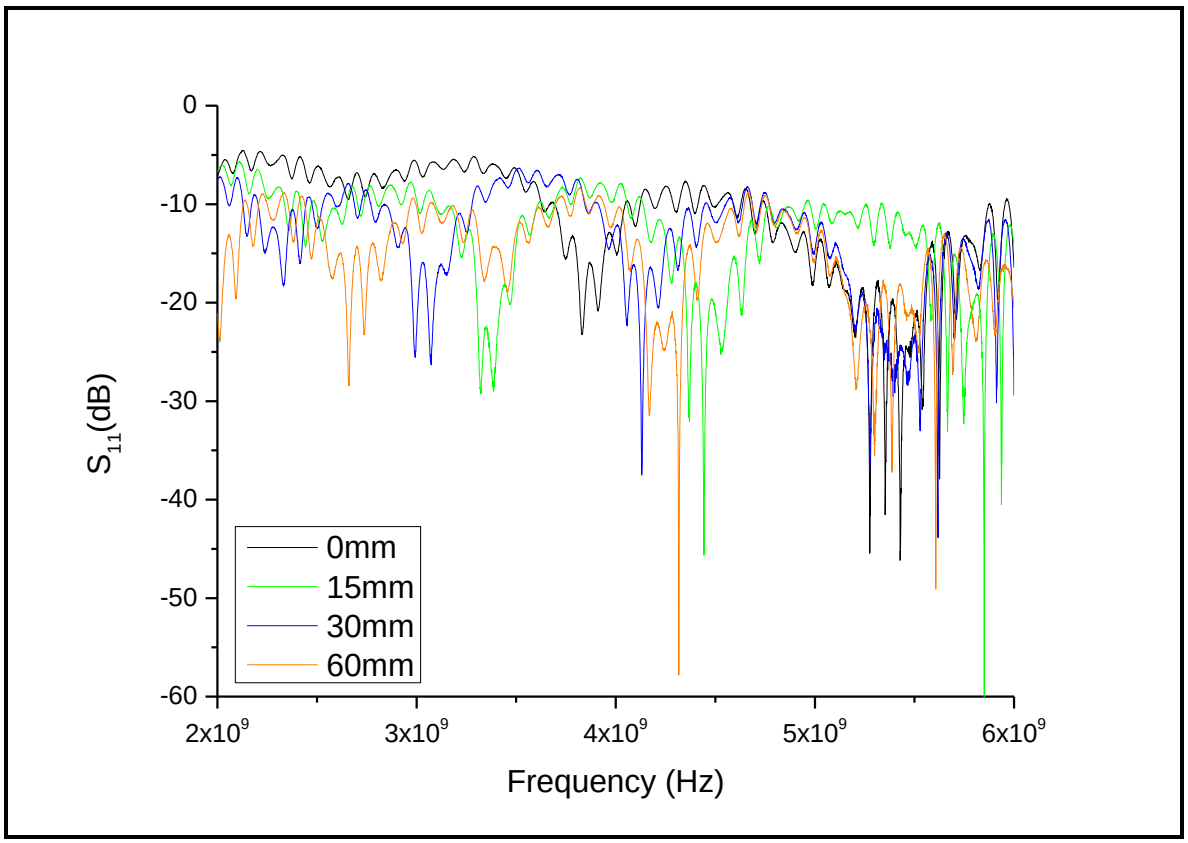

Figure 3.19. S_{11} Water Distance Measurement.

The microwave sensor was modelled and tested in the HFSS software. Figure 3.20 presents the developed sensor, which consists of two antennas. The top antenna is used as a transmitter and the bottom antenna is set up as a receiver. Both antennas have been placed at 33º angle to each other based on preliminary experiment presented in section 3.6.

The purpose of this design is to focus on the desired penetration depth and avoid the interference with objects behind walls. The penetration depth of a concrete structure was greater than 25 cm using a single horn antenna, which is illustrated and proven in section 3.6.1. Therefore, it was essential to focus EM signal at the designated measurement area, which will enable us to collect more valuable data from the reflected signal of a measured object. In this case, only the significant information will be captured. The angle was based on the required penetration depth of the electromagnetic wave throughout measured wall structures. In this setup the penetration depth is approximately 20cm.

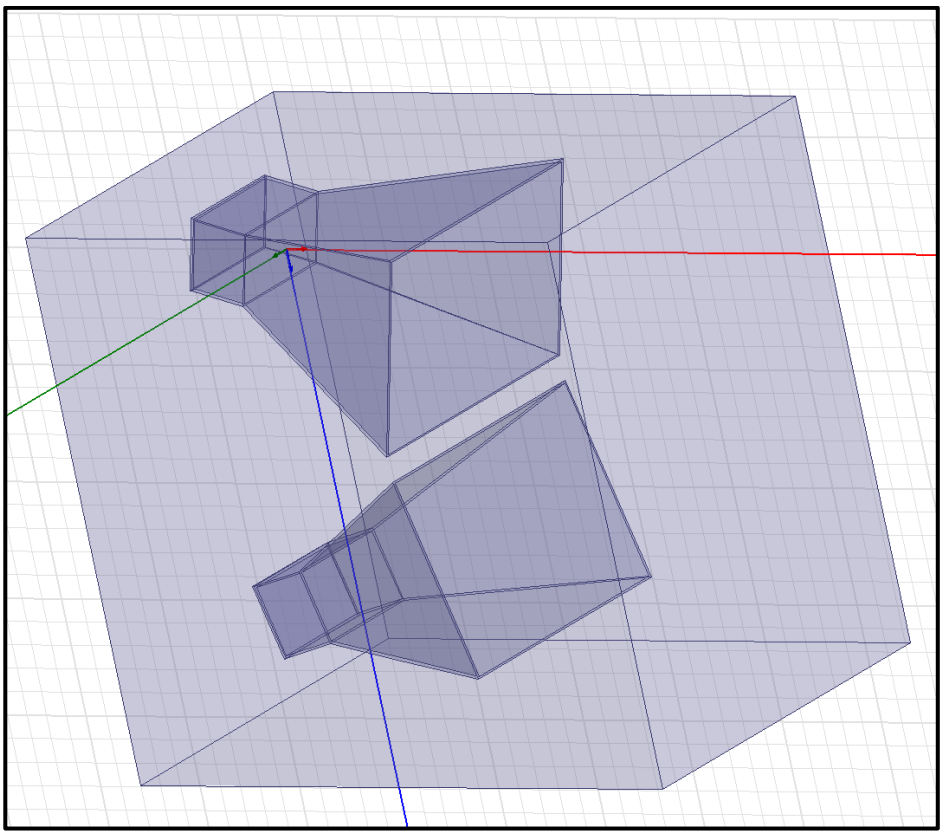

Figure 3.20. HFSS model of microwave sensor.

The simulated model of the final EM sensor and metal plate is shown in Figure 3.21. The metal plate is placed 2cm in front of the sensor to allow the EM radiation to be reflected from the metal plate and received by the bottom antenna.

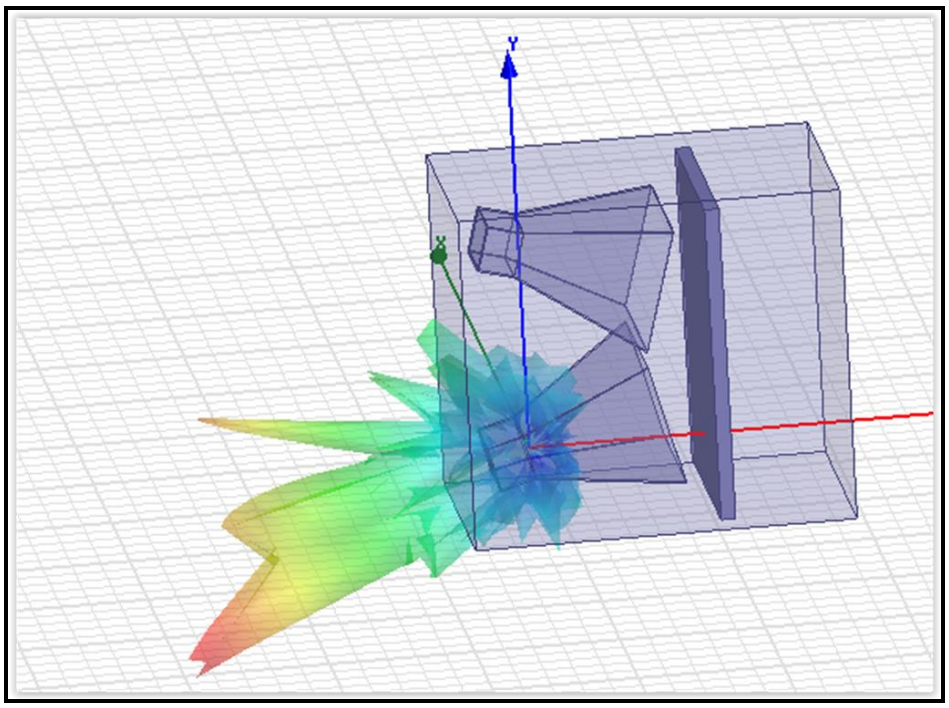

Figure 3.21. HFSS model of EM sensor with metal plate in front.

The analysis of the design with S_{21} parameter is shown in Figure 3.22 (in the 2-6 GHz frequency range) and in Figure 3.23 (in the 6-12 GHz frequency range). The simulation results from both graphs present the reflected power from the metal plate transmitted by the top antenna and received by the bottom antenna. The reflected power is around -10dBm, which is lower than that with a single horn antenna. This could be caused by set angle of the horn antennas, which led to receiving a reflected power from the focused measured area of the object.

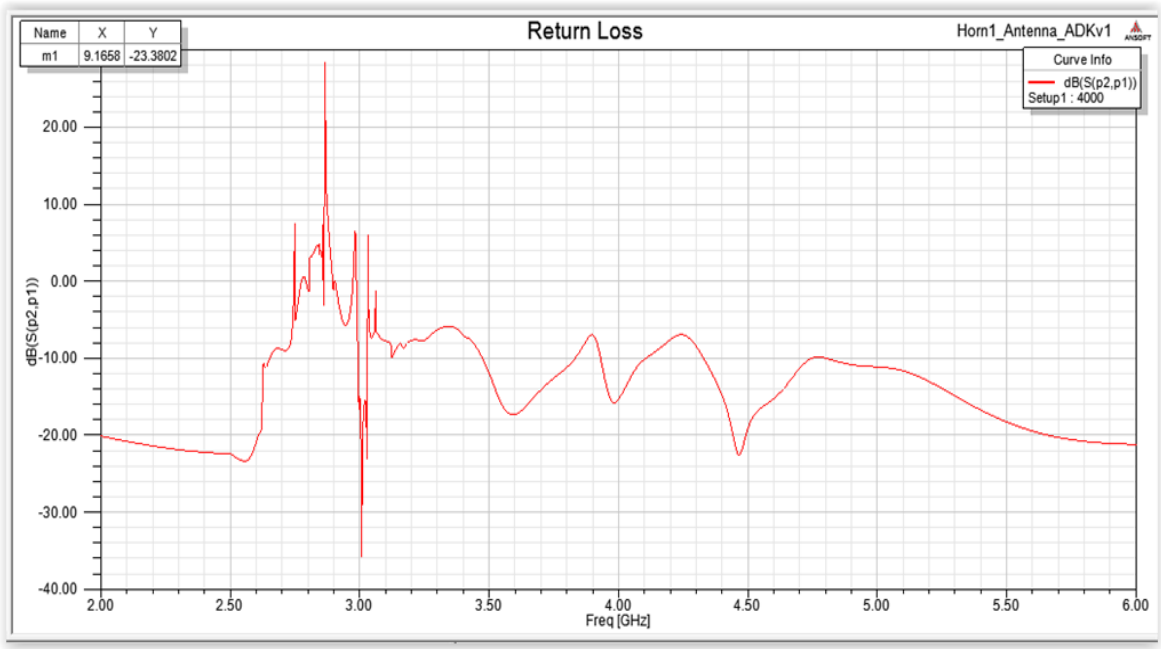

Figure 3.22. HFSS Return loss against Frequency at 2-6 GHz for EM wave sensor with metal plate in front.

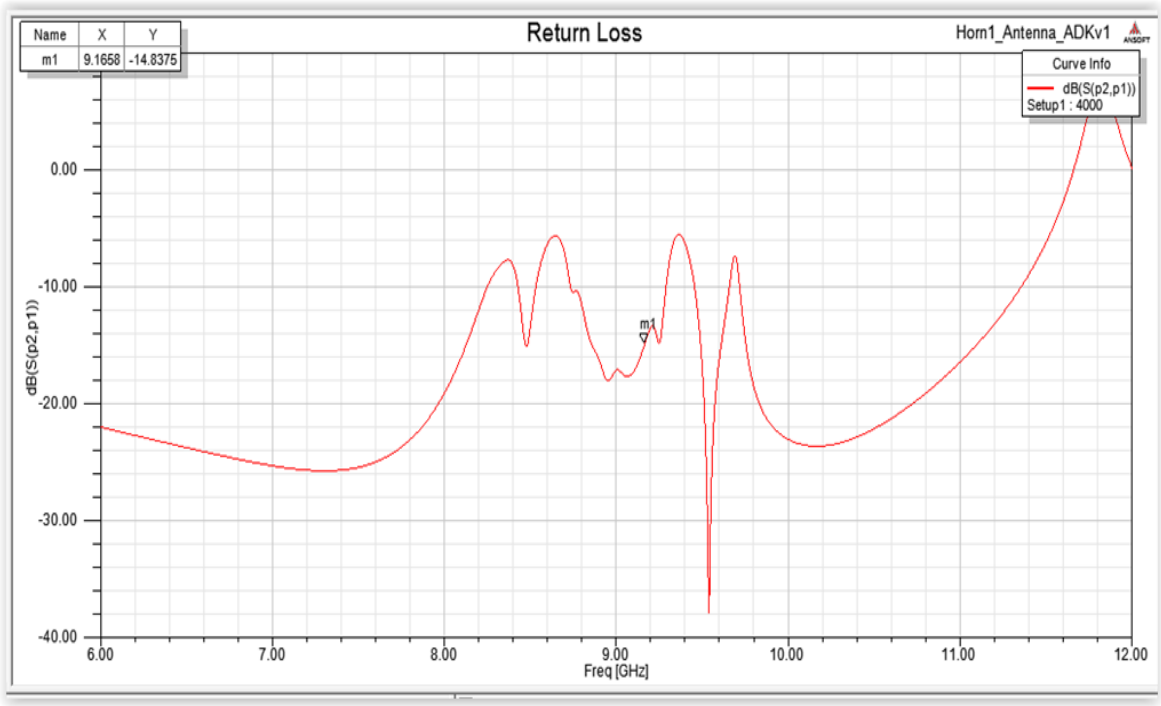

Figure 3.23. HFSS Return loss against Frequency at 6-12 GHz for EM wave sensor with metal plate in front.

3.5. Dielectric Properties of Building Fabrics at Microwave Frequency

Dielectric properties of materials have received increasing attention along with the use of electromagnetic waves in the investigations of material and structural assessment (Agilent 2006). Dielectric properties of a material correlate to other materials characteristics and may be used to determine properties such as moisture content, bulk density, bio-content and chemical concentration (Stuerga 2006). Microwave imaging for building fabrics detection is based on the contrast in dielectric properties of different types of materials and moisture contents (Kirshin *et al.* 2013). Dielectric properties of materials are the relationship between the applied electric field strength E (V/m^2) and the electric displacement D (C/m^2) in the material. Characterization of dielectric properties of material can be implemented by the use of a scalar effective complex permittivity ε_e^* (Equation 15) to account for EM dielectric losses and conductivity of the material (Buyukozturk *et al*. 2006).

$$\boldsymbol{\varepsilon_e^* = \varepsilon_e' - j\varepsilon_e'' = \varepsilon^* + \frac{\sigma''}{j\omega} = \left(\varepsilon' + \frac{\sigma''}{\omega}\right) - j\left(\varepsilon'' + \frac{\sigma'}{\omega}\right)} \qquad \textbf{(15)}$$

where ε_e' is the real part of ε_e^* and represents the ability of a material to store the incident EM energy through wave propagation, ε_e'' is the imaginary part of ε_e^* and represents the degree of EM energy losses in the material, j is the imaginary number. $\varepsilon^* = \varepsilon' - \varepsilon''$ is the complex permittivity (F/m), $\sigma^* = \sigma' - \sigma''$ is the complex electric conductivity (Ω/m), and $\omega = 2\pi f$ is the angular frequency (rad/s) (Buyukozturk *et al.* 2006).

One method to determine the dielectric properties of the materials is the perturbation technique. Resonant cavities are high Q structures that resonate at certain frequencies. A piece of sample material affects the centre frequency (*f*) and quality factor (Q) of the cavity (Balmus *et al.* 2006). From these parameters, the complex permittivity (ε_r) or permeability (μ_r) of the material can be calculated at a single frequency. The perturbation method was used to determine the dielectric properties of building materials. This method uses a rectangular waveguide with iris-coupled end plates. For a dielectric measurement the sample should be placed in a maximum electric field and for a magnetic measurement, in a maximum magnetic field. If the sample is inserted through a hole in the middle of the waveguide length, then an odd number of half wavelengths (n=2k+1) will bring the maximum electric field to the sample location, so that the dielectric properties of the sample

can be measured. An even number of half wavelengths (n = 2k) will bring the maximum magnetic field to the sample location and the magnetic properties of the sample can be measured. Equation 16 determines the perturbation method formula used during measurement.

$$\varepsilon_r' = \frac{V_c(f_c - f_s)}{2V_s f_s} + 1$$

$$\boldsymbol{\varepsilon_r'' = \frac{V_c}{4V_s}\left(\frac{1}{Q_s} - \frac{1}{Q_c}\right)} \qquad \textbf{(16)}$$

Quality factor (Q) formula is shown in Equation 17.

$$\boldsymbol{Q = \frac{f_0}{BW}} \qquad \textbf{(17)}$$

Bandwidth (Figure 3.24) is a measurement of the width of a range of frequencies determined by Equation 18.

$$\boldsymbol{BW = f_2 - f_1} \qquad \textbf{(18)}$$

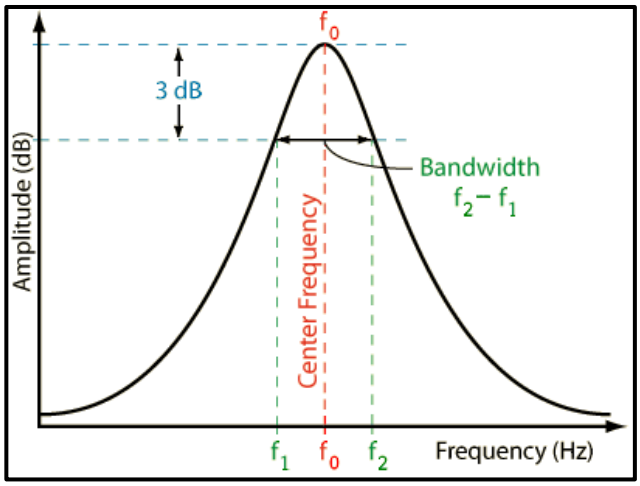

Figure 3.24. Bandwidth. [Adopted from (Tontechnik 2016).]

Figure 3.25 presents the experimental setup for dielectric properties measurement using the perturbation method. During this experiment 2GHz to 3.5GHz waveguide was used. Different materials were tested namely cement, sand, water, cement and sand (mix ratio 1:1.5) Measured materials were placed into a nuclear magnetic resonance (NMR) tube. The NMR tube with selected material was inserted in the middle of the waveguide through the 0.5mm hole.

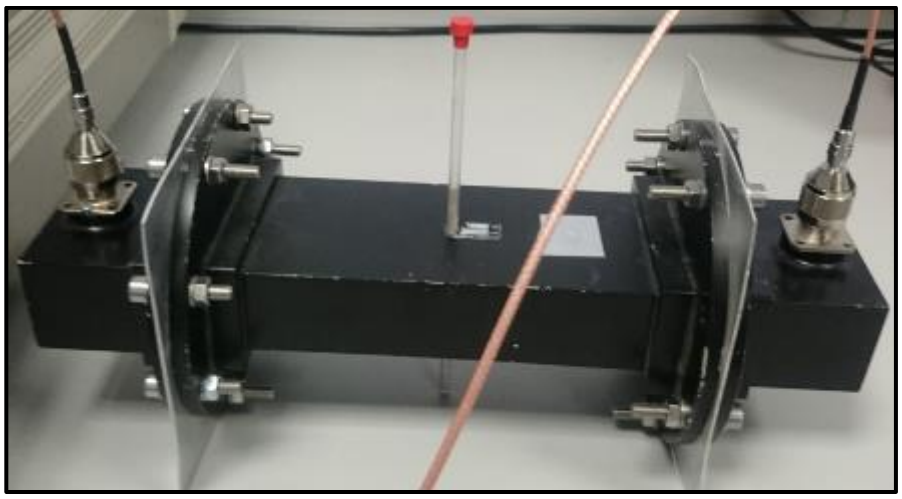

Figure 3.25. Dielectric properties measurement experimental setup.

Building fabrics' dielectric properties have been measured and calculated using formulas 15-17. The results are presented in Table 3.2.

Table 3.2 Building fabrics dielectric properties**.**

Product Description	**Centre Frequency (GHz)**	**F1 (GHz)**	**F2 (GHz)**	**Real Part**	**Imaginary Part**
Cement	3.03553	3.03465	3.03645	2.8024	0.0071
Sand	3.039196	3.037600	3.040373	2.2479	0.0495
Cement and Sand mix ratio 1:1.5	3.035934	3.034400	3.037400	2.7492	0.0857
Water	2.560515	2.5601	2.56094	76.981	-0.046

3.6. Preliminary experiment

The preliminary experiment was set up to identify if microwave spectroscopy that can be used to detect (in a non-destructive manner) different types of construction materials, namely timber, steel and concrete behind the plasterboard. In this experiment two horn antennas 8-12 GHz have been used (Figure 3.26). The top antenna was used as a transmitter and the bottom antenna was used as a receiver. S_{21} data was recorded by a Graphical User Interface in LabVIEW, Figure 3.27 illustrates results from Microwave test set Marconi 6200A, which shows different microwave spectrums while various objects are tested.

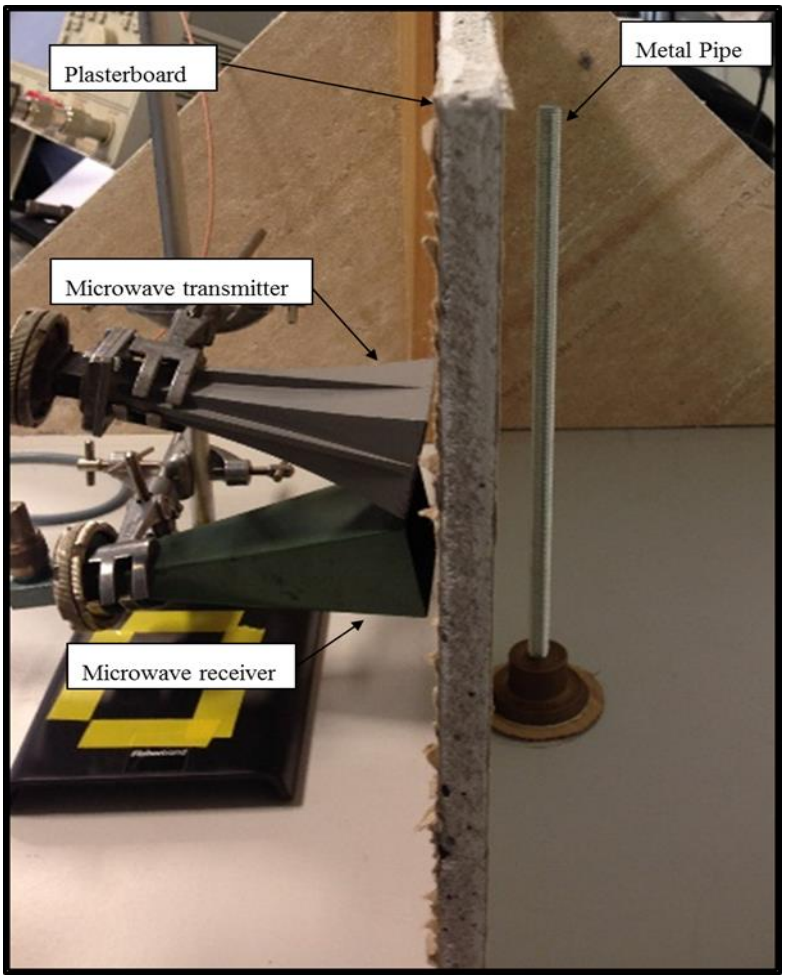

Figure 3.26. Preliminary setup to identify construction materials.

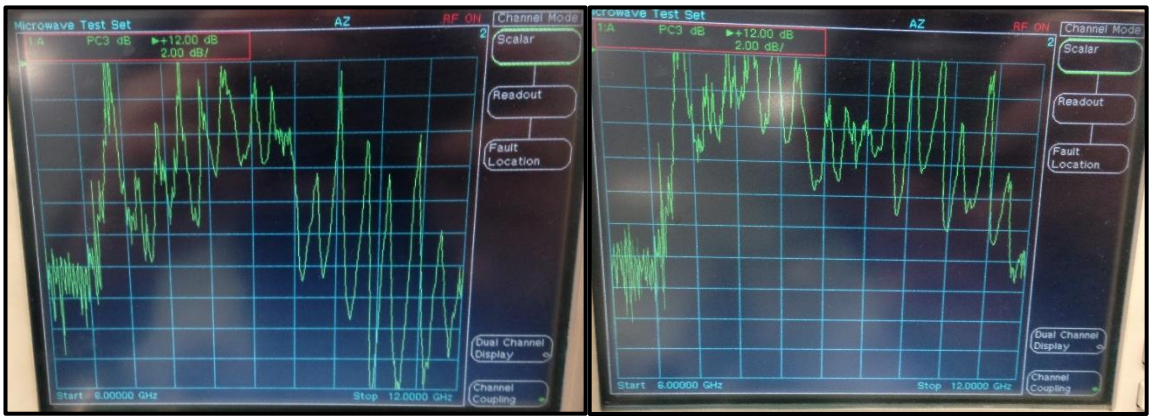

(a) (b)

Figure 3.27. (a) Microwave spectrum for metal pipe displayed on Marconi screen, (b) Microwave spectrum for brick displayed on Marconi screen

3.6.1. Concrete Slabs Penetration Depth with a Single Horn Antenna

This experiment was conducted to calculate the penetration depth of pyramidal horn antennas at a certain frequency range, in the laboratory environment. In this experiment a pre-cast concrete paving slab (600 x 600 x 50mm), grade 20 without any reinforcement bar was used. Figure 3.28 presents the block diagram of concrete penetration depth measurement. Figure 3.29 shows an experimental setup with the single horn antenna to determine penetration depth.

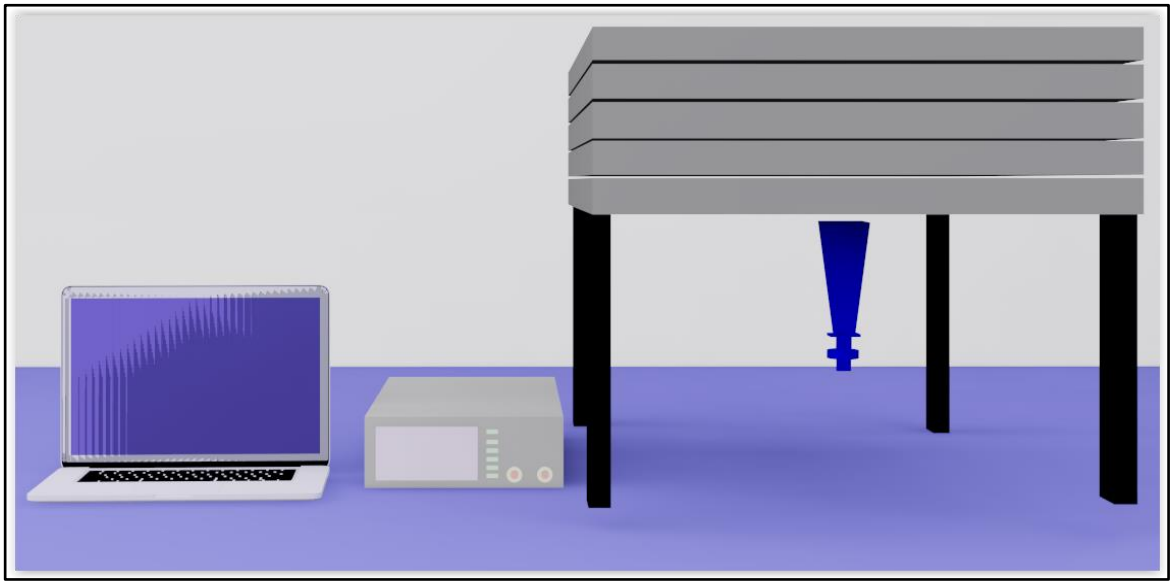

Figure 3.28. Block diagram of concrete penetration depth measurement.

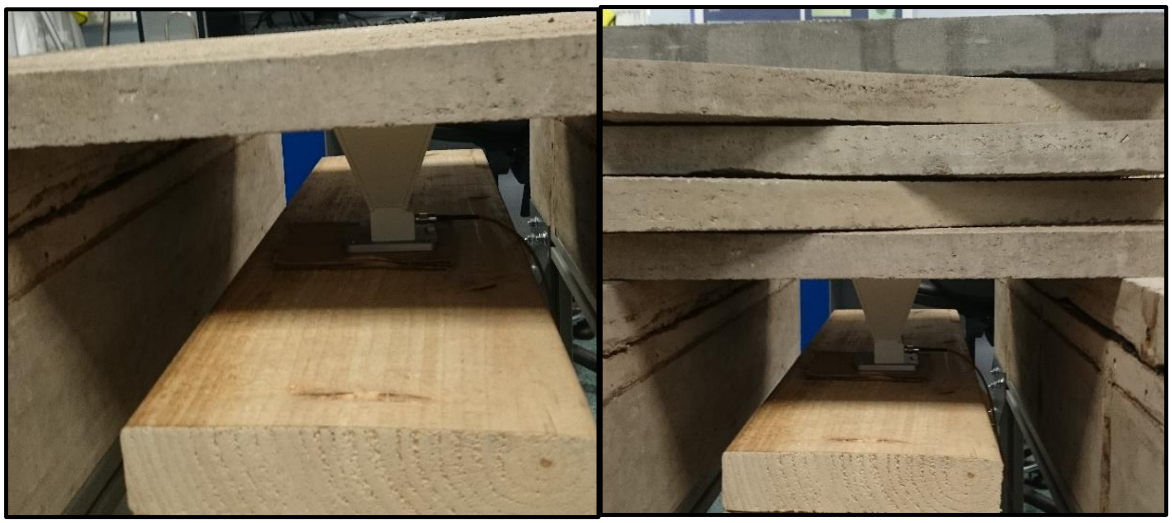

(a) (b)

Figure 3.29. Experimental setup of concrete penetration depth measurement (a) one pre-cast concrete slab (b) five pre-cast concrete slabs.

The measurements are provided by S-parameters in the frequency range between 2GHz and 6GHz, namely $S_{11,}$ i.e. the graph represents reflected power signal from the concrete slabs. There are different depths measured such as 5cm, 10cm, 15cm, 20cm and 25cm. Figure 3.30 shows results of the penetration depth by adding concrete slabs. There is a significant change in the amplitude of the signal across the frequency range between 2GHz and 6GHz. This change was caused by increasing concrete slabs as the microwave reflected energy has decreased by a similar amount (approximately 3dBm) while the concrete layers have increased. There was no further changed when additional slabs were placed.

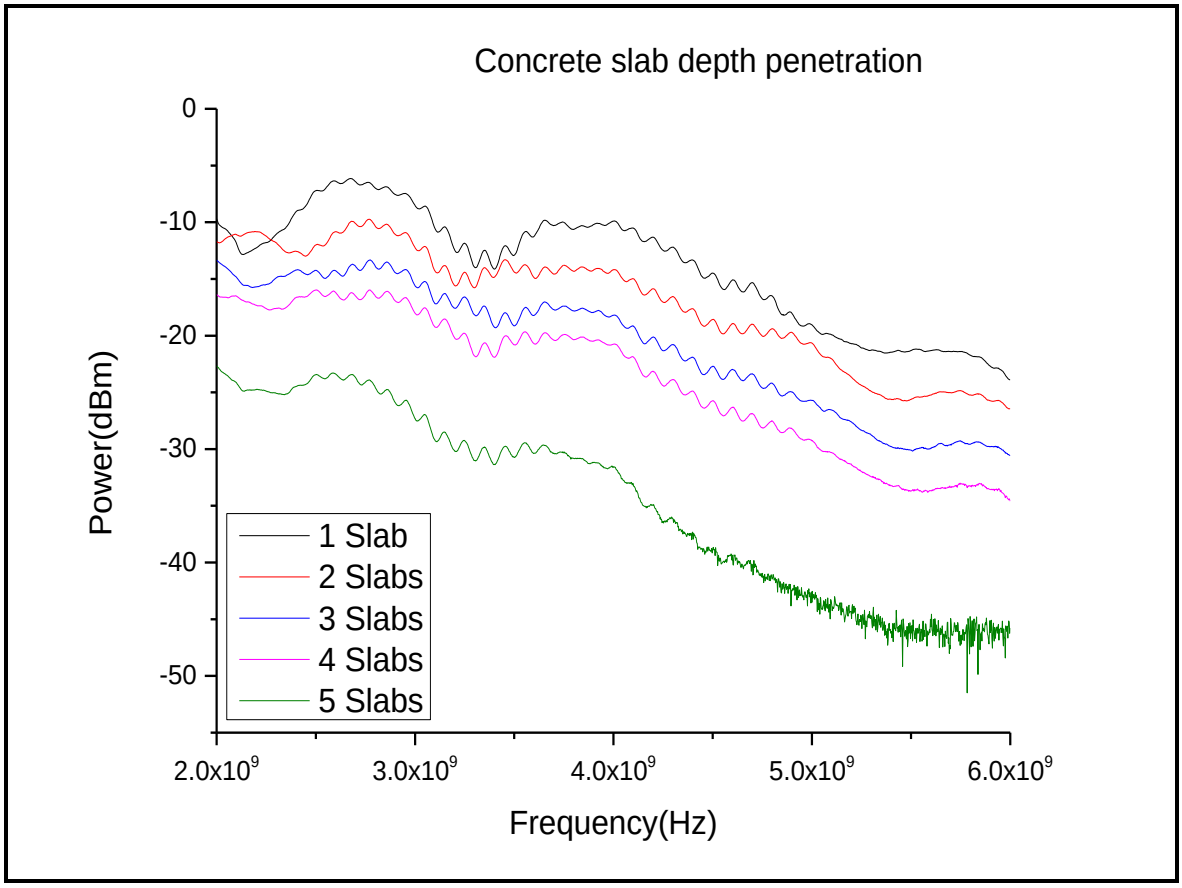

Figure 3.30. Concrete slabs penetration depth.

This experiment was undertaken to confirm the penetration depth of the single horn antenna by increasing the amount of the concrete slabs. Results shows that there is a significant change in attenuation of EM signal at frequency between 2GHz to 6GHz. Results from this experiment illustrated that the horn antenna penetration depth is approximately 25cm. However, the thickness of the common building fabrics is less 25cm and to avoid an interference of an EM signal with external environment, which would lead to false results it

was essential to concentrate the EM signal within the measured building material. Therefore, an additional experimental work will be conducted using two horn antennas.

3.6.2. Concrete Slabs Penetration Depth with Two Horn Antennas

To concentrate the EM wave spectrum within building fabrics, it was required to distinguish an angle between transmitter and receiver. Experimental setup (Figure 3.31) comprises two horn antennas with various angles (15, 33 and 45 degrees) directed to the concrete blocks with a 2cm air gap (contactless measurement) and connected to the PC via VNA for data acquisition using LabVIEW GUI. The measurements were taken from 19cm and 23cm thick concrete blocks.

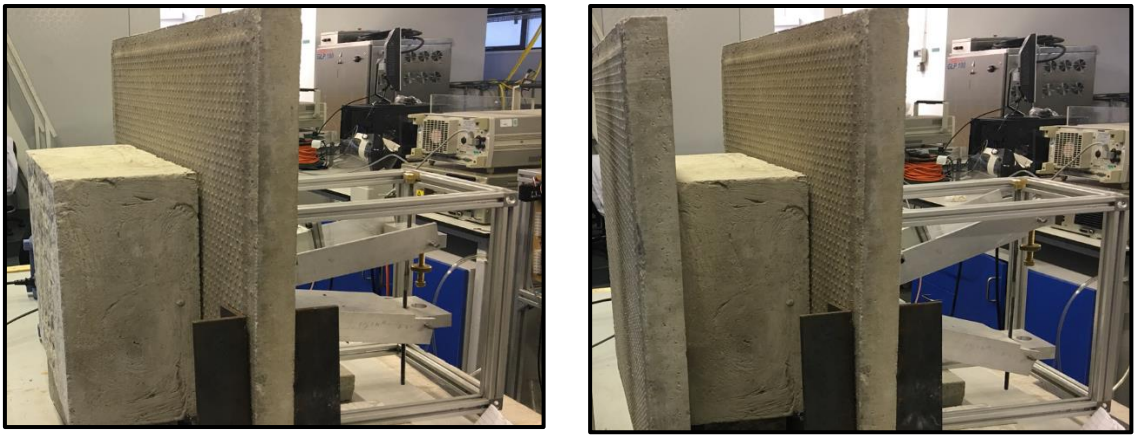

(a) (b)

Figure 3.31. Experimental Setup to determine suitable angle between transmitter and receiver (a) 19cm concrete thickness (b) 23cm concrete thickness.

The measurements are provided by S-Parameter, i.e. a reflected power from the concrete blocks. The spectrum is transmitted to the concrete block from the top horn antenna and the reflected power from the concrete blocks is received by the bottom horn antenna. The results from this experiment are shown in Figure 3.32, i.e. a reflected power from 19cm and 23cm concrete blocks with three different angles, namely 15, 33 and 45 degrees. The results demonstrate that there is a noticeable amplitude change of the spectrum around 4.5GHz with 15 degrees between 19cm and 23cm concrete blocks. This means that the penetration depth of the horn antennas with 15 degrees' angle is greater than 19cm, which would cause an interference of the EM spectrum with an external environment and provide false measurements. However, the thickness of the concrete blocks did not have any impact on

the EM signal with 33 and 45 degrees' angle. Thus, the 33 degrees' angle was selected for this investigation.

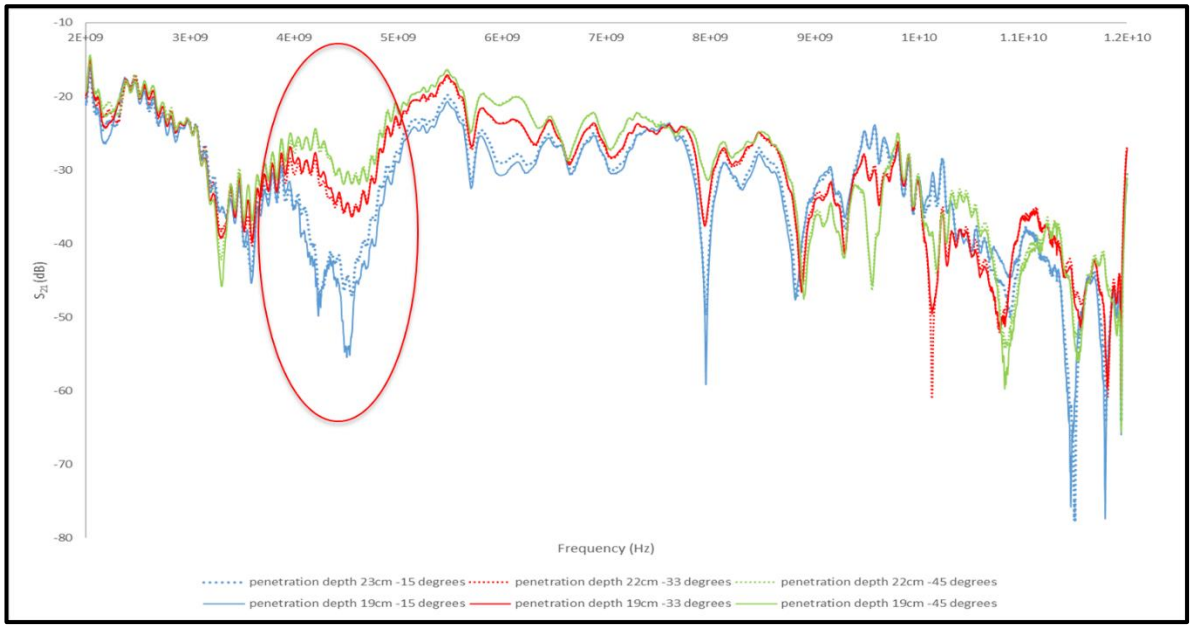

Figure 3.32. Averaged data from the EM sensor with 15, 33 and 45 degrees angle between transmitter and receiver.

3.7. Summary

The fundamental parameters of the antennas were identified and reviewed. Types of antennas have discussed. The pyramidal horn antenna was selected to determine moisture content in building fabrics. The reason for this choice is high penetration depth and high gain which enable to penetrate the building materials. The mathematical model for the performance of the sensors used was evaluated and simulated using HFSS package. Once the model was completed, the antennas simulation shows good response for return loss, total gain and overall performance sensors have been constructed and tested. The pyramidal horn antennas have been purchased from an external supplier. Preliminary experiment for dielectric properties of building materials as well as theoretical model of designed sensor gives a promising results. Undertaken experiment shows the potential of microwave spectroscopy to non-destructive measurements of building fabrics. Further tests will be undertaken and presented in Chapter 4.

Chapter 4 Identification of Building Materials and Foreign Objects

This chapter provides a methodology, results, data analysis and discussion on identification of building materials and foreign objects within structures. Different building materials (e.g. bricks, ash blocks etc.) and foreign objects (e.g. water pipelines, metal, timber and etc.) within a building structure can interfere with an electromagnetic (EM) signal and cause faults in measurements. Thus, it was essential to investigate an effect of different building materials and foreign objects on an EM signal.

Section 4.1 consists of experiments to check whether the microwave spectroscopy will detect foreign objects behind the common building materials. Section 4.2 shows the experiment to determine the location of the foreign object behind the building fabric material. Section 4.3 considers experimental work to determine different building materials.

4.1. Identification of Foreign Objects

This experiment was undertaken to identify different types of foreign objects that could be found within building materials. Foreign objects have to be taken into consideration during electromagnetic (EM) measurements as they could affect the microwave spectrum and cause the false readings.

4.1.1 Methodology

Microwave sensor was connected to the Marconi 6200 microwave test kit and Laptop interface to record the captured data. The frequency range during this experiment was setup between 6GHz and 12GHz. Different foreign objects namely steel rod, timber, concrete block, plastic container filled in with water and air gap were placed behind building fabric materials such as plasterboard, cork board and ceiling plasterboard. The microwave sensor was placed 20mm away from the measured building material and 90mm from a foreign object. The block diagram of the experimental setup is shown in Figure 4.1.

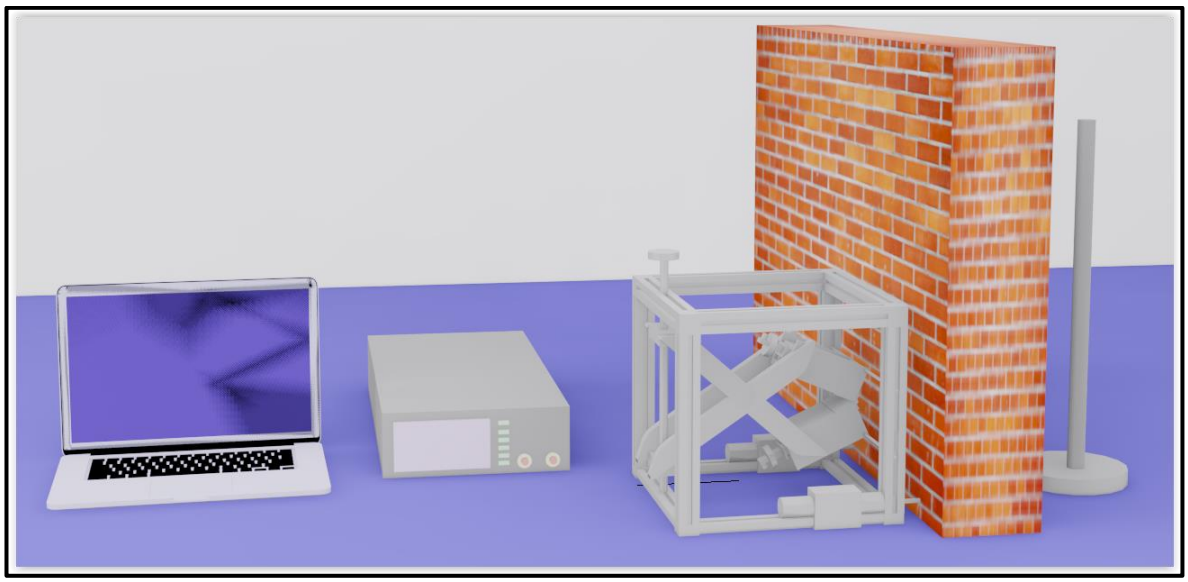

Figure 4.1. Foreign Objects identification block diagram.

4.1.2 Results

Foreign object identification test results are presented in Figure 4.2. The frequency range of the measurements in this experiment is between 6-12 GHz, which is equivalent to the electromagnetic wavelengths between 5-2.5 cm. The measurements were provided by S-parameters namely S_{21} i.e. the graph represents received reflected power signal from the measured material. There are significant changes in the microwave spectrum when different objects are placed behind the plasterboard. The reason for changes is the different dielectric properties of the tested materials, their shape and their size. Microwave signal is transmitted from the top horn antenna and travels through the air into the material, depended on dielectric properties of that material and its absorbance, a part of the signal will be reflected back and part of the signal will go through the material to the air and into the foreign object where another part of the signal will be reflected. Reflected microwave wavelengths will be measured by the second horn antenna. Cut off frequency for this horn antenna is 6.7GHz this is the reason of high noise level at the frequency range between 6GHz to 6.7GHz. The power level for plastic tube with water is between-30dBm to -35dBm at 8GHz, as water absorbs the microwave signal. Metal pipe is reflecting microwave power at approx. 8GHz. Concrete block absorbs microwave spectroscopy at approx. 9GHz the power level is around -32.5dBm. Wood absorbs microwave spectroscopy at approx. 10GHz the power level is around -37.5dBm.

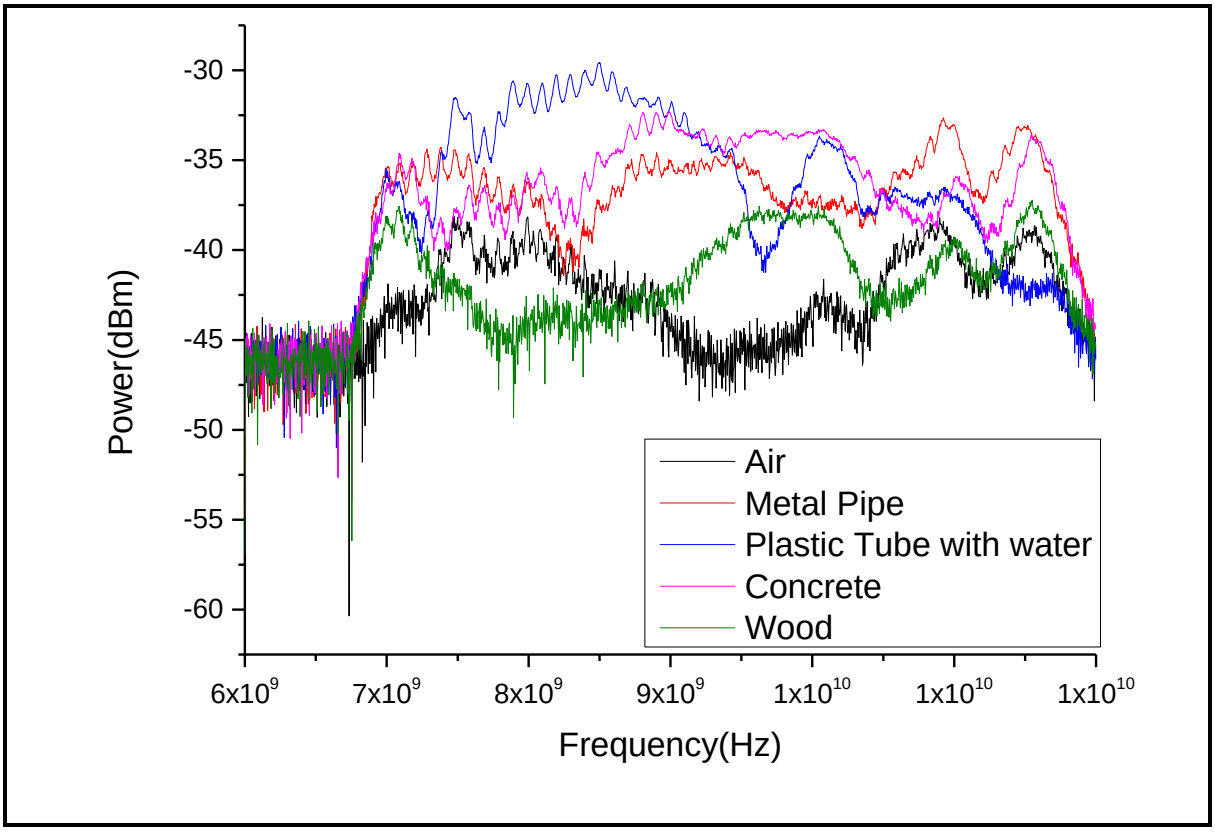

Figure 4.2. Foreign objects identification behind plasterboard.

Figure 4.3 shows results with different objects such as a metal pipe, a plastic container filled with the water, a concrete block, a wood and an air gap placed behind cork board. The purpose of this experiment was to validate if the microwave technique is able to distinguish different surfaces of a wall. The main difference between two materials is dielectric constant and chemical composition, which as a consequence affects microwave spectrum. Therefore, the same object behind different materials will have different EM signature. This is confirmed throughout the results shown in Figure 4.3.

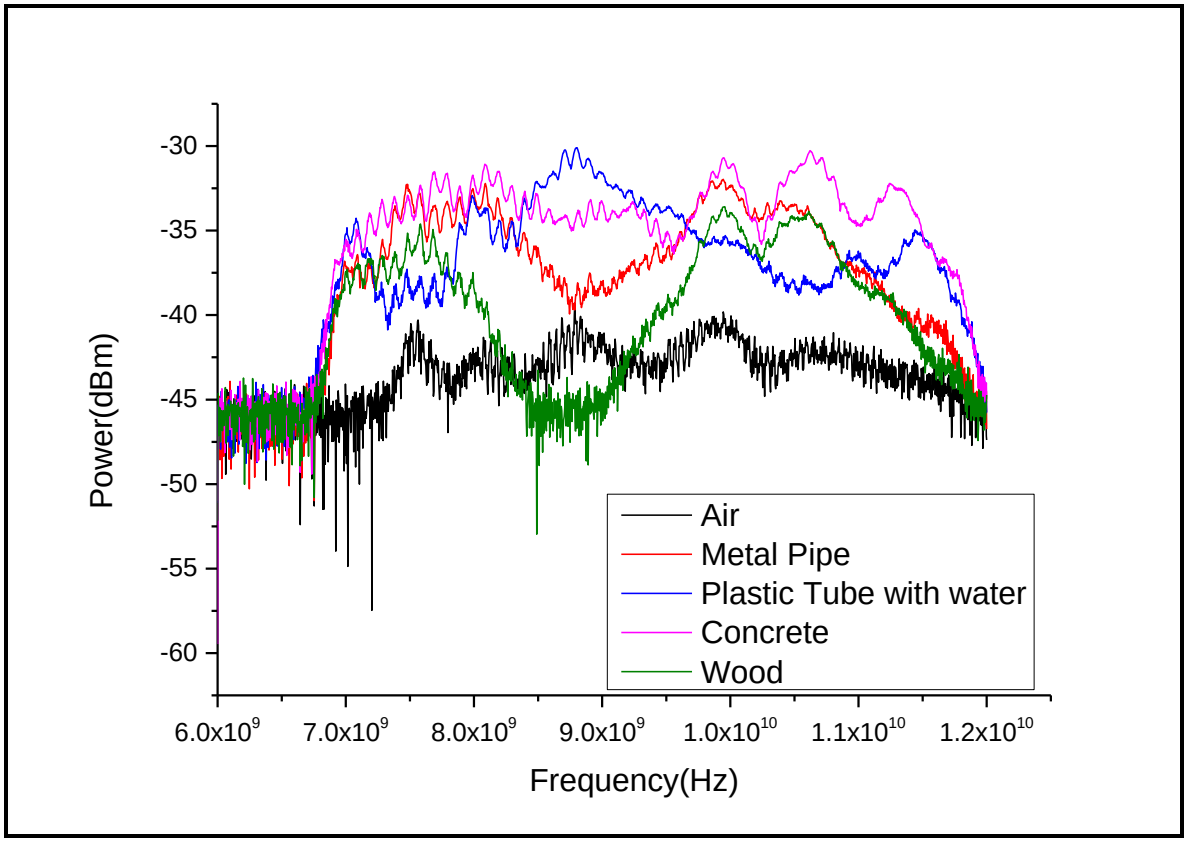

Figure 4.3. Foreign objects identification behind cork board.

Figure 4.4 presents the foreign objects identification test behind ceiling plasterboard material. As can be seen from Figure 4.4 there are still significant changes in the microwave spectrum when ceiling plasterboard is used for measurement. The foreign objects characteristics is similar to Figure 4.2 and Figure 4.3 which enable to justify the microwave characteristic for all independent foreign objects.

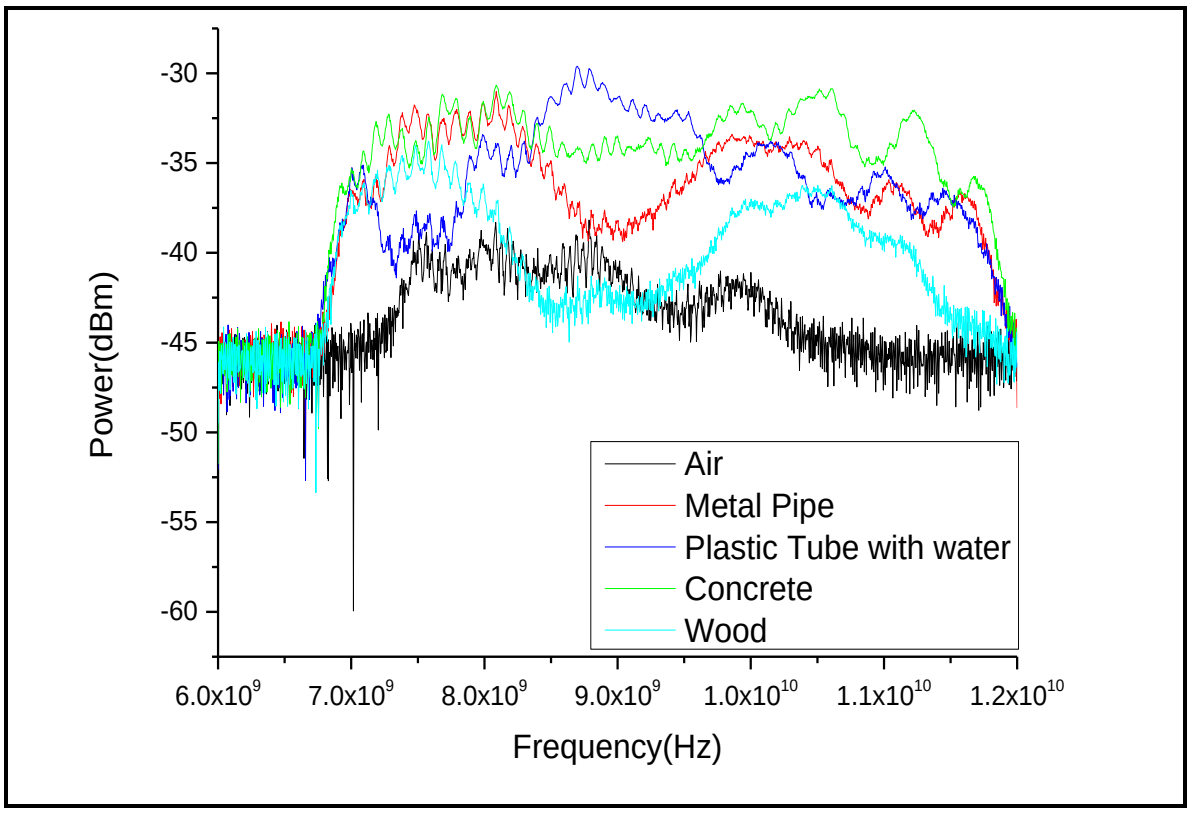

Figure 4.4. Foreign objects identification behind ceiling plasterboard.

Figure 4.5 illustrates the measurements taken using wide band horn antennas to determine foreign objects behind the plasterboard. The measurements were repeated three times then averaged. Results show a clear distinguish between foreign objects at frequency range between 6GHz to 12GHz.

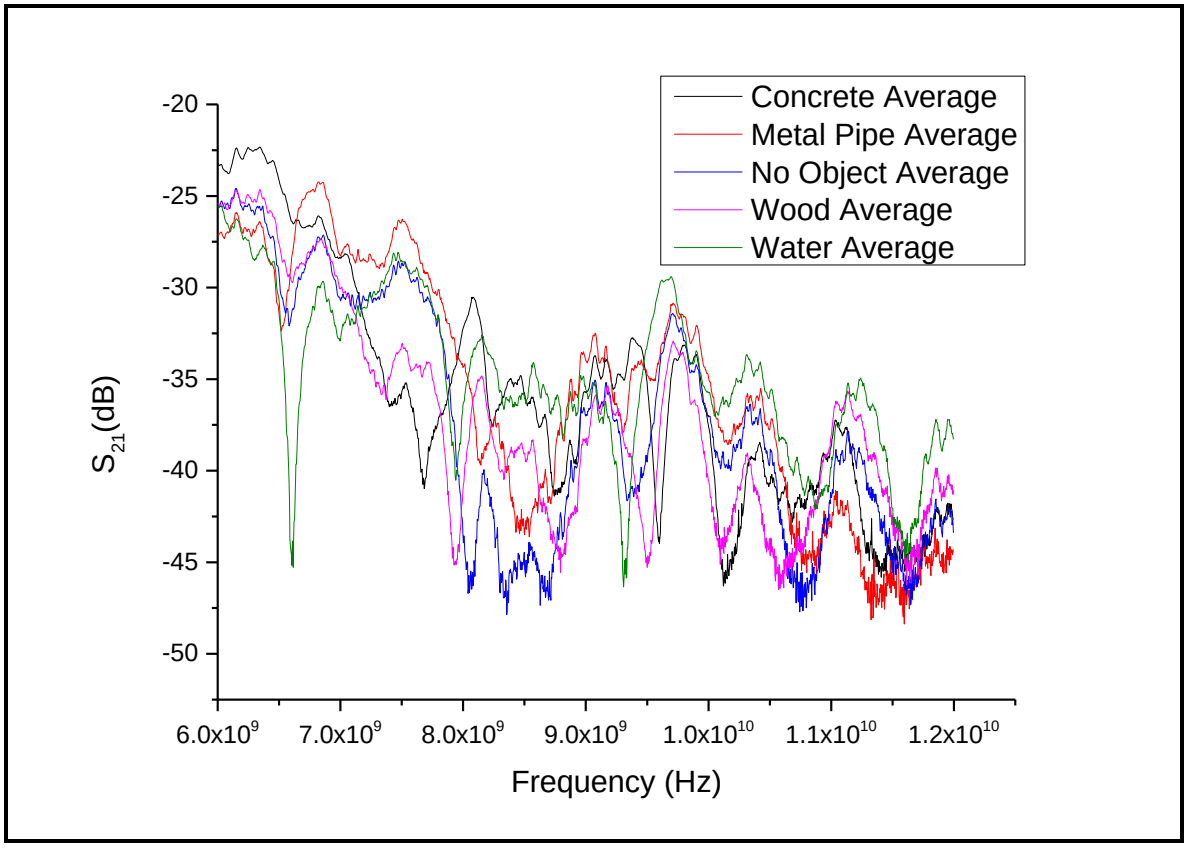

Figure 4.5. Foreign objects identification behind plasterboard using wideband horn antennas.

4.1.3 Analysis

Microwave spectrum was analysed to determine the possibility to predict the foreign object behind the specific material. The Pearson product-moment correlation coefficient was used to prove the symmetry of spectrum received from the measurement of foreign object. Pearson's correlation coefficient returns a value between -1 and 1, where -1 means that there is a strong negative correlation and 1 means that there is a strong positive correlation. Pearson product-moment correlation coefficient formula is presented on Equation 19.

$$r = \frac{n(\sum xy) - (\sum x)(\sum y)}{\sqrt{[n\sum x^2 - (\sum x)^2][n\sum y^2 - (\sum y)^2]}} \quad \textbf{(19)}$$

Figure 4.6 shows the LabVIEW software developed to analyse real-time microwave spectrum and provide the type of material and foreign object based on Pearson correlation.

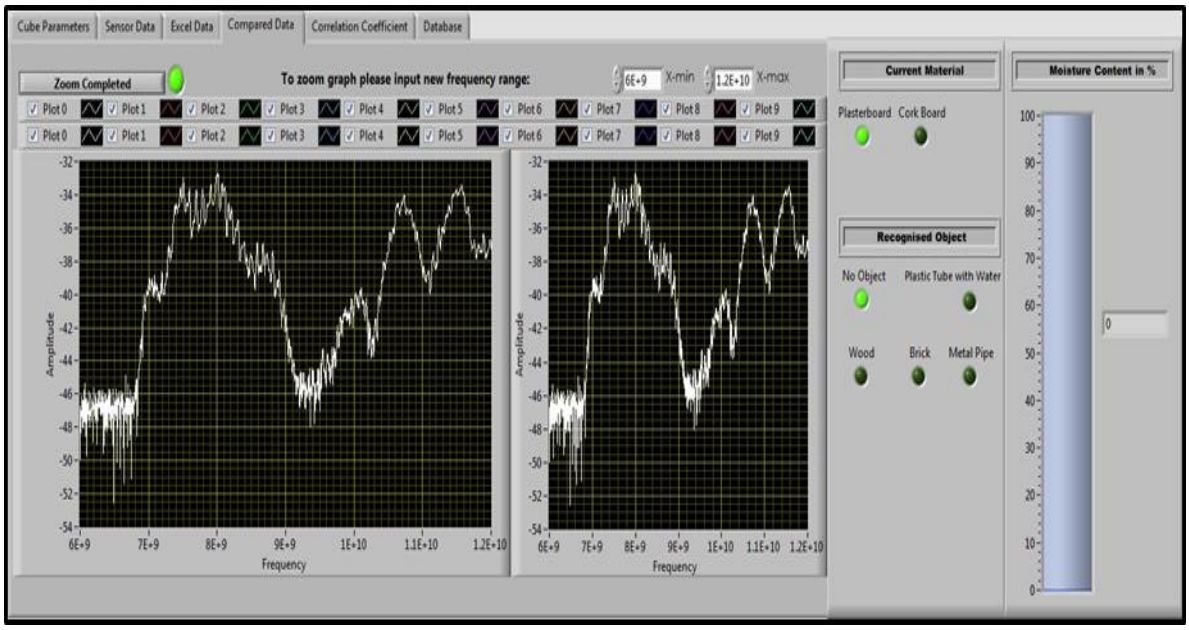

Figure 4.6. LabVIEW Graphical User Interface.

Further data analysis was completed using Principal component analysis (PCA) to determine different foreign objects behind the plasterboard. PCA is a statistical technique that has found application in fields such as face recognition, image compression, and is a common technique for finding patterns in data of high dimension by reducing the amount of the variables (Smith 2002). PCA model was created based on repeatability n=4 using Matlab®. The amplitude changes at 8.5GHz was selected as an optimal frequency to develop the prediction model owing to the repeatability of the dataset. The data was imported into Matlab software and PCA algorithm was applied to create a prediction model. Figure 4.7 presents PCA model for object identification behind plasterboard using data presented on Figure 4.5. PCA model clearly identify different object behind the plasterboard. Water, concrete and wood are closer to each other than metal pipe owing to absorption of the electromagnetic waves by those objects whereas the latter object reflects the electromagnetic waves. Water has the highest dielectric properties among these objects therefore it is further away. Both concrete and wood have similar dielectric properties however concrete block used during this study had larger dimensions then wood sample. Thus, it absorbs more energy and it is closer to water then the wood sample.

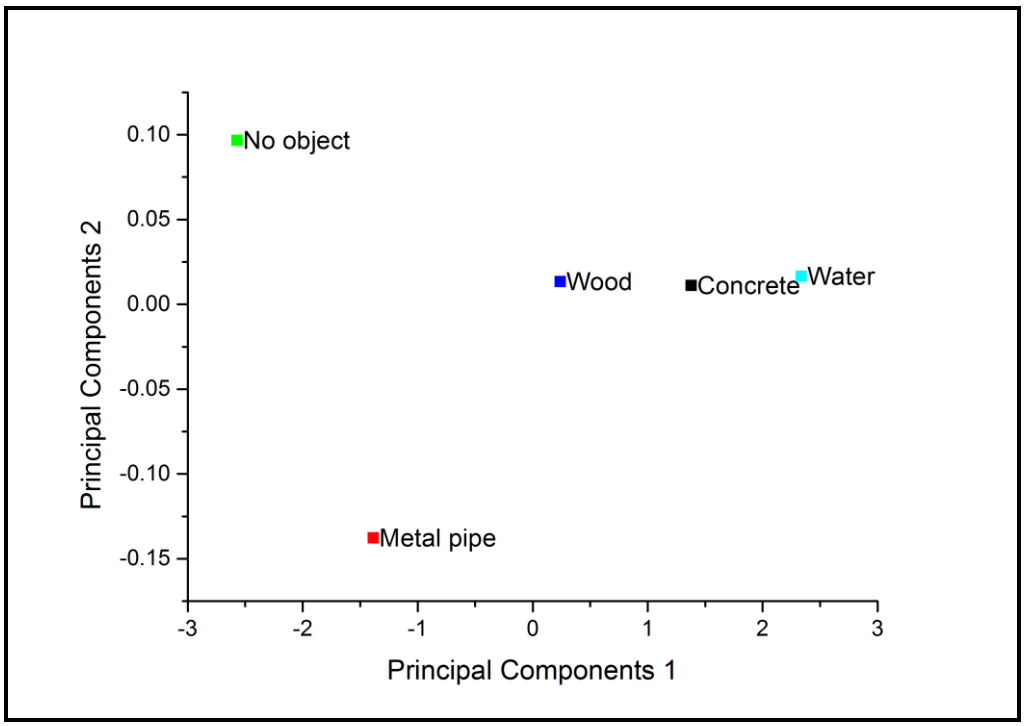

Figure 4.7. PCA model for foreign object detection.

4.1.4 Discussion

Foreign objects identification experiment was carried out to identify if microwave spectroscopy can be used to penetrate throughout building materials namely: plasterboard, ceiling plasterboard and corkboard to determine foreign object behind. The HFSS simulation shows that the position of the foreign object play important role in microwave spectroscopy as there were noticeable changes in the reflection coefficient of the microwave spectrum. Results from the experiment confirms the HFSS simulation (see section 3.4) Different objects as well as different building materials have their own unique microwave characterisation owing to their dielectric properties, shape and possibility to absorb or reflect the microwave waves. To identify the foreign object as well as different material Pearson correlation was used. PCA model was created to predict foreign object behind the plasterboard. Based on the results from this experiment it is necessary to undertake additional experiments to identify the location of the foreign object and identify the type of the building fabrics used in most current structures.

4.2. Foreign Object Location Experiment

In Section 4.1 results show that the microwave spectrum can be affected by the foreign objects. There were significant changes in the microwave spectrum when different objects were placed behind the building materials or when the building material was replaced. This experiment will be undertaken to identify the location of the foreign object. The purpose of this experiment is to find at what distance foreign object will start affecting the microwave spectrum.

4.2.1. Methodology

The location of foreign objects was monitored in real time using a microwave sensor. Linear traverse was used to move objects in precise distances equal to 1cm to monitor changes in the microwave spectrum. The frequency range during this experiment was setup between 6GHz and 12 GHz. Measurements were provided by S-parameters namely S_{21} i.e. the graph represents received reflected power signal from the measured material. Microwave sensor was placed 20mm away from measured material. The experimental setup is presented in Figure 4.8.

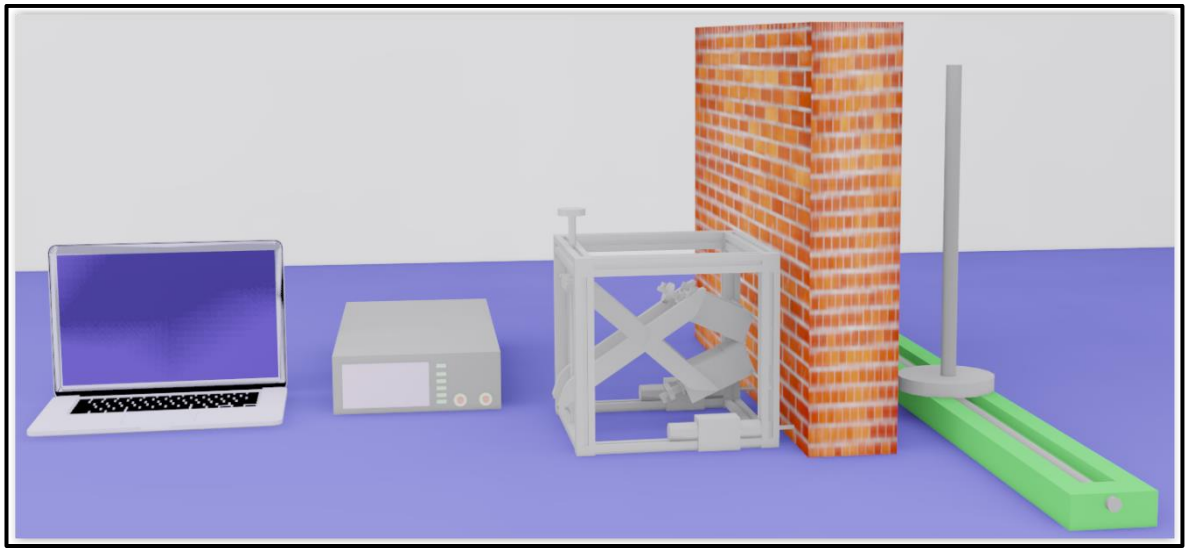

Figure 4.8. Identification of Foreign Object Location block diagram.

4.2.2. Results

It is significant to identify the location of specific objects behind the wall structure such as pipeline and timber construction because it could allow to determine the area with the high level of moisture content which could reduce overall costs of refurbishment. This experiment was undertaken to identify the location of a metal pipe behind the plasterboard. Therefore, this experiment will show how the microwave spectrum is affected by a metal pipe at different positions behind the material. Figure 4.9 presents the results of the test where the steel bar was moving to the left side by 1cm from the centre point of the sensor. Figure 4.10 shows that there is a strong polynomial relationship (R^2= 0.994) between the amplitude shift at 9.7GHz and measured distance. Figure 4.11 presents the results of the experiment where the steel bar was moving to the right side by 1cm from the centre point of the microwave sensor. Data was captured at each stage of the movement. Figure 4.12 shows that there is a strong polynomial relationship (R^2= 0.998) between the amplitude shift at 9.7GHz and measured distance. This shift was caused by the different location of the steel bar that affects the microwave signal reflection angle, which causes different response times that could be used to identify the correct location of the material.

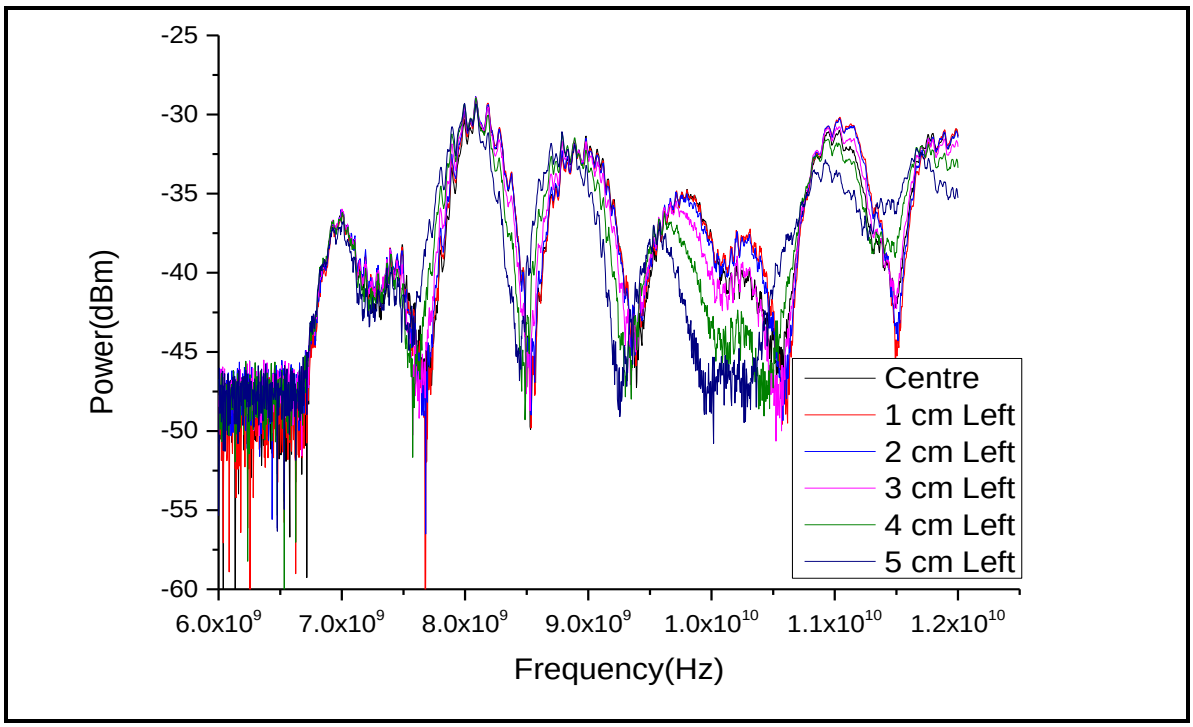

Figure 4.9. Identification of steel bar location- measurement in left direction.

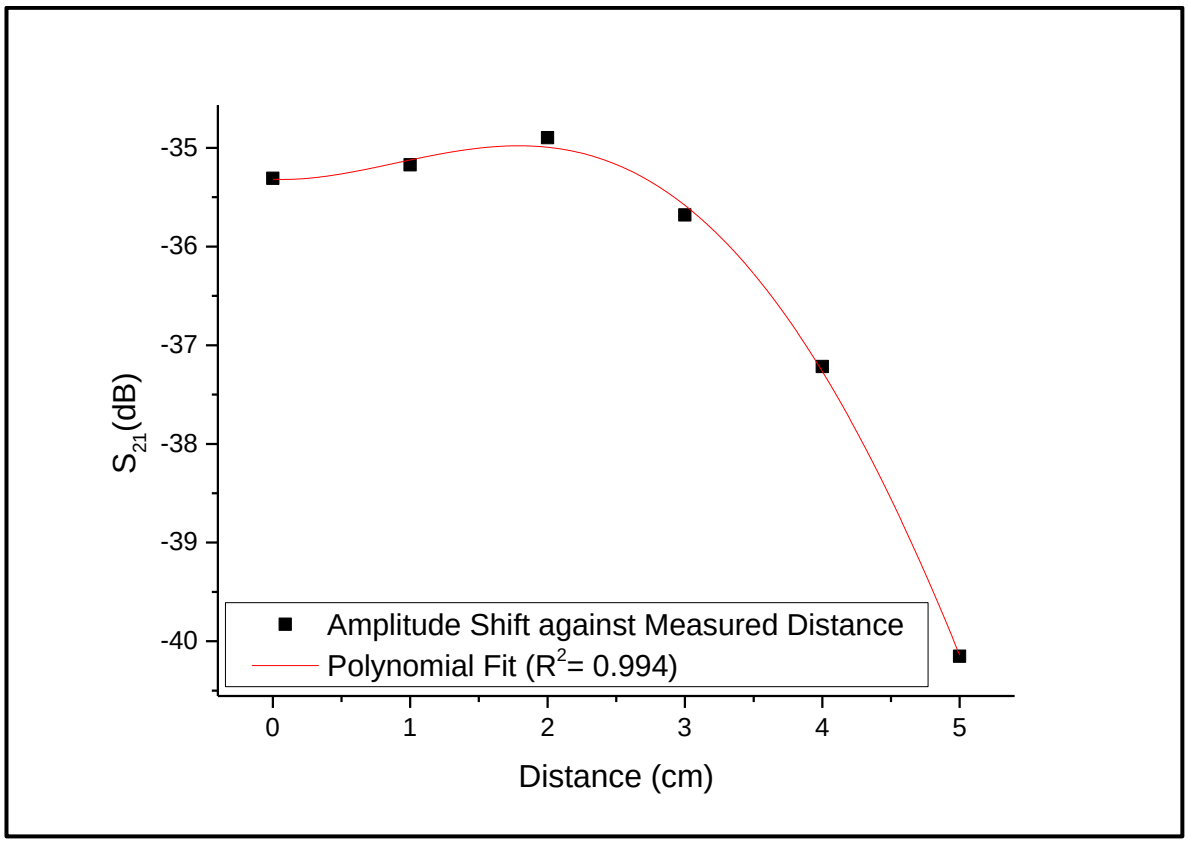

Figure 4.10. Amplitude shift against measured distance to the left at 9.7GHz.

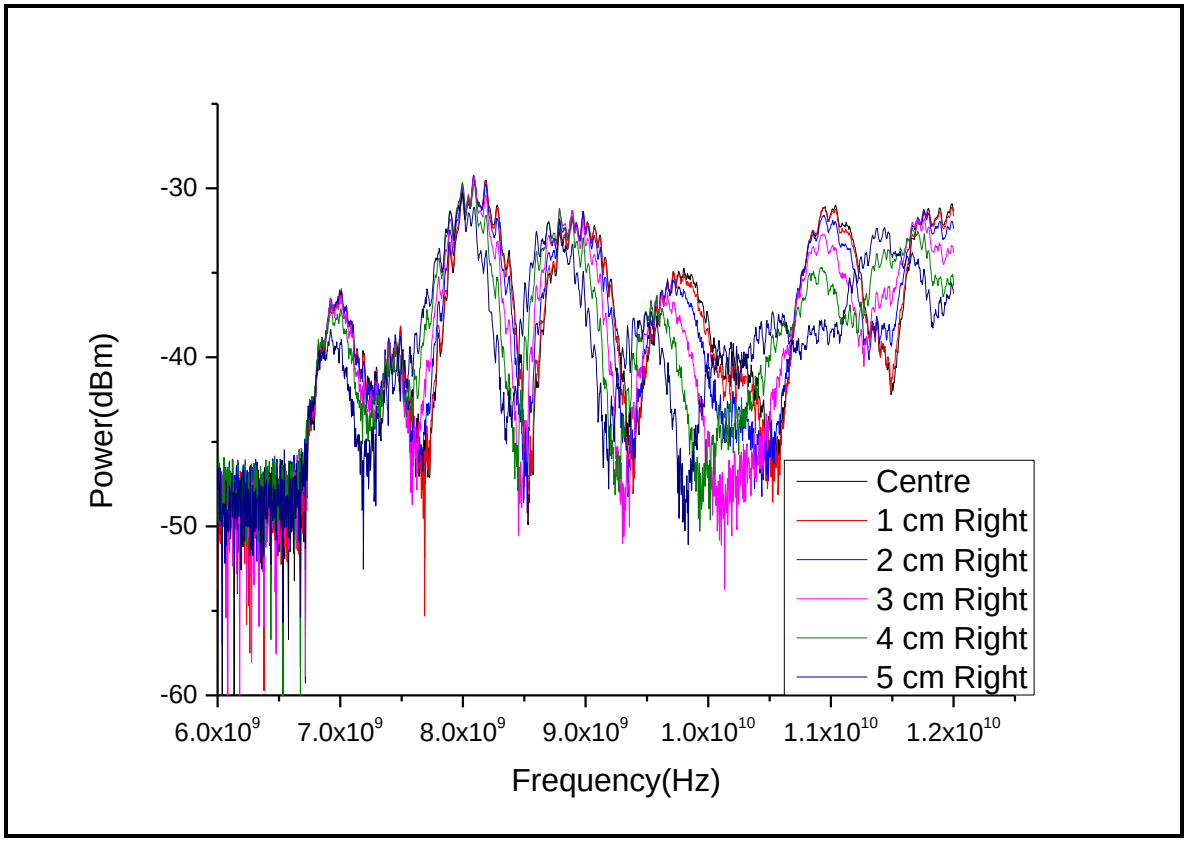

Figure 4.11. Identification of steel bar location- measurement in right direction.

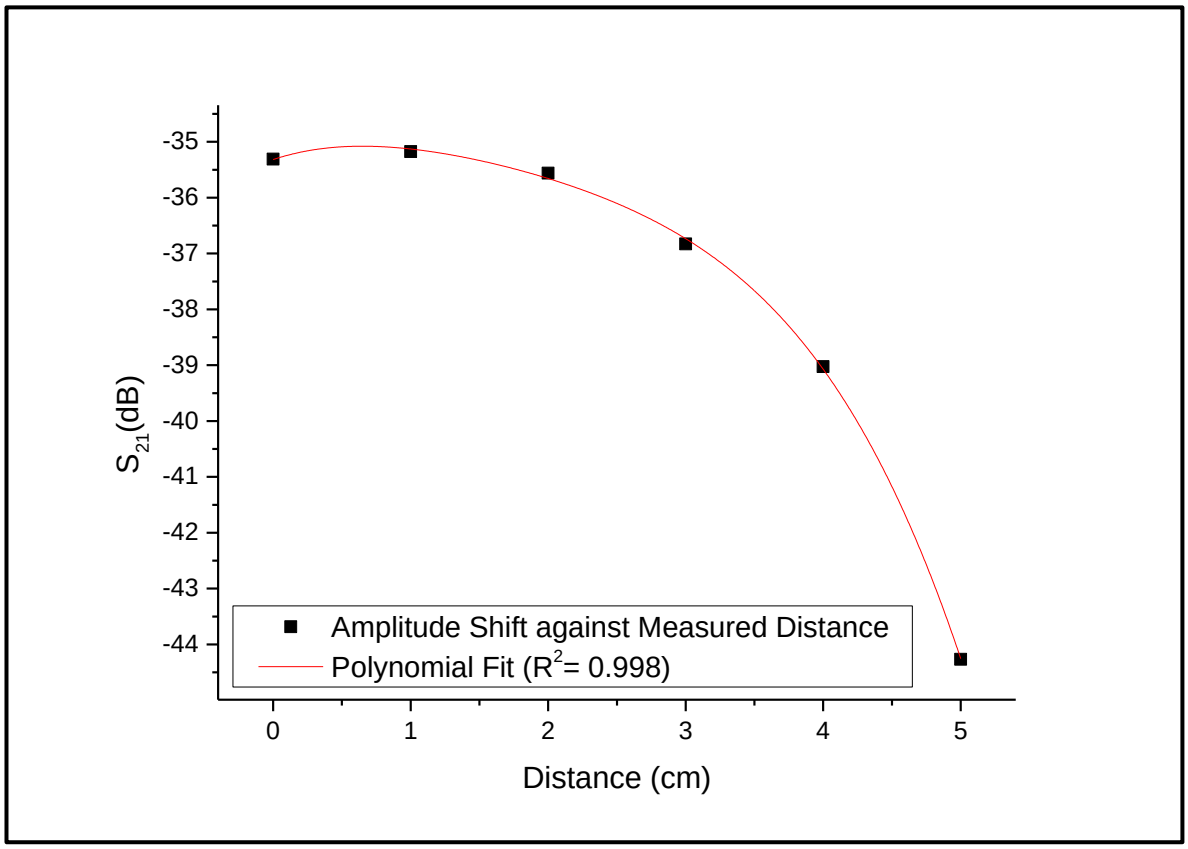

Figure 4.12. Amplitude shift against measured distance to the right at 9.7GHz.

4.2.3. Analysis

Data captured in this experiment was analysed to identify if there is any relationship between measurement of the location to the left and right direction. In both situations there is significant change to the attenuation at 9.7GHz. When the distance between the measured object and centre position increases, the attenuation of EM signal decreases with a polynomial relationship. Figure 4.13 shows the comparison between measurements to different directions. Gathered data enables to distinguish the differences between the directions of the measured material.

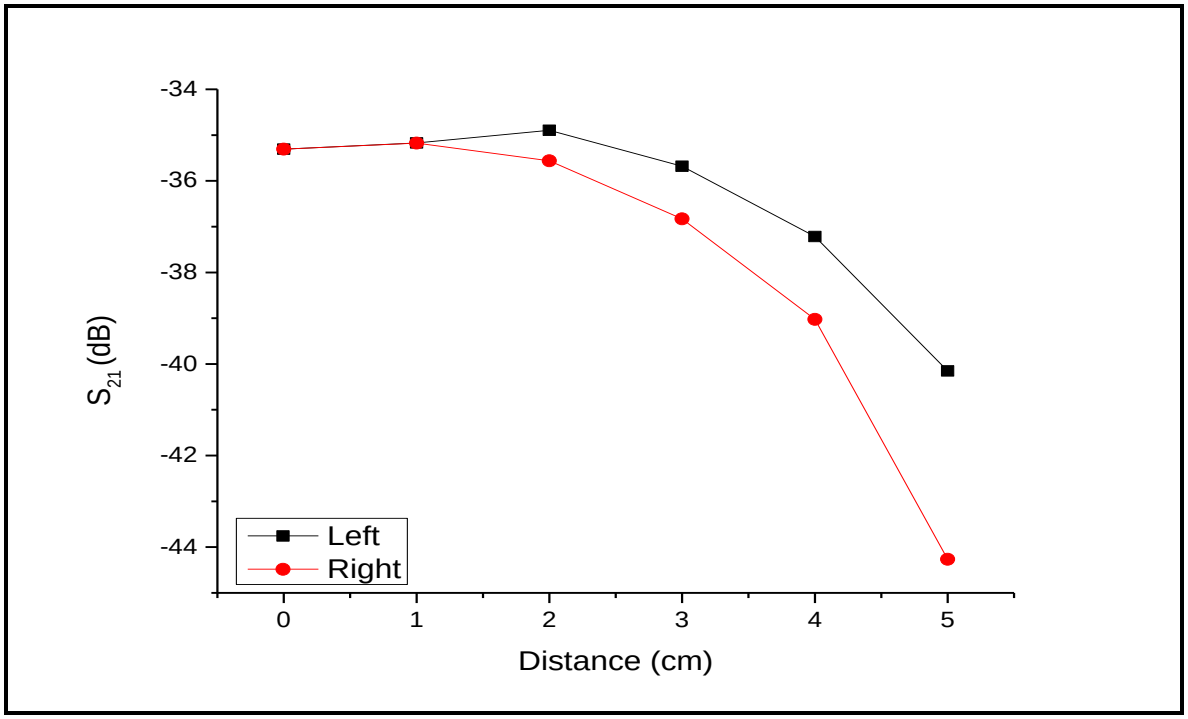

Figure 4.13. Metal pipe movement comparison at 9.7GHz.

4.2.4. Discussion

This experiment was undertaken to confirm if microwave spectroscopy can be used to determine the location of the metal pipe behind the plasterboard. Linear traverse was used to make precise movements which were recorded by self-developed LabVIEW software. Results shows that there is a significant change in attenuation of EM signal at 9.7GHz. Results from this experiment illustrate that the microwave spectrum has a potential use to determine the location of the measured object such as metal pipe. This method will be investigated to identify the location of the reinforcement in the concrete and the results are presented in section 6.3.

4.3. Identification of building fabrics

This experiment was undertaken to identify different building fabrics that are used for building structures. Currently building constructions are made from a variety of materials depending on the building's requirements. Building fabrics has to be taken into consideration during EM measurements as they could affect microwave spectrum and cause false readings.

4.3.1. Methodology

An experiment was conducted to determine different building fabric materials using microwave spectroscopy. It was essential to build in the laboratory environment different types of wall structures from different building fabrics. There were four wall structures built as shown in Figure 4.14: two Brick walls, Ash Block wall and a Dot & Dab wall. All structures were built on special platforms which enables to connect wall structures together namely: Brick to Brick wall or Brick to Ash Block wall. The test was undertaken to identify differences between Brick wall, Ash Block wall, Dot & Dab wall, Brick to Brick wall and Brick to Ash Block Wall. Measurements were provided by S_{21} parameter i.e. the graph represents received reflected power signal from the measured material. The frequency range during this experiment was setup between 6GHz and 12GHz. The EM sensor was placed 20mm in front of the wall surface. Experimental setup is presented in Figure 4.15.

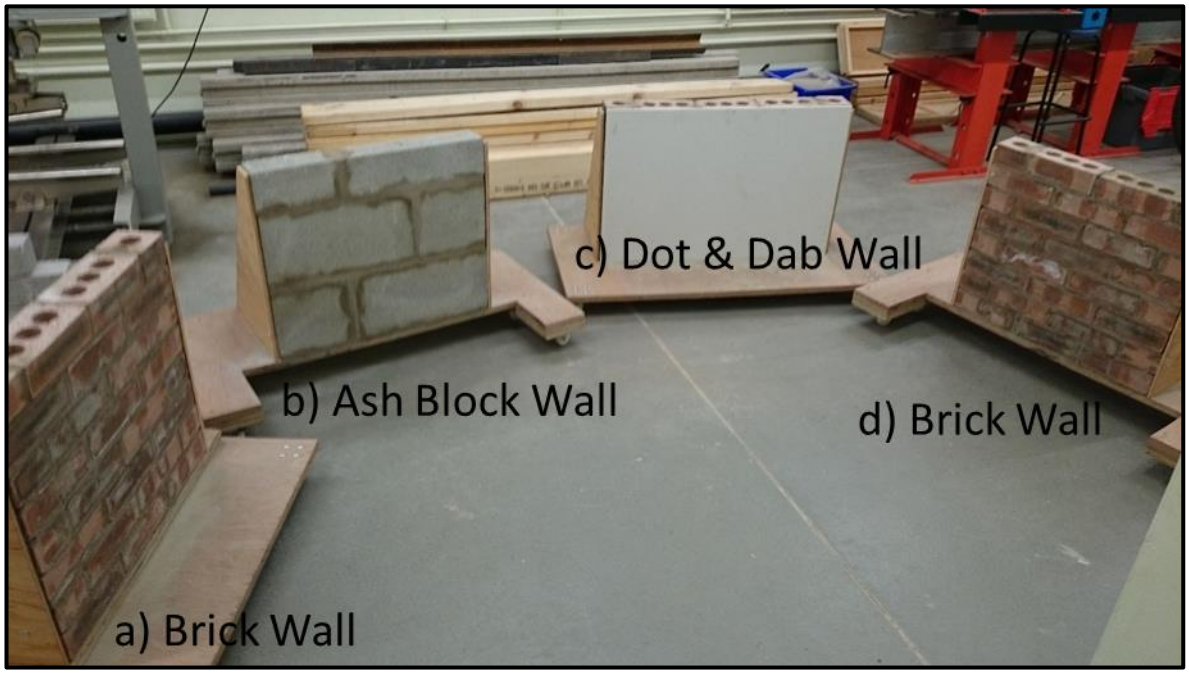

Figure 4.14. Wall structures.

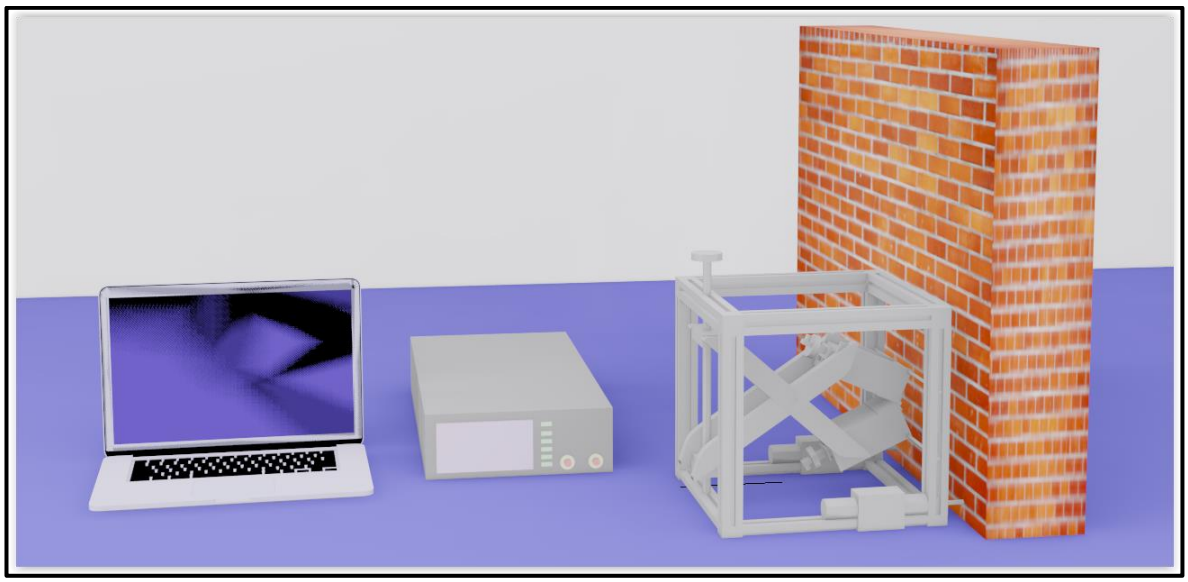

Figure 4.15. Identification of building fabrics experimental setup.

4.3.2. Results

Different building structures such as Ash Block wall, Brick wall, Dot and Dab Brick wall and Brick & Ash Block wall have been used to determine if microwave technology enables to identify different building materials. Results show that the microwave spectroscopy has a significant amplitude shift at frequency between 9GHz and 10GHz, also at that frequency range there are frequency peak shifts due to different chemical and physical properties of the building fabrics. Those properties affect the microwave response which could enable identification of building structures during the test. Figure 4.16 shows the experimental results at the frequency range between 6GHz to 12GHz.

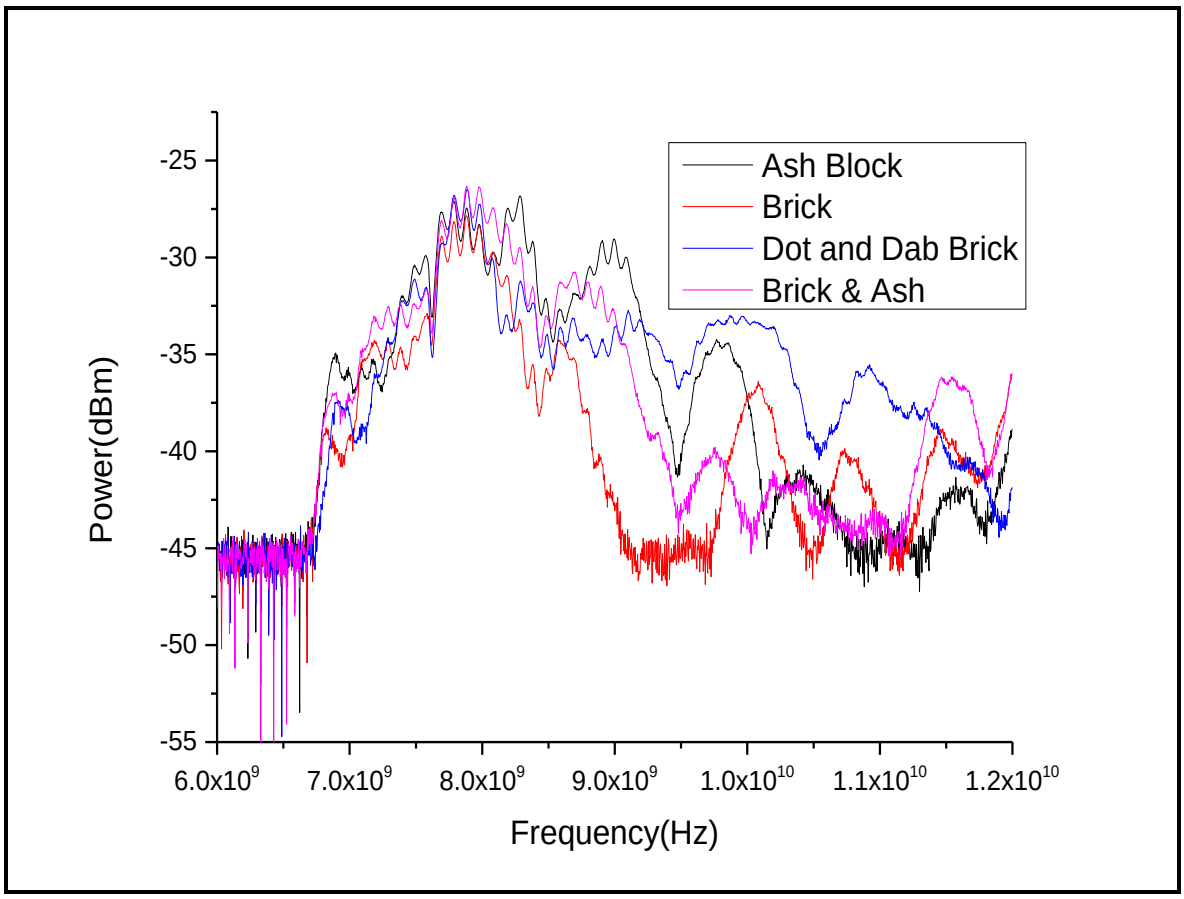

Figure 4.16. Building Structures identification test results.

4.3.3. Analysis

The experimental results in section 4.3.2 show that there is a significant difference in the attenuation of EM wave at 9.48GHz (Figure 4.17). The difference in the attenuation is caused by the dielectric properties of materials and their absorption and reflection of the EM signal. The dielectric properties at 7GHz for the solid brick is 4.6 (Maierhofer & Wsstmann 1998). Autoclaved aerated concrete block has almost three times greater water absorption capacity than clay brick due to its more porous structure (Stojanovic *et al.* 2010). Aerated concrete consists of a cement paste to which a small proportion of aluminium powder is added. During the heating process the aluminium is oxidized producing sufficient hydrogen to aerate the mix into a strong lightweight material. In this case and for small water contents at 3 GHz and 9 GHz the complex permittivity was found to vary between 2-2.5 (Stavrou & Saunders 2003). Brick absorbs approximately -45dB of microwave energy, ash block absorbs approximately -41dB, brick and ash block wall absorbs approximately -43dB and dot and dap approximately -36dB. These results show that the microwave spectroscopy can be used to determine different building materials.

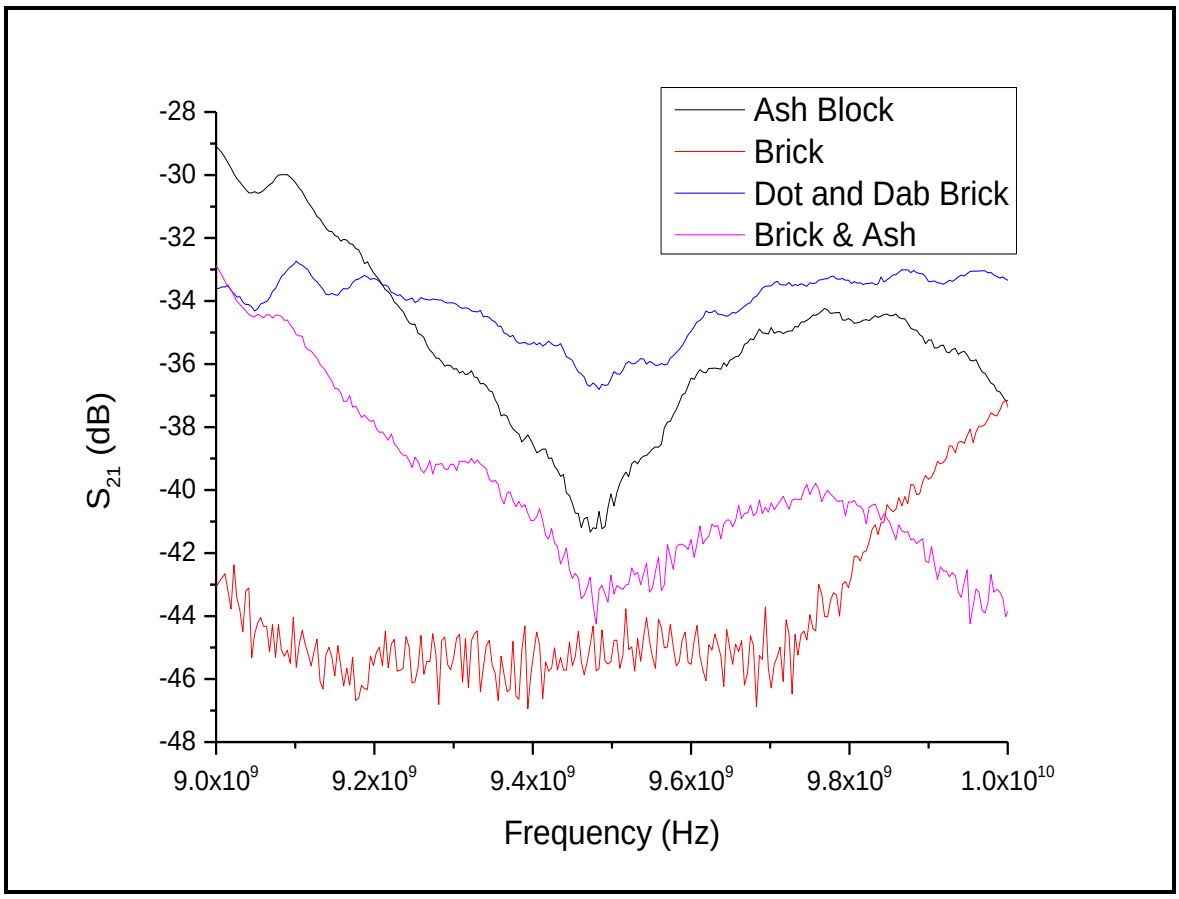

Figure 4.17. Building materials at 9.48GHz.

4.3.4 Discussion

This experiment was undertaken to confirm if microwave spectroscopy can be used to determine different types of building material. The test was undertaken to identify differences between Brick Wall, Ash Block Wall, Dot & Dab Wall, Brick to Brick Wall and Brick to Ash Block Wall. Results show that there is a significant change in the attenuation of EM signal at 9.48GHz. Results from this experiment illustrated that the microwave spectrum has a potential use to identify different building materials.

4.4. Summary

In this chapter a sequence of experimental work to determine location of foreign objects and the detection of different types of building materials was presented. The HFFS simulation showed the potential use of EM waves to determine the location of the measured material. The experimental results confirmed the results from carried out HFSS simulation (see section 3.4). Results from section 4.2.2 shows that there is a significant change in attenuation

of EM signal at 9.7GHz. Results from this experiment illustrated that the microwave spectrum has a potential use to determine the location of the measured object such as metal pipe. Results from section 4.3.2 shows that there is a significant change in attenuation of EM signal at 9.48GHz. Results from this experiment illustrated that the microwave spectrum has a potential use to identify different building materials.

Chapter 5 Monitoring Moisture Content of Building Fabrics

Microwave spectroscopy in Chapter 4 was used to determine different building materials or foreign objects. The results from those experiments are promising, electromagnetic (EM) waves respond to different foreign objects as well as to different building materials. In this chapter experiments will be explored to monitor the moisture content in building fabrics. Moisture content has to be monitored to prevent dampness of building materials and high refurbishment costs. Measurements will distinguish unique microwave spectroscopy for moisture content in monitored materials. Results from this experiments will be used for further analysis. Section 5.1 consists of experiment to check whether the microwave spectroscopy will distinguish moisture content level while monitoring the ceiling plasterboard drying off process. Section 5.2 shows the experiment to monitor the concrete curing process. Section 5.3 considers experimental work to identify the waterproofness of EcoMech Industrial wall material. Section 5.4 shows the experiment to monitor the concrete slab drying off process. Section 5.5 illustrates experiment conducted to monitor concrete behaviour during the drying off process. Section 5.6 shows experiment conducted to monitor concrete behaviour during the drying off process, in a laboratory environment. Section 5.7 summarise results from experiments undertaken to monitor the drying process of different building materials.

5.1. Ceiling Plasterboard drying off

The moisture content of building fabrics is an important parameter in building surveying. To extend the lifespan of the building it is essential to monitor the moisture content of internal and external building fabrics. In experiment microwave spectroscopy will be used to identify if microwave technology could be a potential method to determine moisture levels in the building materials.

5.1.1. Methodology

The preliminary experiment for the measurement of moisture content was conducted with the use of Ceiling plasterboard. The material was soaked in water for two minutes and left

to dry off. The sensor was placed 20mm in front of the material. The weight of the sample and microwave spectrum were recorded every 60 seconds by the program developed in LabVIEW for a period of 24 hours. Figure 5.1 shows the experimental setup used during this experiment.

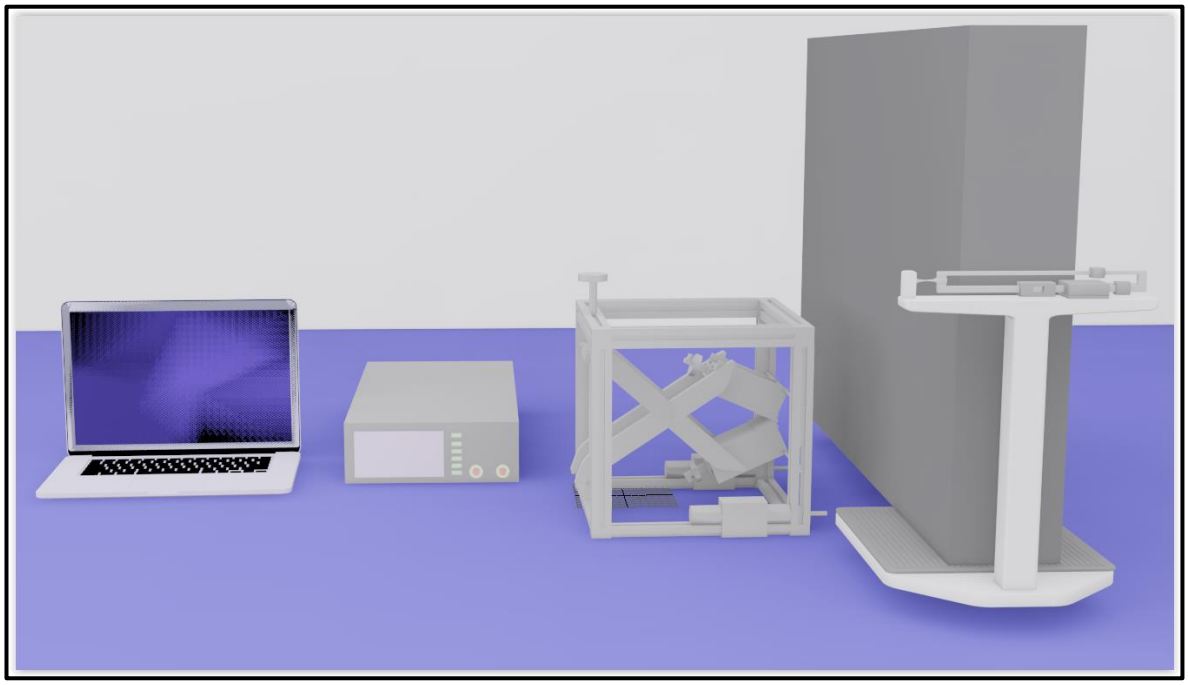

Figure 5.1. Experimental setup of ceiling plasterboard drying off experiment.

5.1.2. Results

Experimental results for drying process of the ceiling plasterboard over 24 hours are presented in Figure 5.2. Microwave spectrum and material weight have been captured once an hour. There is significant amplitude shift across 6GHz to 12GHz frequency range due to the evaporation of the water. Water has high dielectric properties which affects the microwave spectrum. A higher amount of water enables greater power loss of the microwave energy and creates visible changes to the microwave spectroscopy.

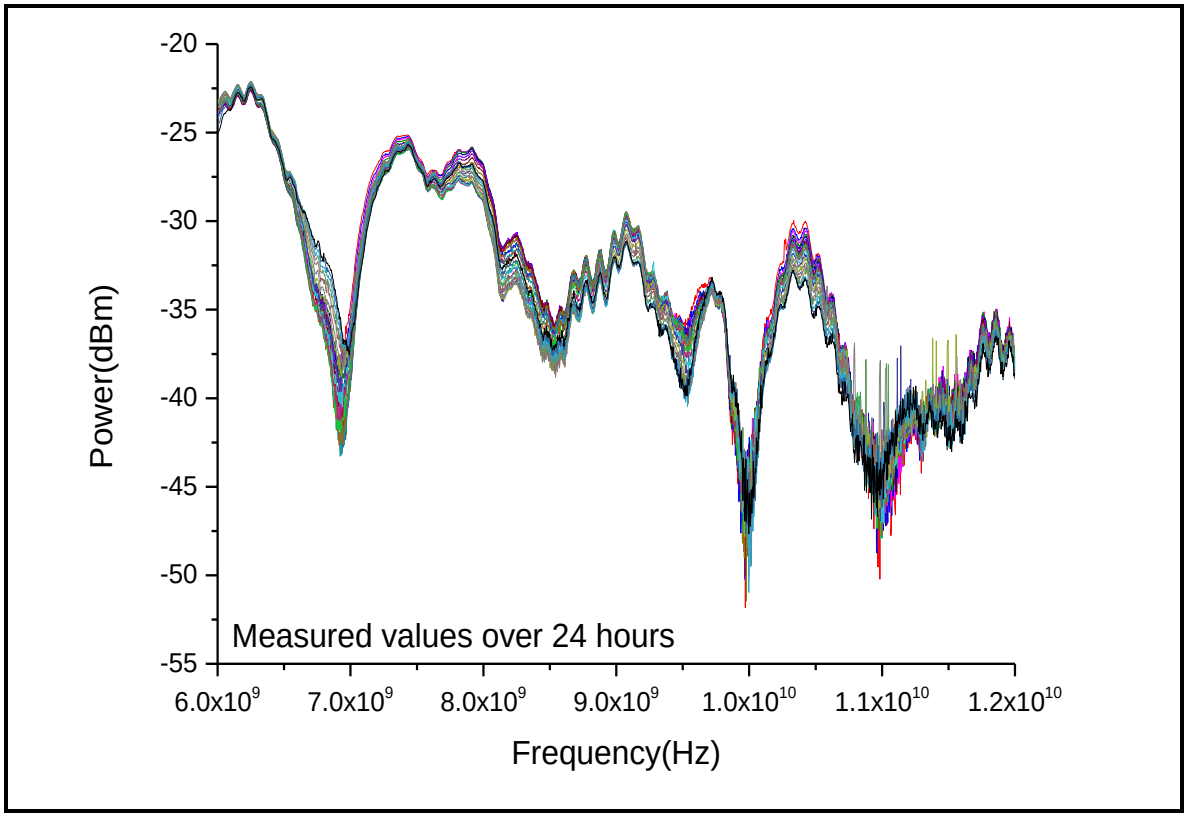

Figure 5.2. Ceiling plasterboard drying process over 24 hours.

Figure 5.3 shows the direct comparison between weight loss and attenuation at 10.3GHz. S_{21} change and material weight loss at the particular frequency decreases linearly ($R^2 = 0.918$) over the period of 24 hours.

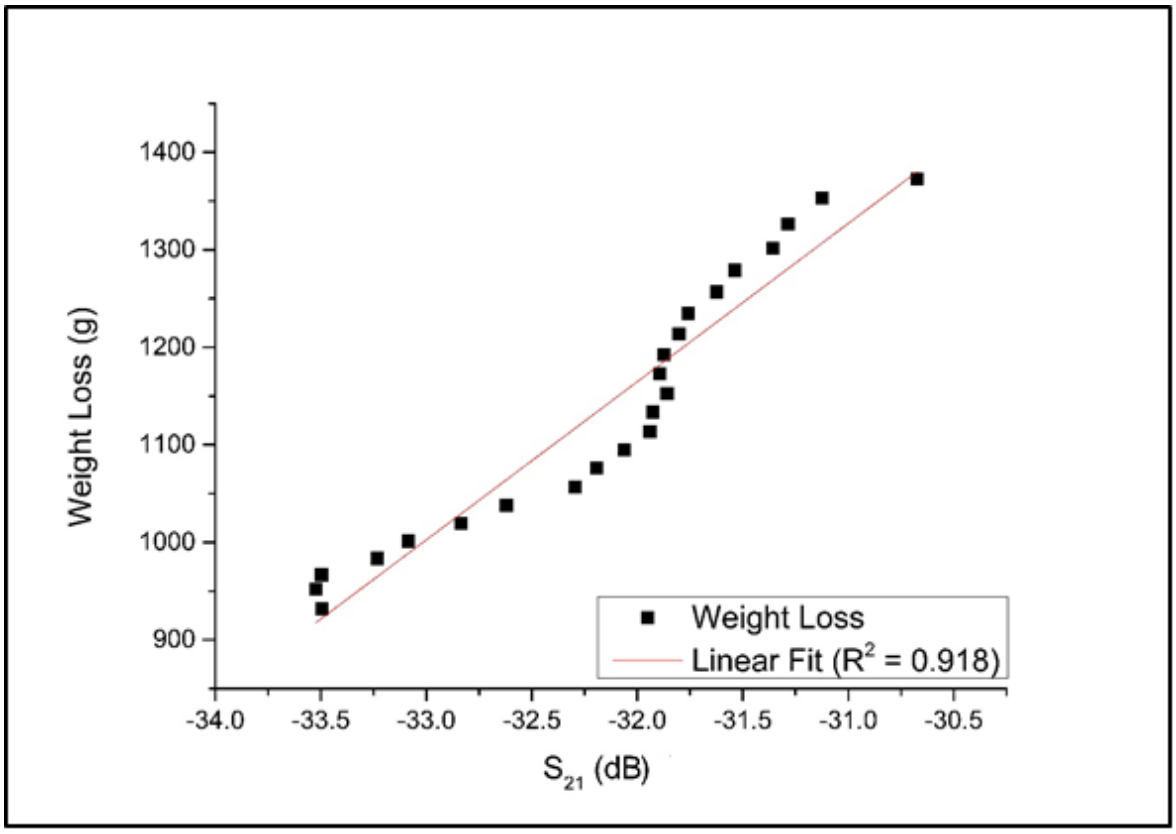

Figure 5.3. Ceiling plasterboard comparison between weight loss and attenuation at 10.3GHz.

5.1.3. Analysis

During drying of porous material, a critical level is defined in such a way that for moisture contents above that level, liquid exists mainly as free water and as only bound water below that level. The energy absorption is low when the moisture content is below critical and the dielectric properties have values close to those of a skeleton porous material. Above the critical level the dielectric properties are much higher and have values that tend towards that of the free water. Hence, the dielectric loss will decrease as the material dries and consequently the effectiveness of dielectric heating or drying reduces as the product dries out. There is a high linear correlation between material weight loss and attenuation at 10.3GHz. Figure 5.4 shows the prediction method using Partial Least Squares Regression (PLSR) which is a technique that reduces the predictors to a smaller set of uncorrelated components and performs least squares regression on these components instead of on original data. PLS regression is mainly used in chemical, drug, food and plastic industries. A common application is to develop the relationship between spectral measurements which includes multiple variables that are often correlated with each other's and chemical

composition or other physio-chemical properties (Minitab 2016). Two model were calibrated for both EM attenuation and moisture content, The EM attenuation model has good accuracy, with $R^2 = 0.892$ and Root Mean Square Error of Prediction (RMSEP) = 3.97g for the validation set.

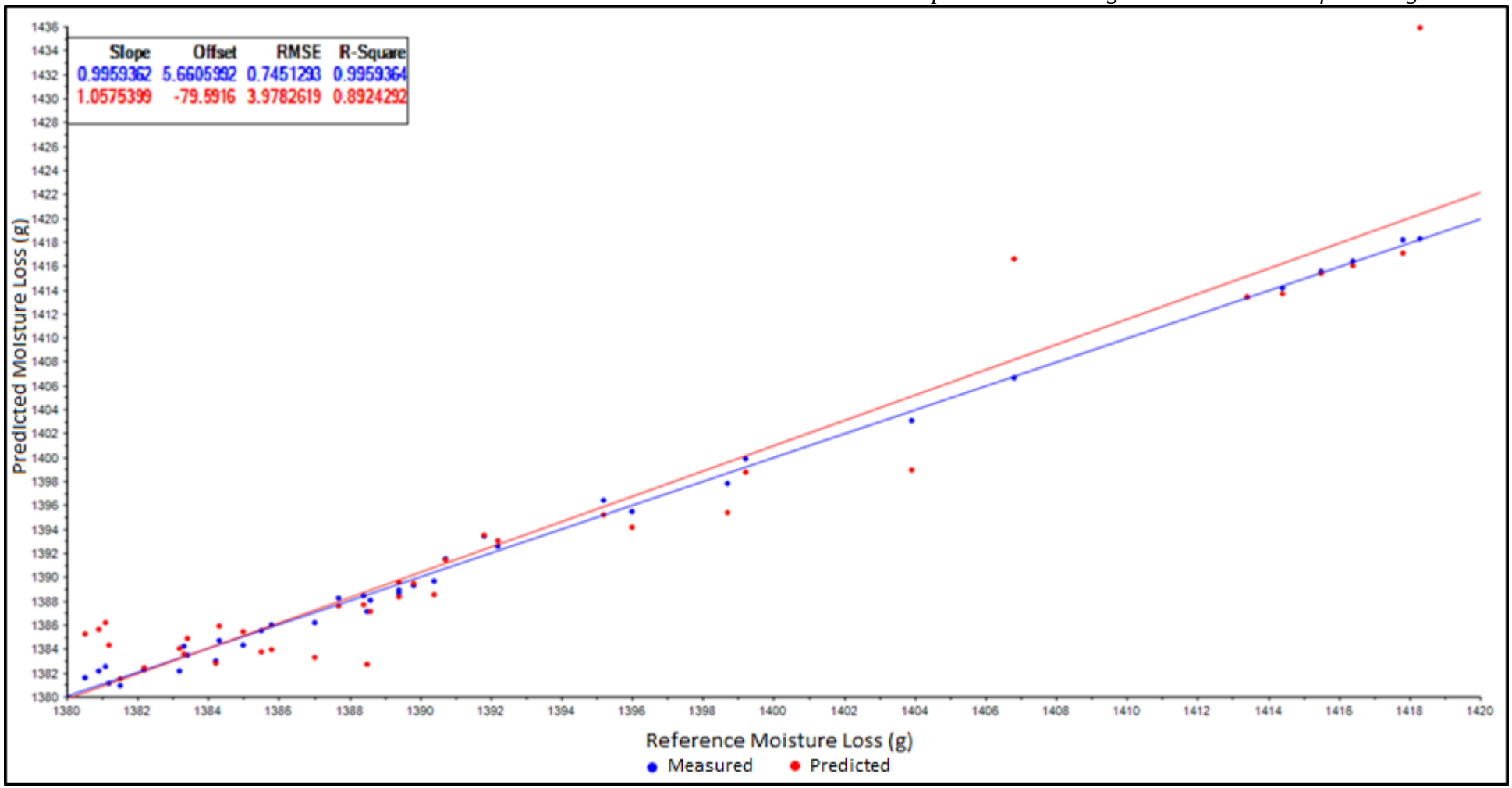

Figure 5.4. Measured and predicted moisture loss from electromagnetic wave sensor.

5.1.4. Discussion

This experiment was undertaken to confirm if microwave spectroscopy can be used to determine the moisture content of the ceiling plasterboard during the drying off process. Results shows that there is a significant change in attenuation of EM signal across 6GHz to 12GHz frequency range while the water evaporates from measured material. There is a high linear correlation between material weight loss and attenuation at 10.3GHz. The prediction model using PLS method has good accuracy, with $R^2 = 0.892$ and Root Mean Square Error of Prediction (RMSEP) = 3.97g for the prediction set.

5.2. Concrete Curing Process

This experiment was conducted to monitor concrete curing process. The purpose for this test was to identify if EM sensor could monitor water evaporation from concrete. Curing has strong influence on the properties of hardened concrete. Adequate curing will increase durability, strength, water tightness, abrasion resistance, volume stability, and resistance to freezing. Exposed slab surfaces are especially sensitive to curing as strength development and freeze-thaw resistance of the top surface of a slab can be reduced significantly when curing is defective (Kosmatka *et al.* 2003).

5.2.1. Methodology

This experiment was undertaken while concrete flat roof was being built. A microwave sensor was placed 20mm under the concrete roof structure to monitor in real time the curing process of the wet concrete over twenty-eight days, data was recorded every 30 minutes. The frequency range during this experiment was 6GHz to 12GHz. Figure 5.5 shows the experimental setup of this test.

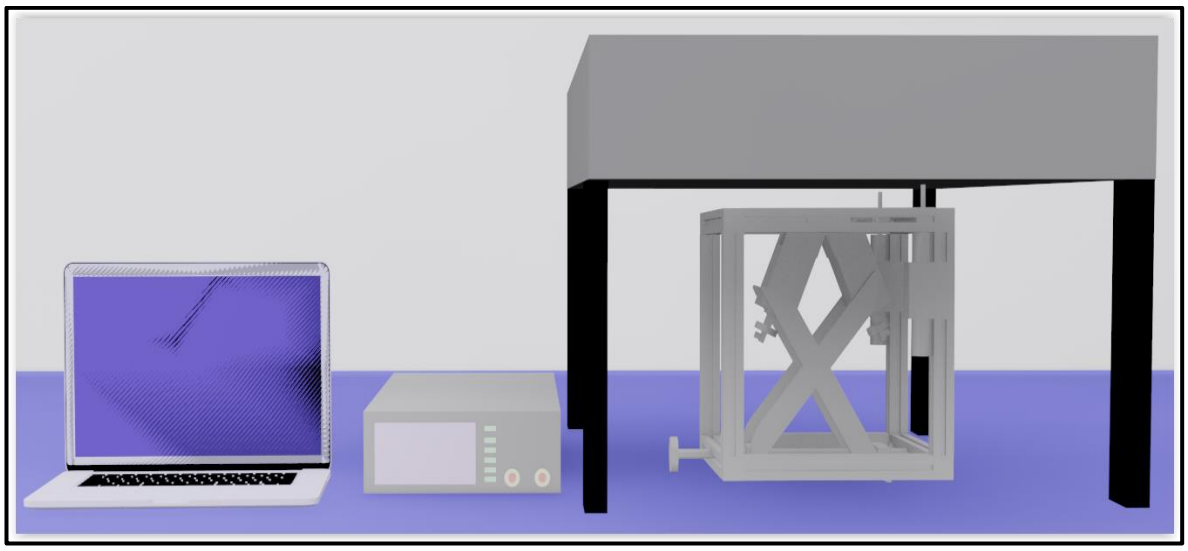

Figure 5.5. Concrete flat roof structure curing process.

5.2.2. Results

The curing process of the concrete is a significant process due to the strengthening properties of concrete. It was found that most concrete requires a minimum of 28 days to finalise the curing process. This experiment was conducted to monitor the changes of the concrete properties by capturing the data every 30 minutes. Figure 5.6 shows the results of the experiment. The microwave spectrum has a visible amplitude shift across the frequency range between 6GHz and 12GHz due to changes in concrete dielectric properties caused by the water evaporating process.

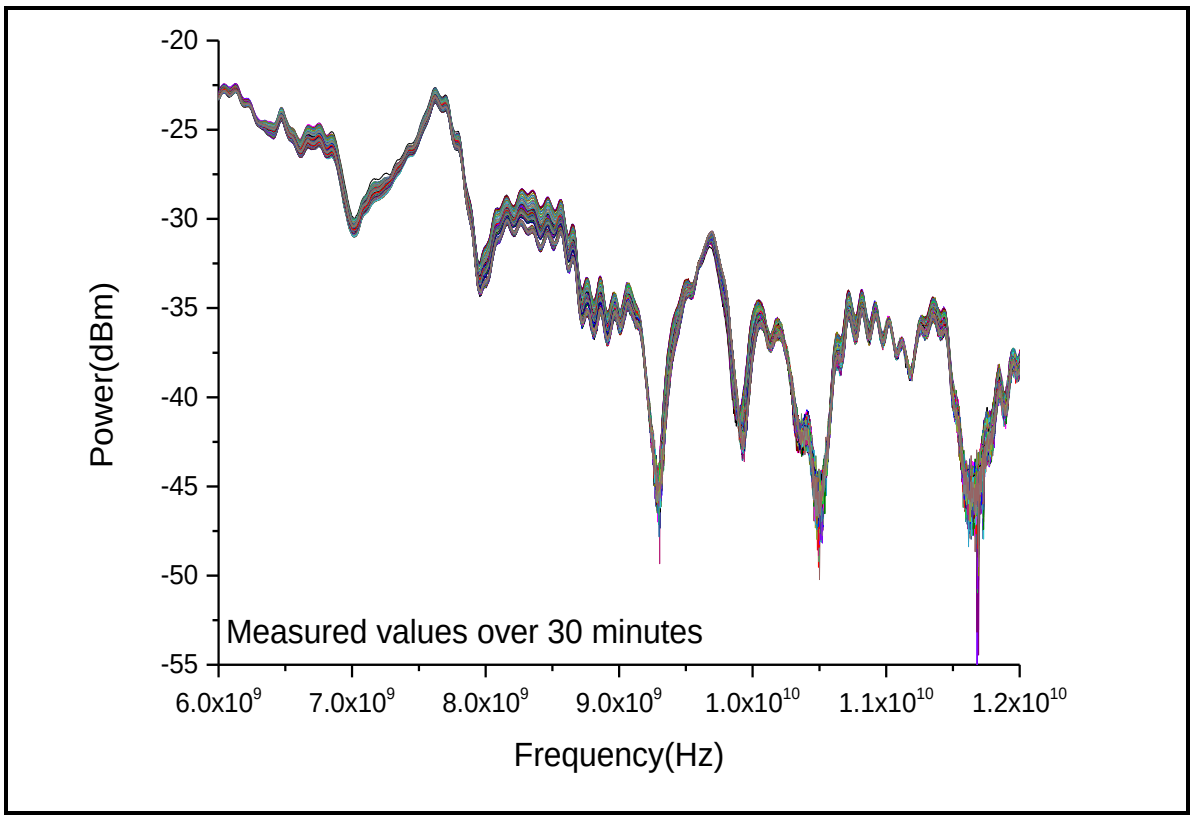

Figure 5.6. Concrete flat roof structure curing process.

5.2.3. Analysis

Dielectric properties are much higher on the begging of the experiment and have values that tend towards to the free water. The dielectric loss will decrease as the material will cure and consequently the effectiveness of dielectric heating or curing reduces as the product dries out.

5.2.4. Discussion

This experiment was undertaken to confirm if microwave spectroscopy can be used to monitor the concrete flat roof structure during curing process. Results shows that there is a significant change in attenuation of EM signal across 6GHz to 12GHz frequency range while the water evaporates from measured material.

5.3. EcoMech Industrial Wall Structure

EcoMech panels were tested under four different scenarios with and without the EM sensor. The tests varied from surface testing of water content to soaking the panel in water and monitoring the drying process to enable calibration of the sensor technology. Those experiments have been undertaken to identify the waterproofness of the tested material.

5.3.1. Methodology

The four dominant testing conditions are as follows:

5.3.1.1 External board water absorption

The aim of the test was to measure the water resistance capability of the external magnesium board surface. Figure 5.7 shows the section of the wall panel tested and how it was placed underneath the frame created to hold the experimental setup.

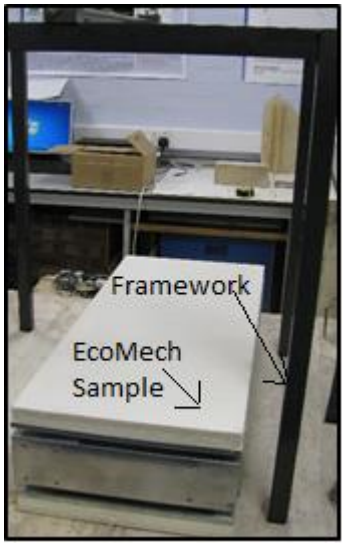

Figure 5.7. Sector of the wall panel tested placed in the framework.

Two glass pipes were fixed on the magnesium board surface to test its water resistance as shown in Figure 5.8. Each of the glass tubes was filled with 750 ml of water. Glass tube A was directly attached to the surface of the panel and had its base fixed using silicon sealant to avoid water leakage from the edges. Glass tube B was indirectly attached to the surface of the panel with an aluminium sheet in between the panel surface and the glass tube. The edges were again sealed using silicon sealant. The aluminium sheet was used to test the

difference between the absorbance with and without any intermediate surface between the panel and the tube (i.e. it was the control, allowing the accommodation of any significant evaporation).

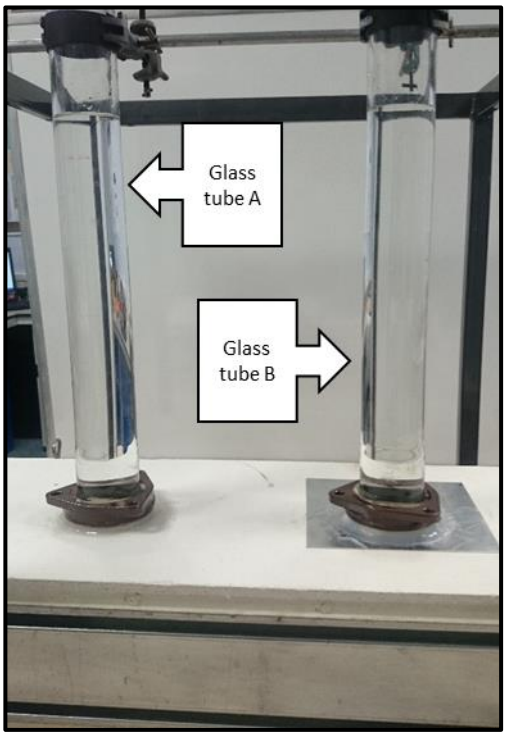

Figure 5.8. Glass tubes with 750ml water fixed on the experimental panel to test the water absorption of the surface.

The measurements were taken in terms of water absorption versus time for both the glass tubes. An interesting parameter to test was the water ingress into the magnesium board. The results are presented in Figure 5.14. The results for water absorption on the surface of the wall panel are presented in Table 5.1. The start height of the water sample in both the glass tubes is at 41.8 cm correspond to 750ml with a decrease (absorption) to 38.8 cm in the case of the glass tube directly attached to the surface of the wall panel without the aluminium sheet.

Table 5.1. Water absorption data comparison, glass tubes attached to the board and the aluminium surface.

hh:mm	EcoMech Board (cm)	Aluminium sheet (cm)
00:00	41.8	41.8
01:18	41.6	41.8
04:10	41.4	41.8
08:52	41.1	41.8
23:42	39.5	41.8
54:48	38.8	41.8

It can be seen that the water absorption of almost 3 cm (Table 5.1) was observed in the case of the glass tube directly attached on the surface of the section of the panel compared to no change in the water levels of the tube attached indirectly on to the surface through the steel plate. This shows that the magnesium board surface allows water permeation and may absorb moisture/water. Water has penetrated through the surface of the magnesium board, causing staining – it was noted that this staining was not permanent and the board finish recovered upon drying. The change in the water levels is also presented in the form of a graph in

Figure **5.9**

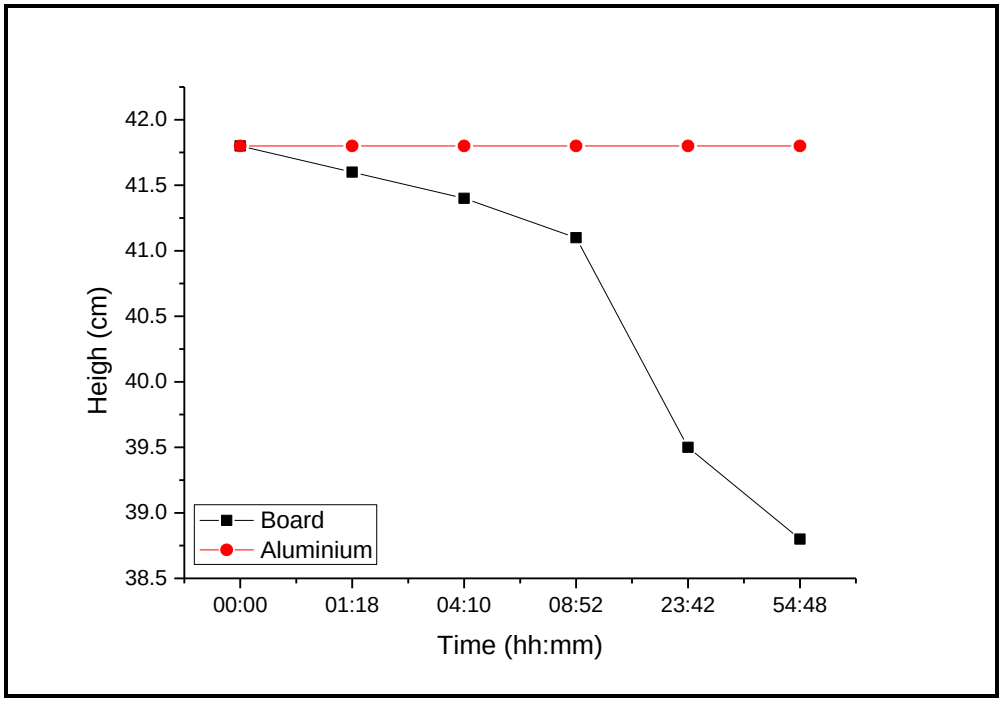

Figure 5.9. Comparison of water absorption between the glass tubes directly and indirectly connected to the surface of the panel.

5.3.1.2 Internal insulation water absorption

This test was to determine the water absorption levels of the internal foam (polyurethane insulation), particularly since magnesium board was found to be heavily water resistant. A hole was drilled into the magnesium board outer surface only to insert a glass tube through it. The experimental arrangement is shown in Figure 5.10.

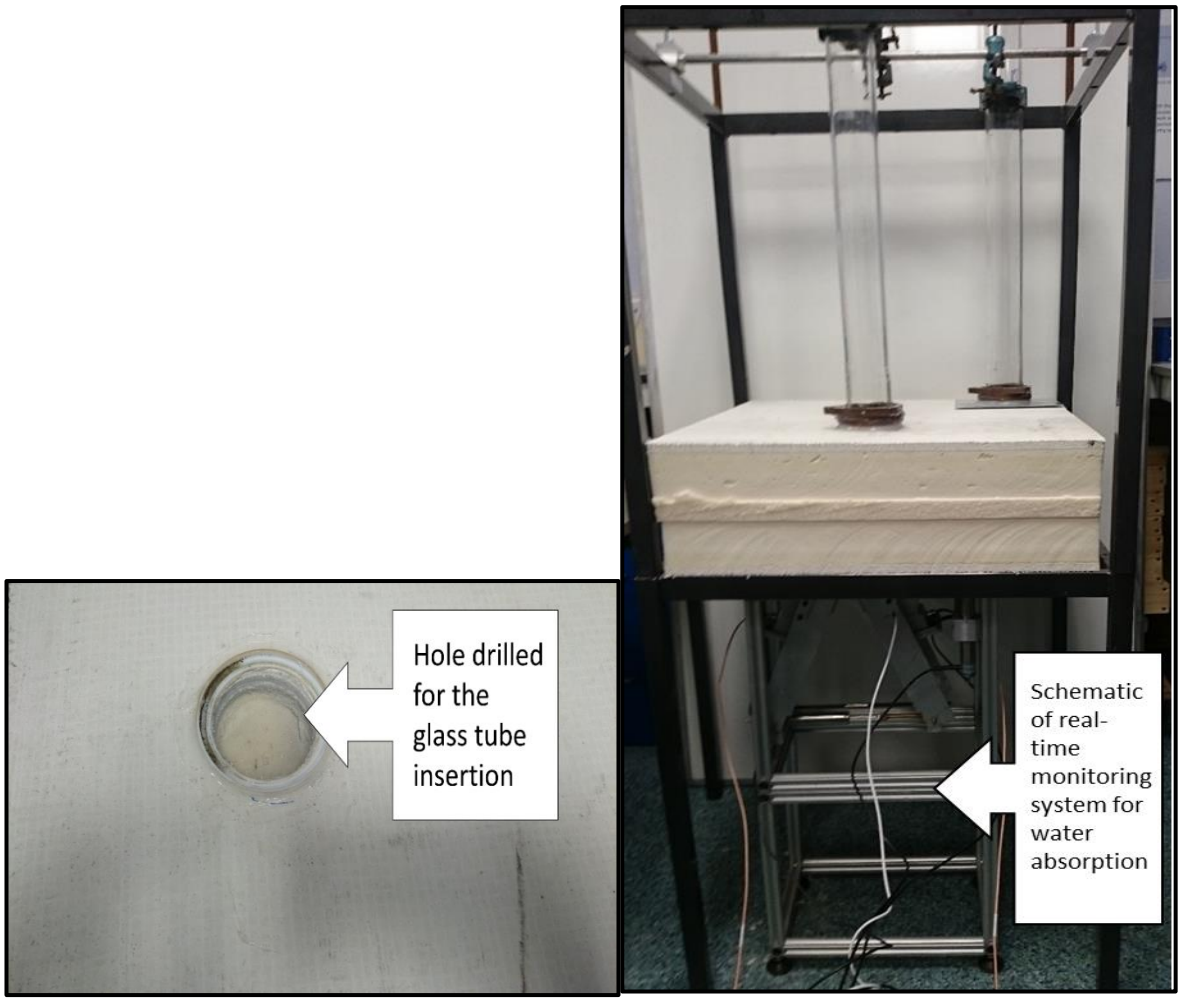

Figure 5.10. Experimental setup to monitor internal water absorption.

The process of water absorption was monitored using sensor technology in real-time. Results are presented in Figure 5.15. The results of the water absorption internally into the

foam/polyurethane filling are presented in Table 5.2. The change in the water levels is also presented in the form of a graph in Figure 5.11.

Table 5.2. Water absorption data comparison, glass tubes filled with water attached through the hole into the foam as well as the other attached to the aluminium surface.

hh:mm	EcoMech Board (cm)	Aluminium sheet (cm)
00:00	41.8	41.8
01:00	41.6	41.8
02:14	41.5	41.8
06:38	41.3	41.8
12:17	41.1	41.8
22:11	40.8	41.8
24:23	40.8	41.8

It shows that over the period of one day there was a 1 cm decrease in the water levels hence showing water ingress into the filling.

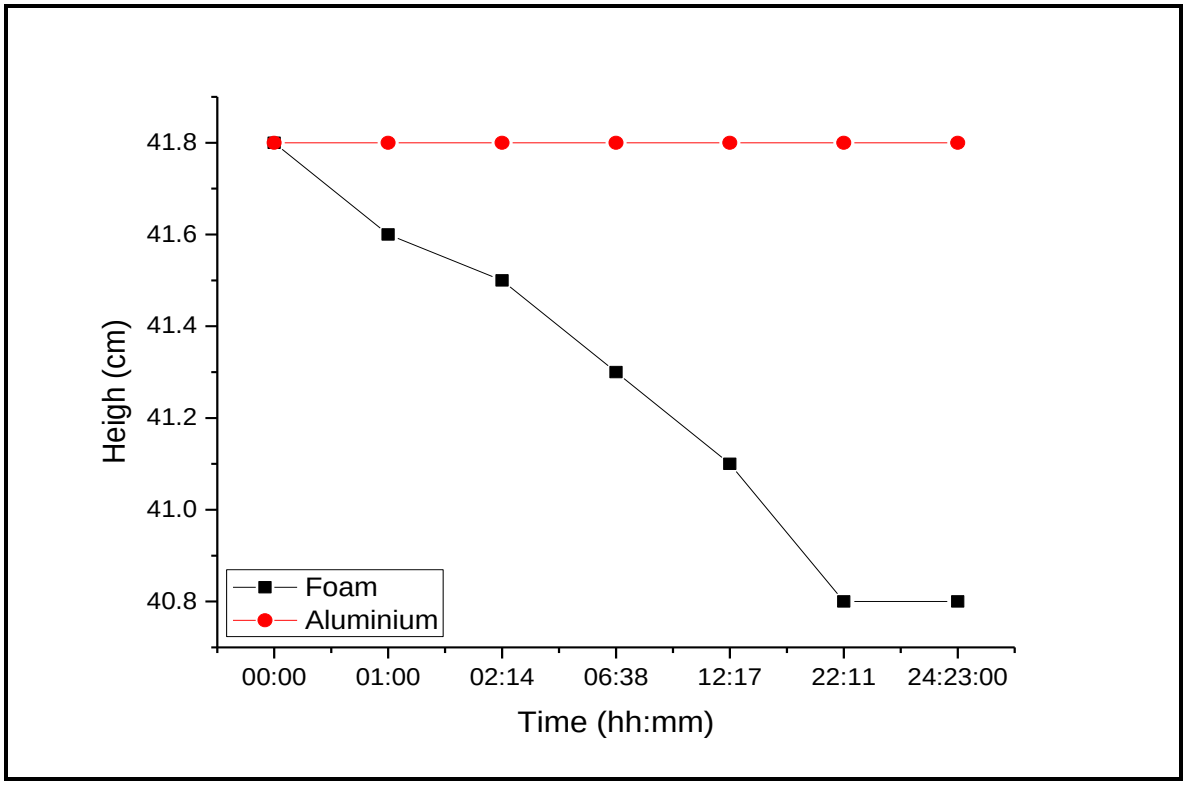

Figure 5.11. Comparison of water absorption between the glass tubes passing through the

surface of the panel into the polyurethane filling and attached indirectly on to surface of the panel through stainless steel plate (no hole drill).

5.3.1.3 Surface spray and monitoring the drying process

Water was sprayed on the external magnesium board surface of the wall panel and data was recorded for the drying process through the use real-time sensors as shown in Figure 5.12.

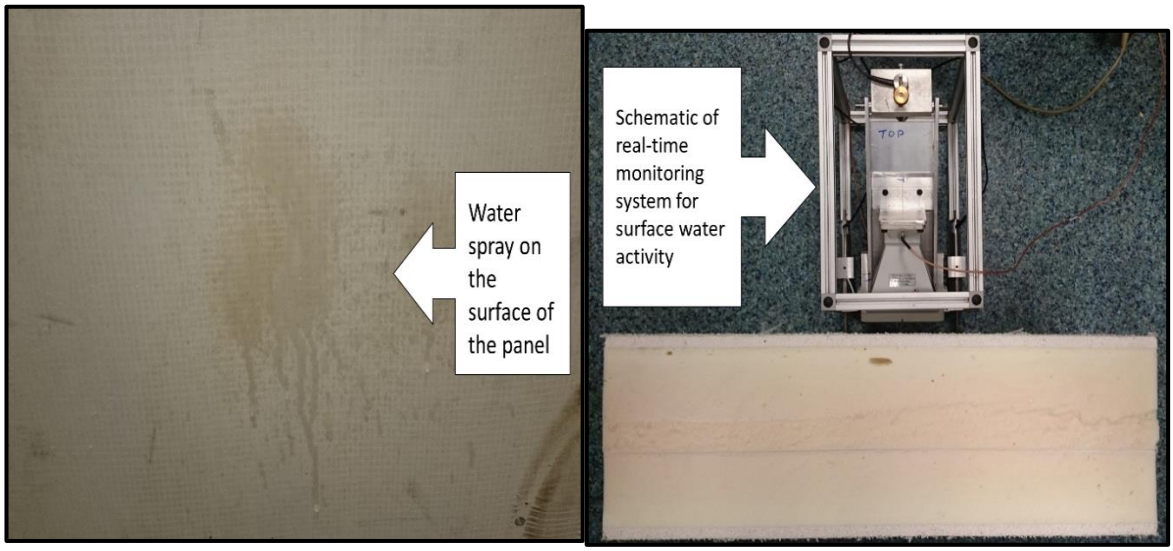

(a) (b)

Figure 5.12. Real-time surface monitoring of the drying process using sensors.

The aim was to monitor the surface drying process of water on the section of the wall panel. It was also to study the robust performance of the sensors to capture the data, i.e. drying versus time. The results are presented in Figure 5.16.

5.3.1.4 Soaking the whole panel and monitoring the drying process

A whole section of the wall panel supplied was soaked into the water and left to dry. Data was recorded every five minutes to monitor the drying of the panel (i.e. from the sensor system and also from a set of weighing scales). For comparison purposes a conventional engineering wall brick was also soaked and left to dry off for the same duration as the panel to monitor the relative difference in the rate of drying and sensor response. The absorption of water was also calculated for both the wall panel and the conventional wall brick. The section of the wall panel soaked is shown in Figure 5.13.

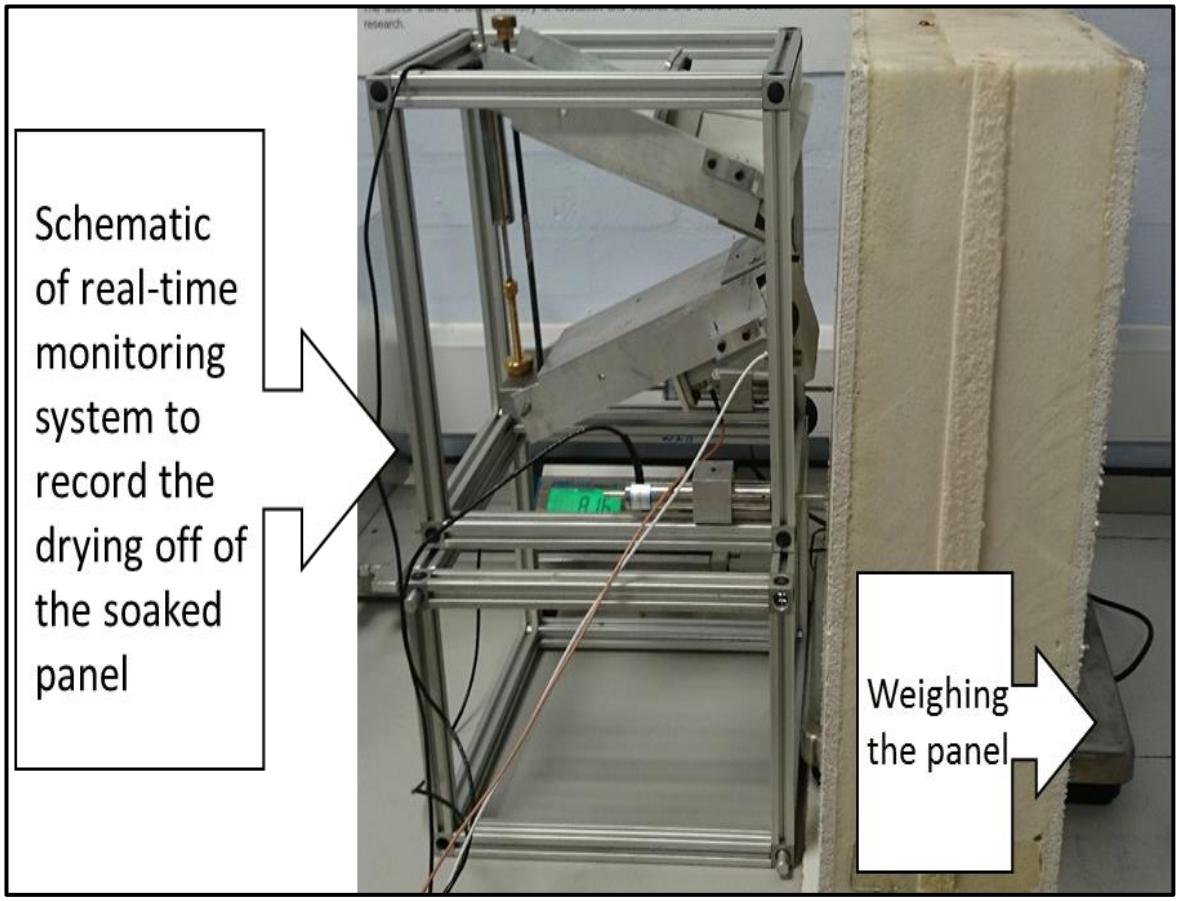

Figure 5.13. Experimental setup for monitoring the dry off wall panel. Wall panel was weighed before and after soaking and the drying off was monitored through the use of sensors.

Both the section of the wall panel and brick were first weighed before soaking. The weight was recorded to compare it with the weight after the soaking process. Bespoke LabVIEW software was used to capture the data from the sensor and weighing scale simultaneously to give a consistent time base. The measurement results are shown in Figure 5.17.

5.3.2. Results

5.3.2.1 External board water absorption

Figure 5.14 presents the results of the microwave spectrum during external wall drying process. Data was captured every 5 minutes. Microwave amplitude changes while the water penetrates the magnesium board surface. This effect can be seen due to the high dielectric properties of water which affect the microwave spectroscopy.

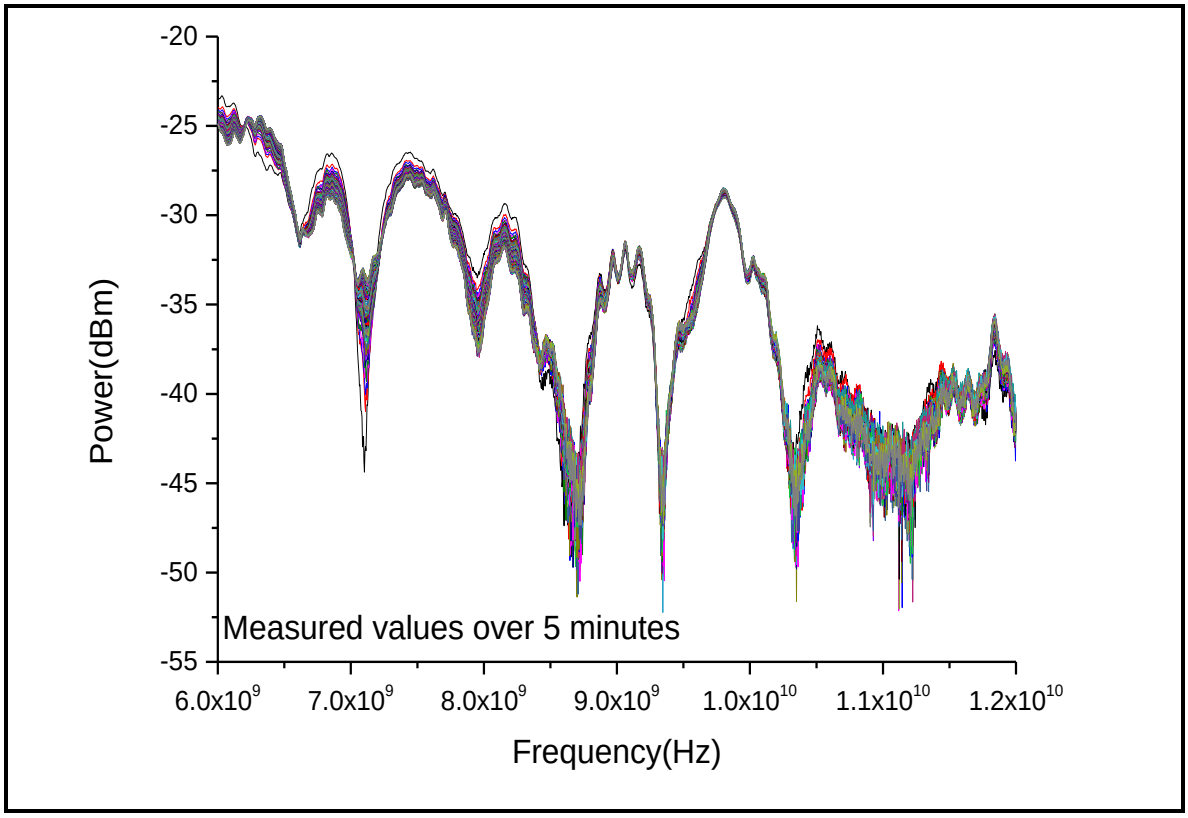

Figure 5.14. EcoMech external wall drying process.

5.3.2.2 Internal insulation water absorption

Figure 5.15 presents the results of the internal drying process. Data was captured every 10 minutes. Microwave amplitude changes while the water penetrates the polyurethane board surface. This effect can be seen due to the high dielectric properties of water which affect the microwave spectroscopy.

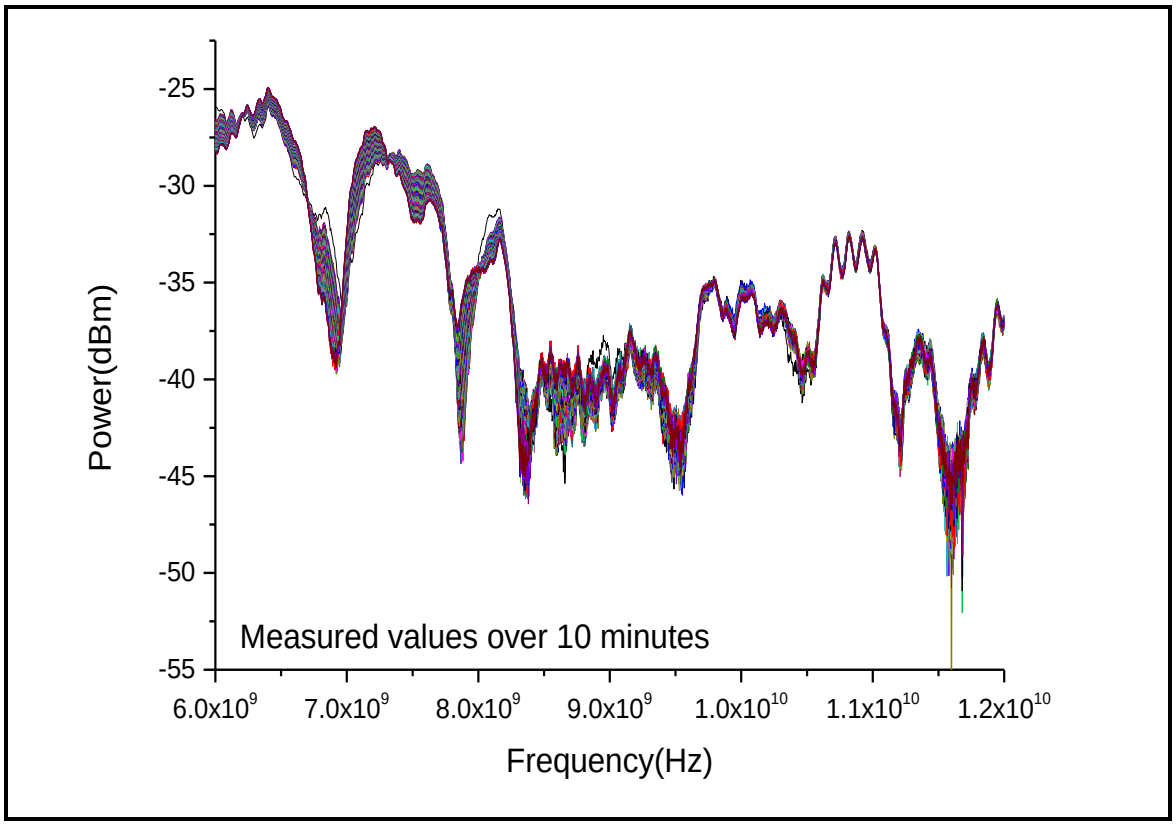

Figure 5.15. EcoMech polyurethane filling foam drying process.

5.3.2.3 Surface spray and monitoring the drying process

Monitoring the spraying of the external board surface is presented in Figure 5.16. Data was collected every 10 seconds. There is significant amplitude shift across 6GHz to 12GHz frequency range due to the evaporation of the water. Water has high dielectric properties which affects the microwave spectrum. The lower amount of water enables the reduction of the power loss of the microwave energy and creates visible changes to the microwave spectroscopy.

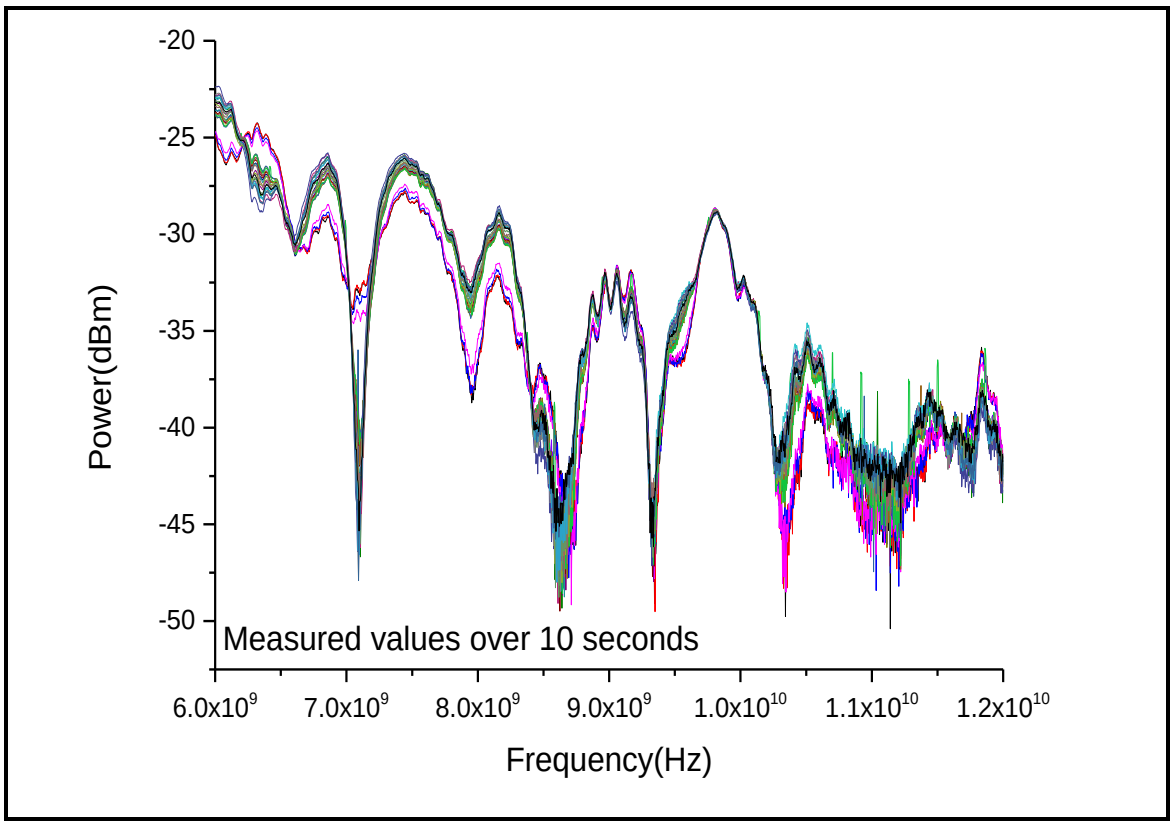

Figure 5.16. EcoMech external board spraying process.

5.3.2.4 Soaking the whole panel and monitoring the drying process

Figure 5.17 presents the results of soaking the EcoMech panel over 24 hours and monitoring the drying process. Data (EM spectrum and weight loss) was captured every 20 minutes. The change in the reflected signal is caused by the evaporation of the water from the measured material. There is a noticeable amplitude decrease across the full EM spectrum. Therefore, the spectrum was correlated against weight loss of the measured sample in order to select the optimal frequency range for weight loss determination. Figure 5.18 demonstrates a linear correlation between weight loss and the EM spectrum. It can be seen in the figure that an amplitude change at the frequency range between 7.39GHz and 7.5GHz presents a very strong linear relationship ($R^2 = 0.95$) with the weight loss.

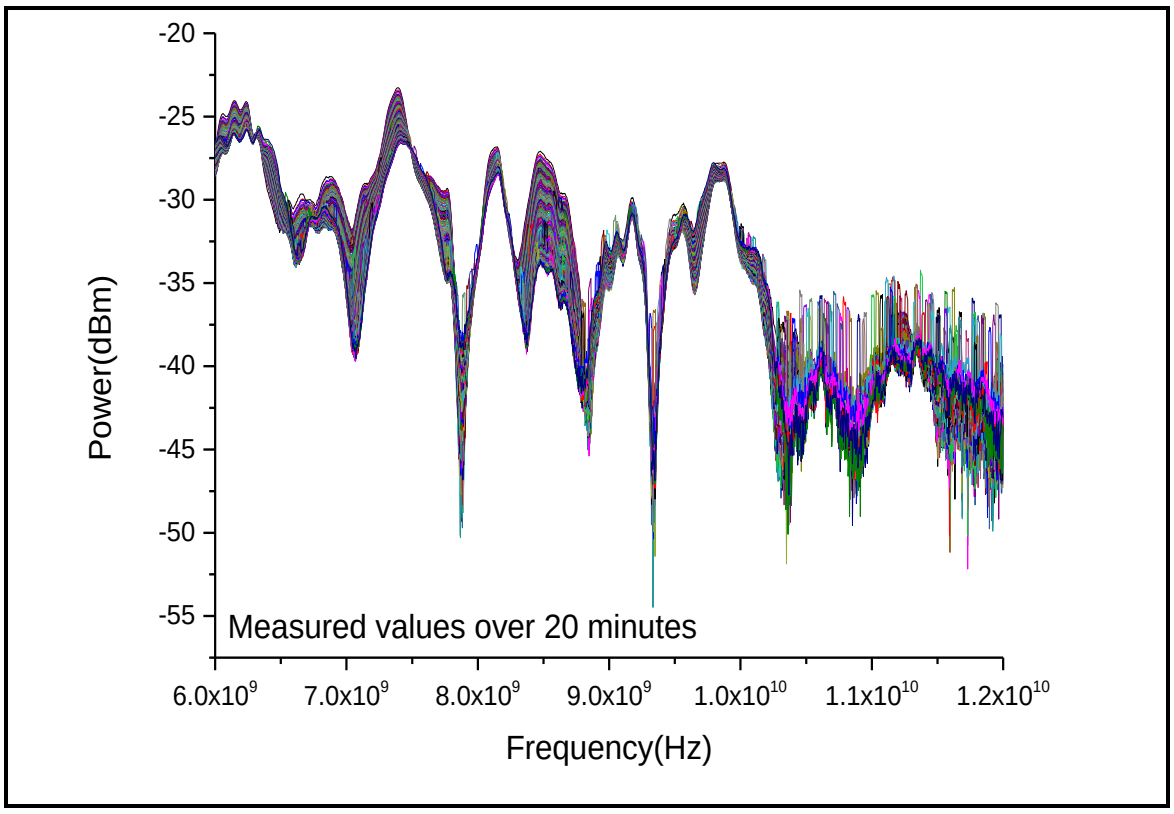

Figure 5.17. Soaking whole EcoMech panel and monitoring drying process.

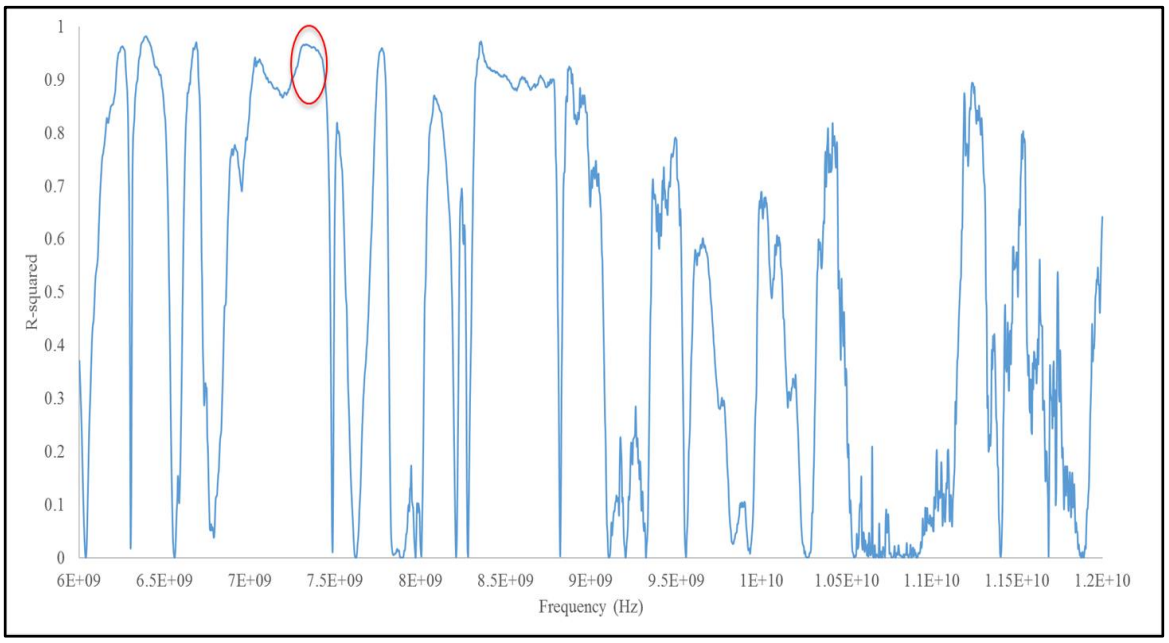

Figure 5.18. R-squared of weight loss and amplitude shift across full frequency spectrum.

Figure 5.19 shows the S_{21} reflection coefficient at 7.39GHz over the measurement period. Data was normalised to a percentage change for direct comparison. As can be seen the S_{21} change and material weight loss at this particular frequency decreases over the time.

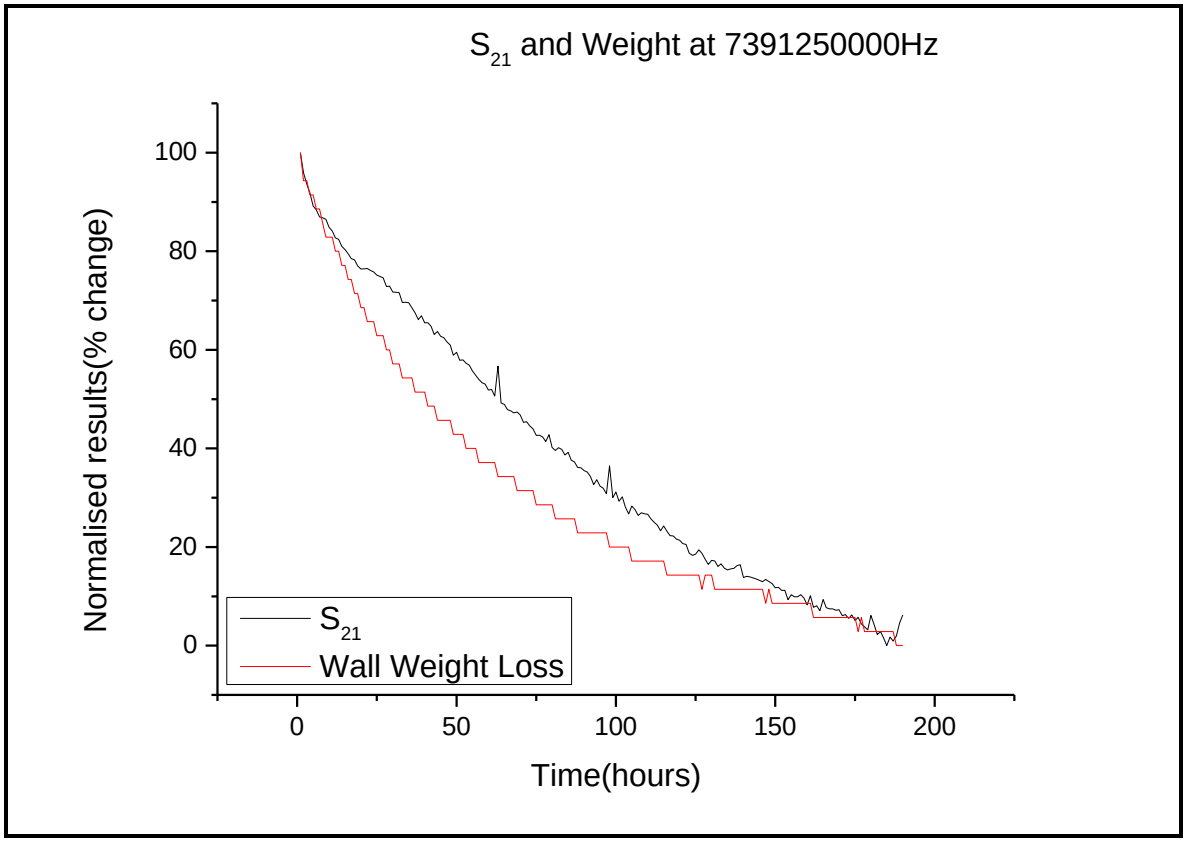

Figure 5.19. S_{21} change at 7.39GHz over period of drying process.

Figure 5.20 shows linear best fit at 7.39GHz over the period of measurement for weight loss. R^2 = 0.95 which is a reasonably accurate result for correlation between S_{21} parameter and moisture loss in the EcoMech sample.

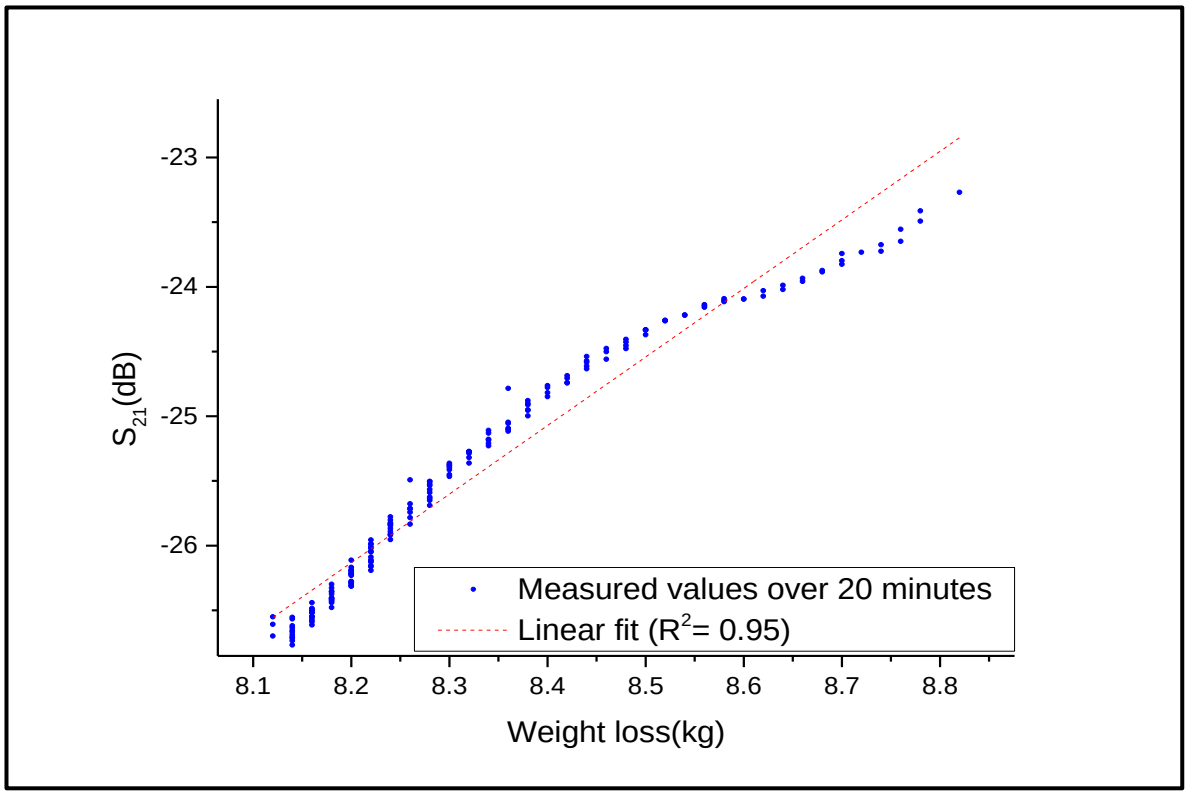

Figure 5.20. Linear best fit (R^2 = 0.95).

5.3.3. Analysis

Experimental results from external board water absorption, internal insulation water absorption and surface spray and monitoring the drying process shows that dielectric properties of porous material increases while water content is supplied into the measured material and have values that tend towards to the dielectric properties of the free water. The dielectric loss will decrease as the material dries and consequently the effectiveness of dielectric reduces as the product dries out. Experimental results for soaking the whole panel and monitoring the drying process shows that there is a high linear correlation between material weight loss and attenuation at 7.39 GHz, R^2 = 0.95. Figure 5.21 shows the prediction method using Partial Least Squares Regression (PLS). Two models were calibrated for both EM attenuation and moisture content, The EM attenuation model has a good accuracy, with R^2 = 0.986 and Root Mean Square Error of Prediction (RMSEP)= 0.020kg for the prediction set.

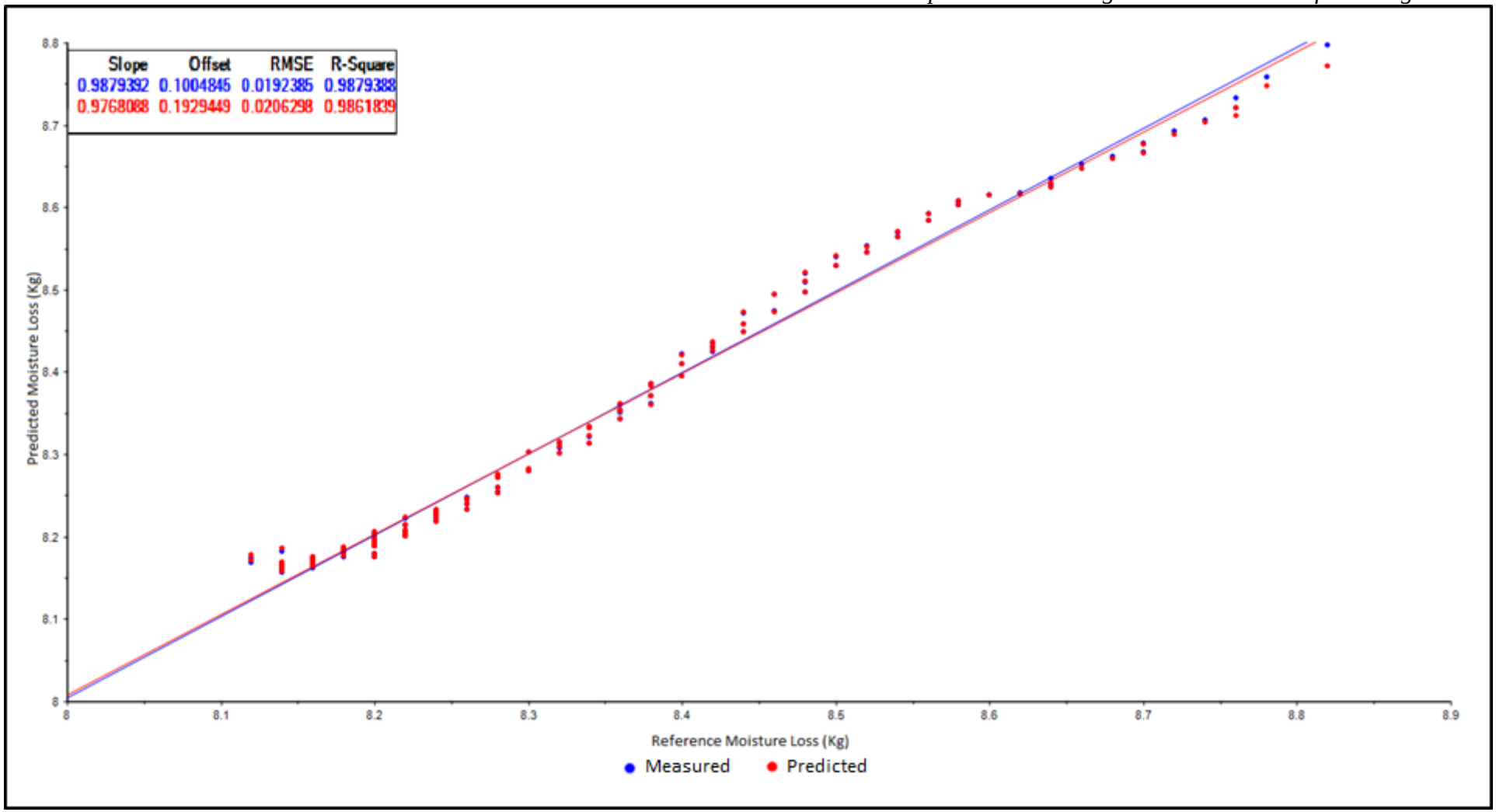

Figure 5.21. Measured and predicted moisture loss from electromagnetic wave sensor.

5.3.4. Discussion

EcoMech panels were tested under four different scenarios with and without the EM sensor. The tests varied from surface testing of water content to soaking the panel in water and monitoring the drying process to enable calibration of the sensor technology. Those experiments have been undertaken to identify the waterproofness of the tested material. Results show that there is a significant change in the attenuation of EM signal across 6GHz to 12GHz frequency range while the water evaporates from measured material. There is a high linear correlation between material weight loss and attenuation at 7.39GHz. The prediction model using the PLS method has a good accuracy, R^2 = 0.986 and Root Mean Square Error of Prediction (RMSEP) = 0.020kg for the prediction set.

5.4. Concrete Paving Slab Moisture Drying off Process

Concrete paving slab will be used in this experiment to simulate the concrete flat roof structure to monitor the moisture evaporation process. Concrete flat roof structure in tropical countries is exposed to high rains and high humidity which cause the damage to the waterproof membrane and damage to concrete structure.

5.4.1. Methodology

This experiment was conducted to monitor concrete behaviour during the drying off process, in a laboratory environment. A preliminary roof structure was made from a pre-cast concrete paving slab (600 x 600 x 50mm), grade 20 without any reinforcement bar. A microwave sensor was placed under the concrete structure 20mm from the building material. The frequency range during this experiment is between 6GHz to 12 GHz. The experimental setup is shown in Figure 5.22.

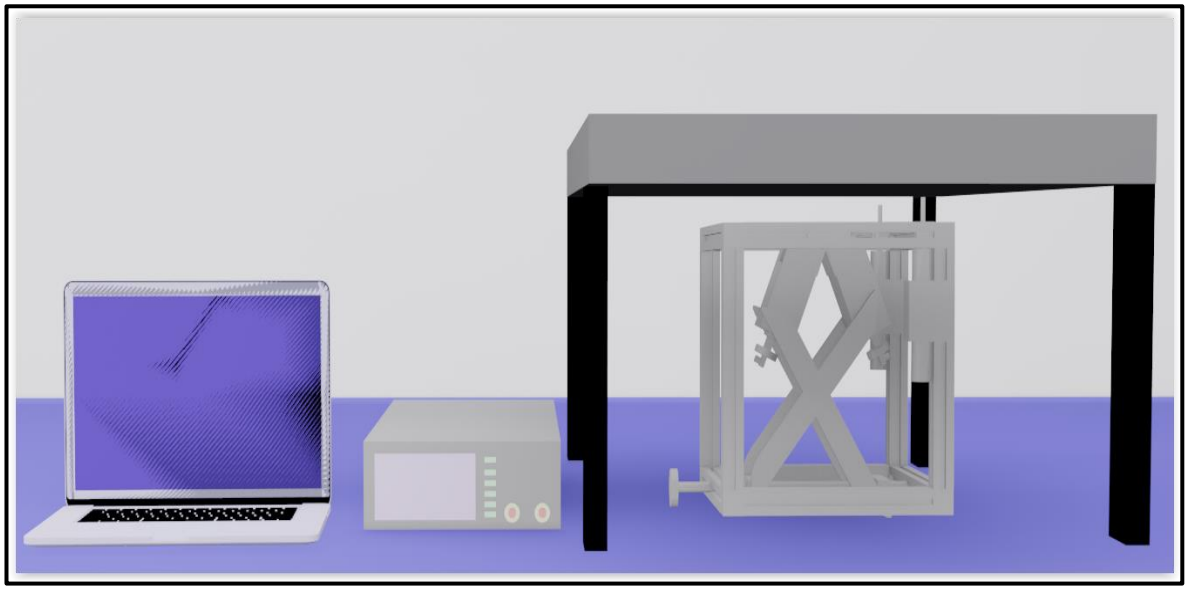

Figure 5.22. Concrete slab drying off process, experimental setup.

5.4.2. Results

The results of the concrete slab drying process are presented in Figure 5.23. Measured data was recorded every 30 seconds. Evaporating water from the concrete slab changes the dielectric properties of the concrete material as well as reflecting different amounts of microwave energy which cause the significant change in the microwave reflection coefficient.

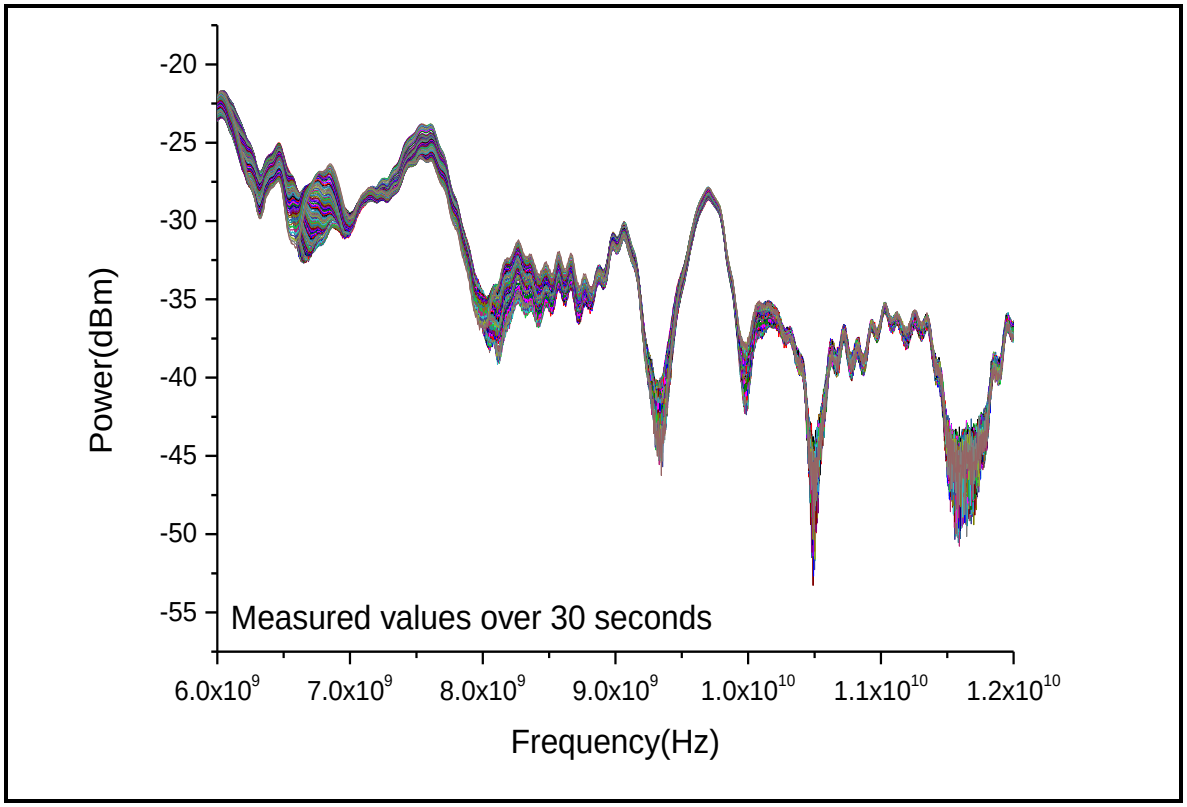

Figure 5.23. Concrete slab drying process.

5.4.3. Analysis

Experimental results from concrete slab drying off process show that dielectric properties of porous material increase while water content is supplied to the measured material and have values that tend towards the dielectric properties of the free water. The dielectric loss will decrease as the material dries and consequently the effectiveness of dielectric reduces as the product dries out.

5.4.4. Discussion

This experiment was undertaken to confirm if microwave spectroscopy can be used to monitor the concrete slab drying process. Results show that there is a significant change in attenuation of EM signal across 6GHz to 12GHz frequency range while the water evaporates from measured material.

5.5. Concrete Structure Moisture Drying off Process

The preliminary experiment in section 5.4 to monitor the drying process of concrete paving shows that EM waves can be used to monitor the evaporation process as microwave spectrum is affected when the amount of water/ moisture in concrete paving slab decreasing. This experiment will determine moisture drying off process in concrete flat roof structure built into Malaysian standards (case study) requirements attached in Appendix A.

5.5.1. Methodology

This experiment was conducted to monitor concrete behaviour during the drying off process, in a laboratory environment. A preliminary roof structure was made to Malaysian concrete flat roof structure standards (see Appendix A) without any reinforcement bar. A microwave sensor was placed under the concrete structure 2cm from the building material. The EM wave frequency during this experiment is between 6GHz and 12GHz. The experimental setup is shown on Figure 5.24.

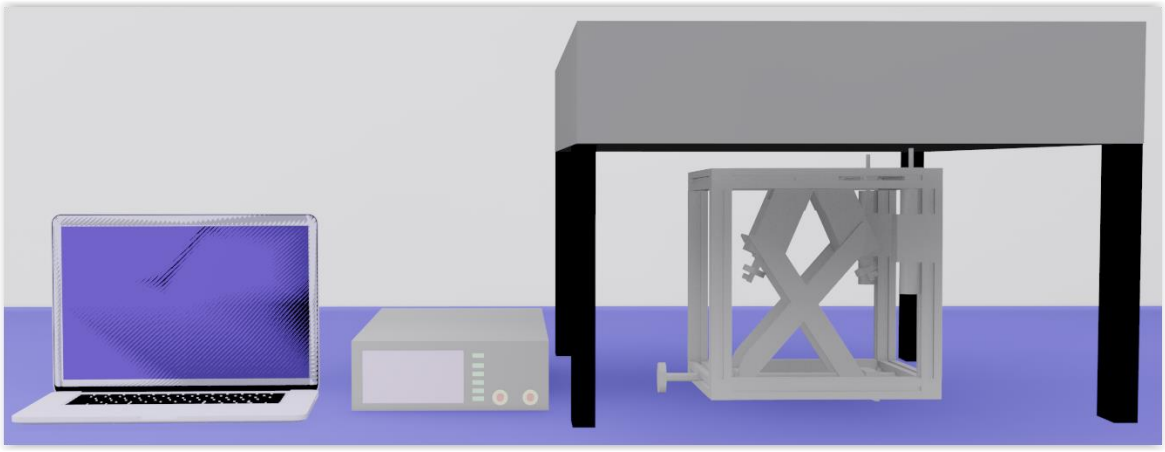

Figure 5.24. Concrete flat roof structure drying off process.

5.5.2. Results

Figure 5.25 presents the results of the drying process of the concrete roof structure. Data was recorded every 20 minutes. There is a slight amplitude shift across the measured frequency range due to the small amount of moisture content in the concrete slab. Moisture evaporates which changes the dielectric properties of concrete.

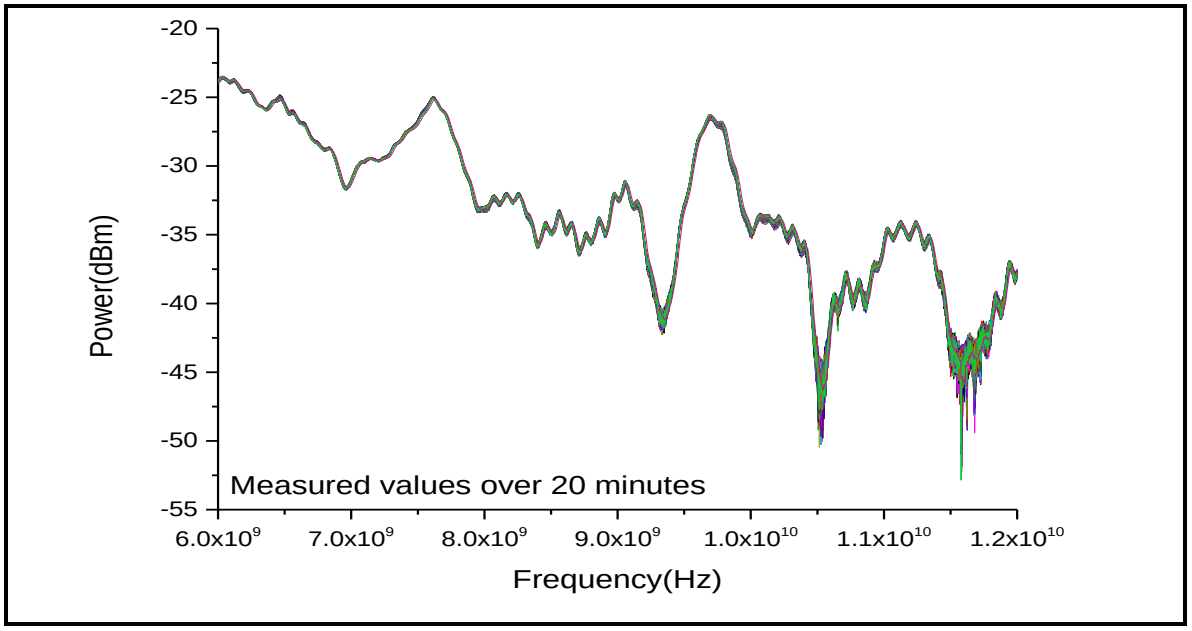

Figure 5.25. Concrete flat roof structure drying process.

5.5.3. Analysis

Experimental results from concrete flat roof structure drying off process shows that dielectric properties of porous material increases while water content is supply into the measured material and have values that tend towards to the dielectric properties of the free water. The dielectric loss will decrease as the material dries and consequently the effectiveness of dielectric reduces as the product dries out.

5.5.4. Discussion

This experiment was undertaken to confirm if the microwave spectroscopy can be used to monitor the concrete flat roof structure drying off process. Results show that there is a change in attenuation of EM signal across 6GHz to 12GHz frequency range while the water evaporates from measured material.

5.6. Concrete Blocks Moisture Drying off Process

This experiment was conducted to monitor concrete behaviour during the drying off process, in a laboratory environment. A preliminary concrete cubes were made from Malaysian concrete flat roof standards (see Appendix A) without any reinforcement bar.

5.6.1. Methodology

The microwave sensor was positioned in front of the concrete block with a 20 mm gap as indicated in Figure 5.26. The sample was not touched or moved during the experimental work, and all other conditions such as temperature and light remained nominally the same during the test. The sensor was connected to a Rohde & Schwarz Vector Network Analyser (VNA) and a laptop, which captured and stored data via software developed in LabVIEW. Concrete blocks were placed in a container with water and left submersed for 24 hours. Each concrete block was weighted before and after being placed into the water. Measurements were taken every 30 minutes over a 24-hour period. The experiment was repeated three times (n=3).

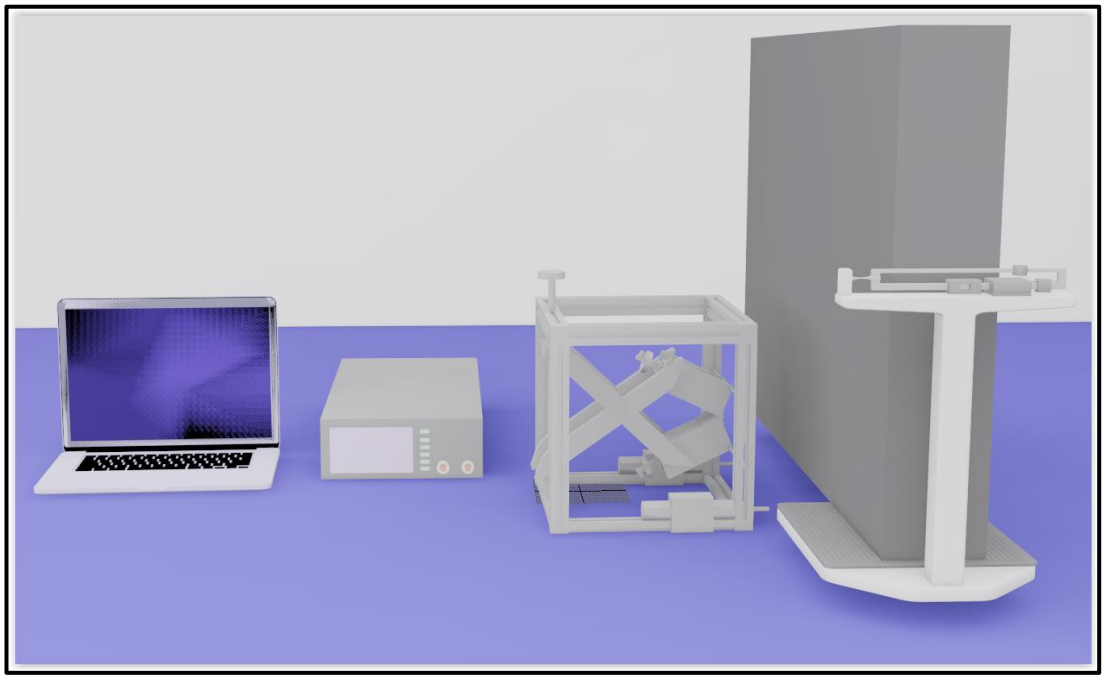

Figure 5.26. Concrete cubes drying off process, experimental setup.

5.6.2. Results

Figure 5.27 shows the S_{21} measurements of the concrete cube taken every 30 minutes during a 24-hour period. It can be seen that there is 12 dB difference between the first and last measurements, which is a noticeable change in EM wave signature while the sensor is continuously taking measurements of the concrete block. Repeatability of the experiment confirms the results presented.

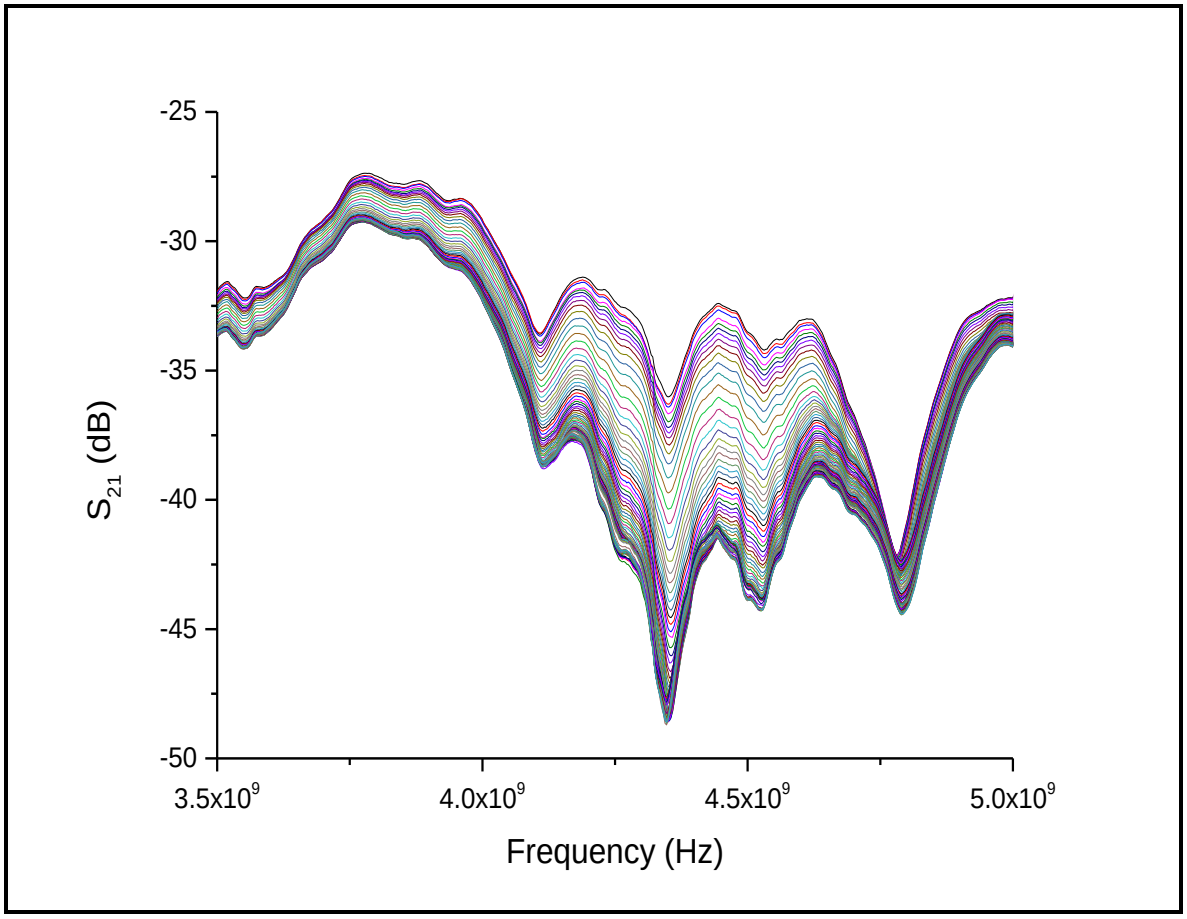

Figure 5.27. S_{21} measurements from the EM sensor, measurements were taken once per half an hour in the frequency 2-12GHz, but for clarity data measurements 3.5-5GHz are presented.

5.6.3. Analysis

Experimental results from concrete cubes show that dielectric properties of porous material increases while water content is supply into the measured material and have values that tend towards to the dielectric properties of the free water. The dielectric loss will decrease as the material dries and consequently the effectiveness of dielectric reduces as the product dries out. Figure 5.28 represents a prediction model to determine moisture content of concrete that

was developed using Partial Least Squares Regression (PLSR) analysis in Matlab software. The frequency range with the strongest regression coefficients were selected as the optimal frequency range for moisture content prediction, namely from 3.5-5GHz. The experimental values are plotted and displayed in Figure 5.28. The model demonstrated a good capability to predict moisture content of concrete with $R^2_{prediction}$ = 0.9958 and RMSEP (Root Mean Square Error of prediction) = 0.0138.

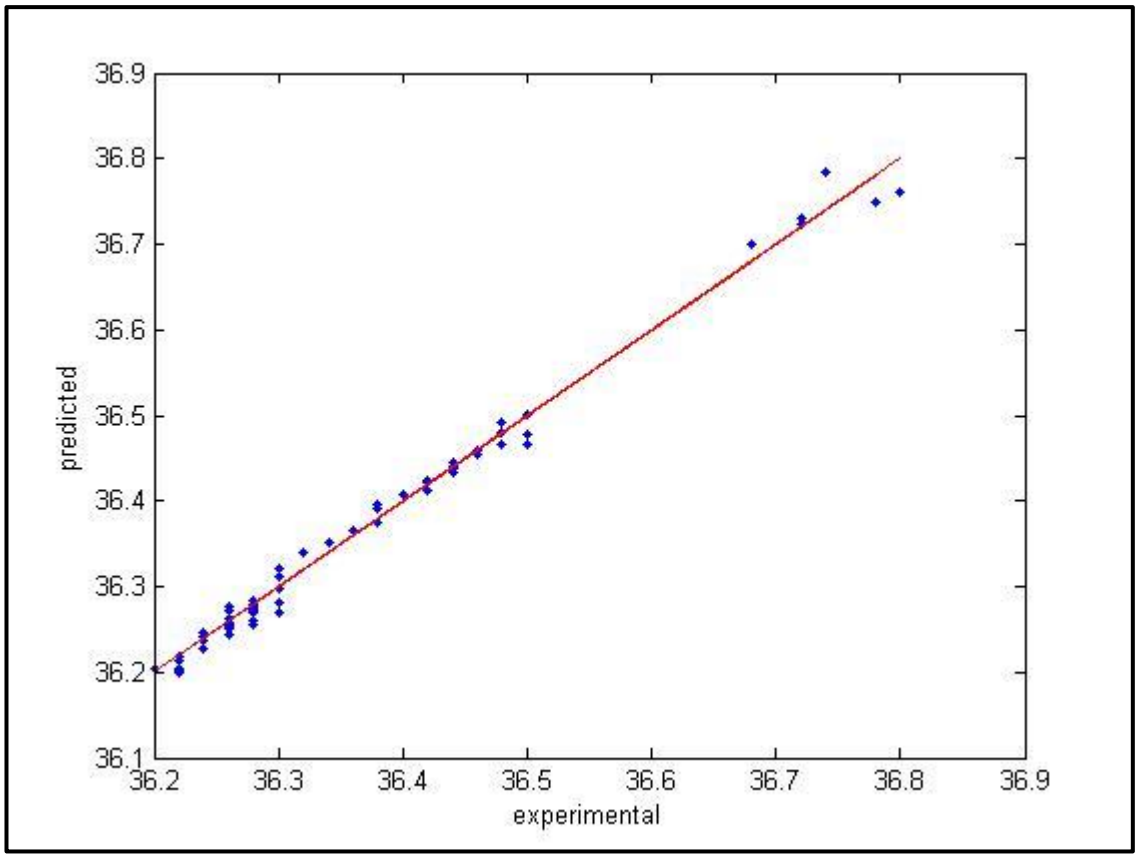

Figure 5.28. Experimental and predicted moisture content from EM sensor.

5.6.4. Discussion

This experiment was taken to monitor the drying off process of the concrete cube. Results show that there is a significant change in attenuation of EM signal across 3.5GHz to 5GHz frequency range while the water evaporates from measured material. The prediction model using PLS method has good accuracy, with R^2 = 0.9958 and a root mean square error of prediction (RMSEP) of 0.0138.

5.7. Summary

In this chapter a sequence of experimental work to monitor the moisture content in building fabrics was presented. Results from section 5.1.2 illustrated that microwave spectroscopy can be used to monitor the moisture content of the ceiling plasterboard during the drying off process. Results show that there is a significant change in attenuation of EM signal across 6GHz to 12GHz frequency range while the water evaporates from measured material. There is a high linear correlation between material weight loss and attenuation at 10.3GHz. The prediction model using PLS method had good accuracy, $R^2 = 0.892$ and Root Mean Square Error of Prediction (RMSEP) = 3.97g for the prediction set. Also microwave spectroscopy can be used to monitor the concrete flat roof structure during curing process. Results from section 5.2.2 shows that there is a significant change in attenuation of EM signal across 6GHz to 12GHz frequency range while the water evaporates from measured material. The tests of EcoMech panel varied from surface testing of water content to soaking the panel in water and monitoring the drying process. Results in section 5.3.2 shows that there is a significant change in attenuation of EM signal across 6GHz to 12GHz frequency range while the water evaporates from measured material. There is also a high linear correlation between material weight loss and attenuation at 7.39GHz. The prediction model using PLS method had good accuracy, with $R^2 = 0.986$ and RMSEP = 0.020kg for the prediction set. Microwave spectroscopy can be used to monitor the concrete slab drying (section 5.4.2) and concrete flat roof structure (section 5.5.2) drying off process. Results show that there is a significant change in attenuation of EM signal across 6GHz to 12GHz frequency range while the water evaporates from measured material. Results in Section 5.6.2 shows that there is significant change in attenuation of EM signal across 3.5GHz to 5GHz frequency range. The prediction model using PLS method has good accuracy, with $R^2 = 0.9958$ and a root mean square error of prediction (RMSEP) of 0.0138.

Chapter 6 Case Study: Detection of Defects in Concrete Flat Roof Structure

Microwave spectroscopy in Chapter 5 was used to determine moisture content in building materials. This Chapter will examine a Malaysian case study on detection of defects in concrete flat roof structures. Roof leakages of high-rise buildings involving concrete flat roof design in tropical countries such as Malaysia continue to be a serious problem. Almost all of the buildings have concrete flat roof design. In addition, it is recognized widely that the incorrect installation of materials and components during construction contributes to the occurrence of defects. For instance, membrane layers even when installed by an authorized manufacturer continue to face durability problems and poor performance a few years later.

In this chapter experiments will be explored to determine defects in concrete flat roof structure which are the cause of the water ingress into the building materials. Section 6.1 shows preliminary experiment for membrane failure detection on concrete paving slab. In section 6.2 experimental work to determine membrane failure in concrete flat roof structure constructed to Malaysian building standards will be presented. Section 6.3 shows the experiment to determine the location of the reinforcement in the concrete flat roof structure. Section 6.4 summarise experiments undertaken to determine defects in the concrete flat roof structure.

6.1. Concrete Slabs

In this experiment concrete paving slab will simulate concrete flat roof structure to determine the defects of waterproof membrane layer which cause the water ingress into the concrete structure.

6.1.1. Methodology

A preliminary roof structure for testing was made from a pre-cast concrete paving slab (600 x 600 x 50mm), grade 20 without any reinforcement bar and with an applied rubber membrane. The paving slab was placed on a metal frame 620mm high as indicated in Figure 6.1. This height is to ensure easy access for the sensor antenna during the experiment.

Figure 6.1. Concrete paving slab on metal structure.

A typical waterproof rubber membrane was applied tight into a wooden frame above the slab to imitate the flat roof membrane. The membrane was placed on the top of the slab as shown in Figure 6.2.

Figure 6.2. Concrete paving slab with a membrane layer.

One of the membrane samples was subjected to penetration damage with the creation of a 10mm diameter hole. This is to allow water ingress, simulating membrane failure, to the concrete roof as shown in Figure 6.3.

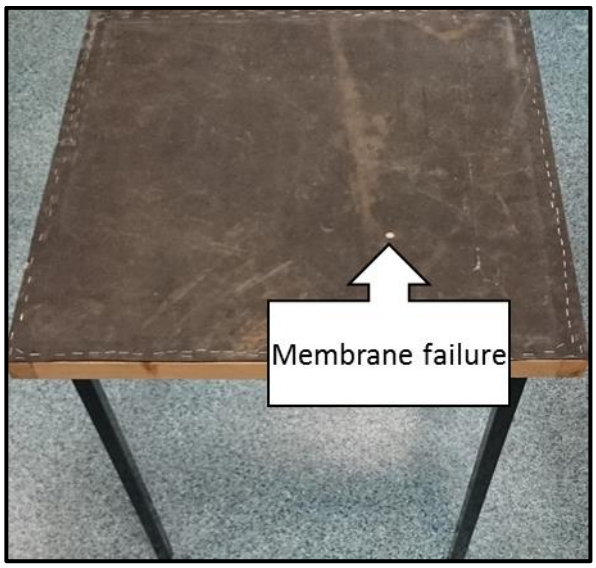

Figure 6.3. Membrane with fault.

The microwave sensor was placed 20mm beneath the concrete structure. The applied frequency range was between 6GHz and 12GHz. The sensor was connected to the Marconi Microwave test set and a laptop, which captured and stored data via bespoke software developed in LabVIEW as indicated in Figure 6.4.

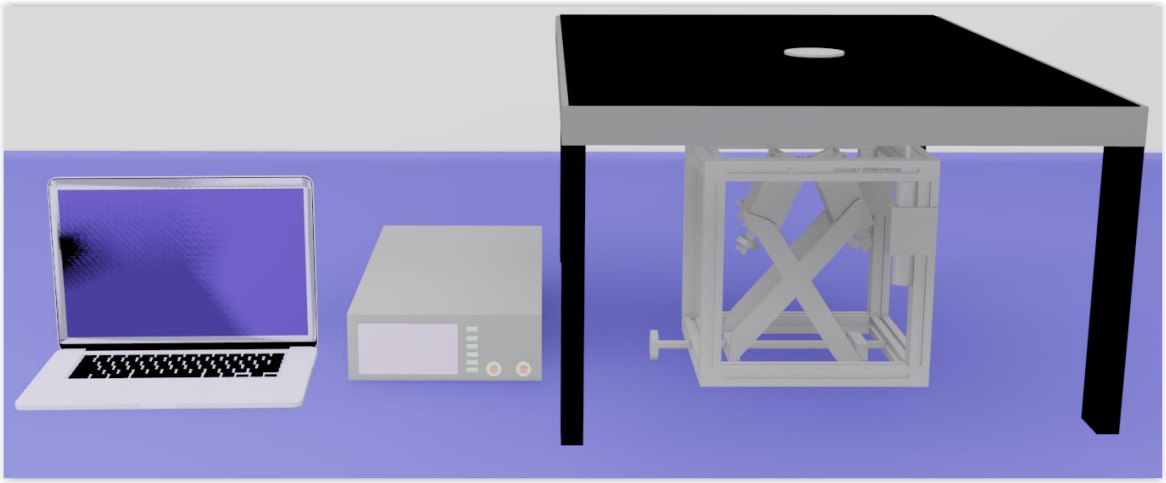

Figure 6.4. Experimental setup.

6.1.2. Results

The membrane layer is a significant part of the concrete flat roof as it protects roof structure from moisture content penetration. Figure 6.5 presents the experimental results of membrane failure on the concrete slab. There are three parameters that have been reviewed. Firstly, the concrete slab was covered with a dry membrane layer, then the membrane layer was filled with water and finally, the membrane was damaged and water started penetrating the

concrete slab. Each of the settings was recorded. There is a significant change in the amplitude of the microwave spectrum in the frequency range between 8GHz and 9.5GHz. This change was caused by water which started penetrating the concrete slab when the membrane layer was faulty. As well there is a significant difference between the dry membrane layer and the membrane filled with water due to the high dielectrics properties of the water.

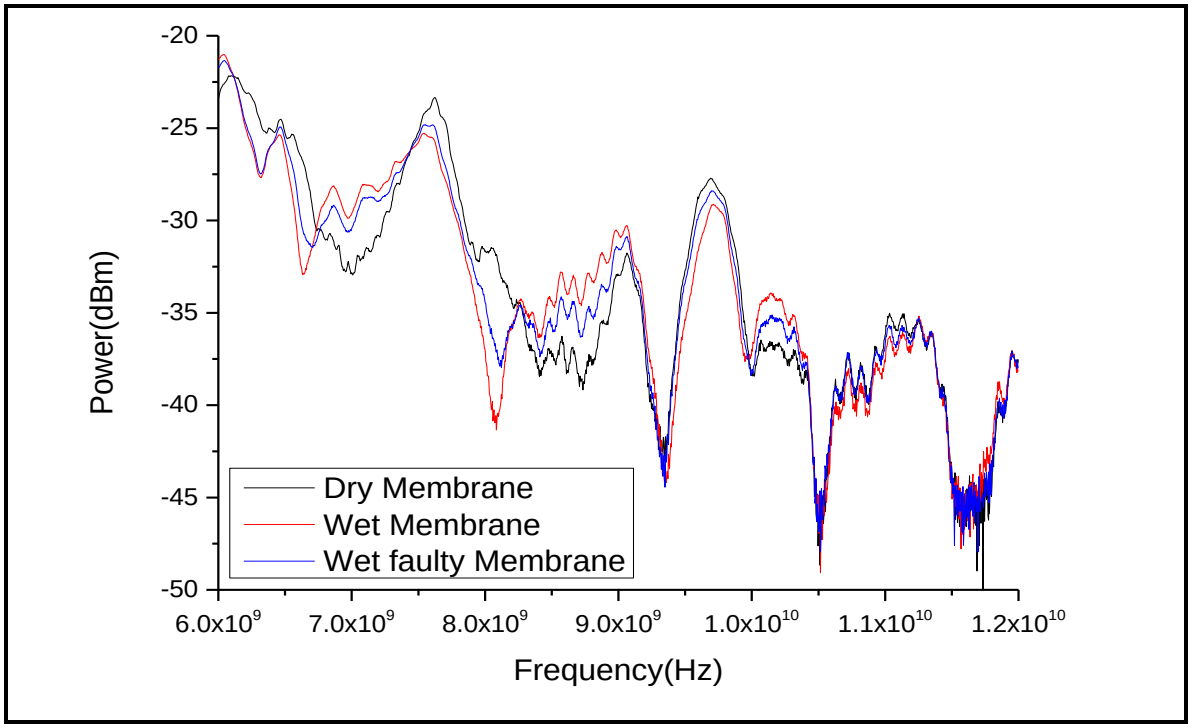

Figure 6.5. Membrane failure on concrete slab.

6.1.3 Analysis

The experiment from section 6.1.2 shows that microwave spectroscopy responds to changes applied to concrete slabs. There is a significant attenuation shift at frequency between 8GHz to 9.5GHz. This change is caused by water content applied into the membrane with and without failure. The S_{21} power for dry membrane is approximately -40dBm, for wet faulty membrane -37dBm and for wet Membrane -35dBm. The reason for those results is that water has high dielectric properties as measured in section 3.5 and absorbs microwave energy which causes the change in EM attenuation.

6.1.4 Discussion

This experiment was undertaken to confirm if microwave spectroscopy can be used to determine waterproof membrane failure on paving slab. Results show that there is a significant change in attenuation of EM signal at frequency between 8GHz to 9.5GHz. Results from this experiment illustrated that the microwave spectrum has a potential use to identify damages to membrane.

6.2. Malaysian Concrete Flat Roof Structure

Preliminary experiment in section 6.1 shows that EM waves can be used to determinate the membrane damage with the concrete paving slab. This experiment will determine the membrane damage in concrete flat roof structure constructed to Malaysian standards (see Appendix A).

6.2.1. Methodology

It was critical to design and build concrete flat roof structures which would enable multiple tests to be undertaken in a laboratory environment. One structure was built without reinforcement (Figure 6.6) and the second structure was built with reinforcement (Figure 6.7).

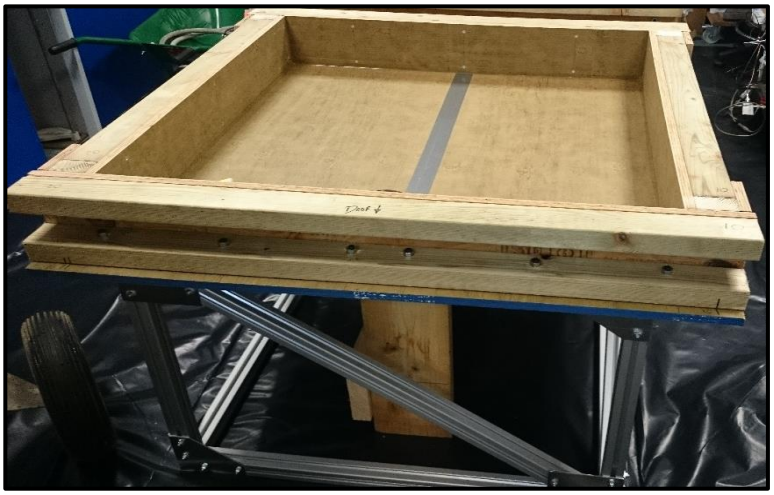

Figure 6.6. Roof structure without reinforcement.

The roof structure without reinforcement had dimensions 100cm x 100cm x 23cm and was created to Malaysian flat roof concrete proportion standards (see Appendix A).

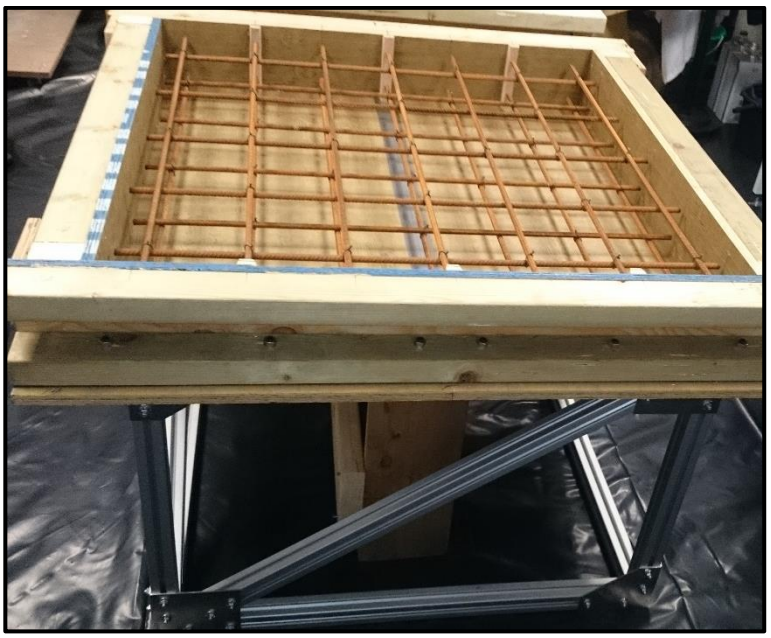

Figure 6.7. Roof structure frame with reinforcement.

The roof structure with reinforcement had dimensions 100cm x 100cm x 23cm and was created to Malaysian flat roof concrete proportion standards (see Appendix A). Therefore, it has reinforcement bars located at the same distance apart as suggested in Malaysian roof structure.

The flat roof structure had a waterproof membrane between the screed layers. A waterproof membrane rubber sheet was used to determine if it is possible to detect any faults. Figure 6.8a presents the roof structure with a membrane without any faults, Figure 6.8b presents the roof structure with a membrane with a fault.

(a) (b)

Figure 6.8. (a) Roof with a membrane layer (b) Roof with damaged membrane layer.

6.2.2. Results

Figure 6.9 presents the results of the membrane failure detection on the concrete flat roof structure. There are four conditions that have been reviewed. Firstly, a membrane layer without defects was placed on the concrete roof structure without reinforcement; then a defective membrane layer was placed on the concrete flat roof structure without reinforcement. Also a membrane layer without defects was tested on the concrete roof structure with reinforcement as well as a damaged membrane layer. Data on each of the conditions were been captured. There is a significant shift of frequency peak at approximately 4GHz which indicates differences between concrete roof structures with and without reinforcement due to the changes in dielectric properties of the roofs' structures when the steel reinforcement is placed in the measured area. Also there is significant amplitude shift which indicates when the membrane layer is faulty due to the water penetration of the concrete structure as well as changes made to the membrane (defects).

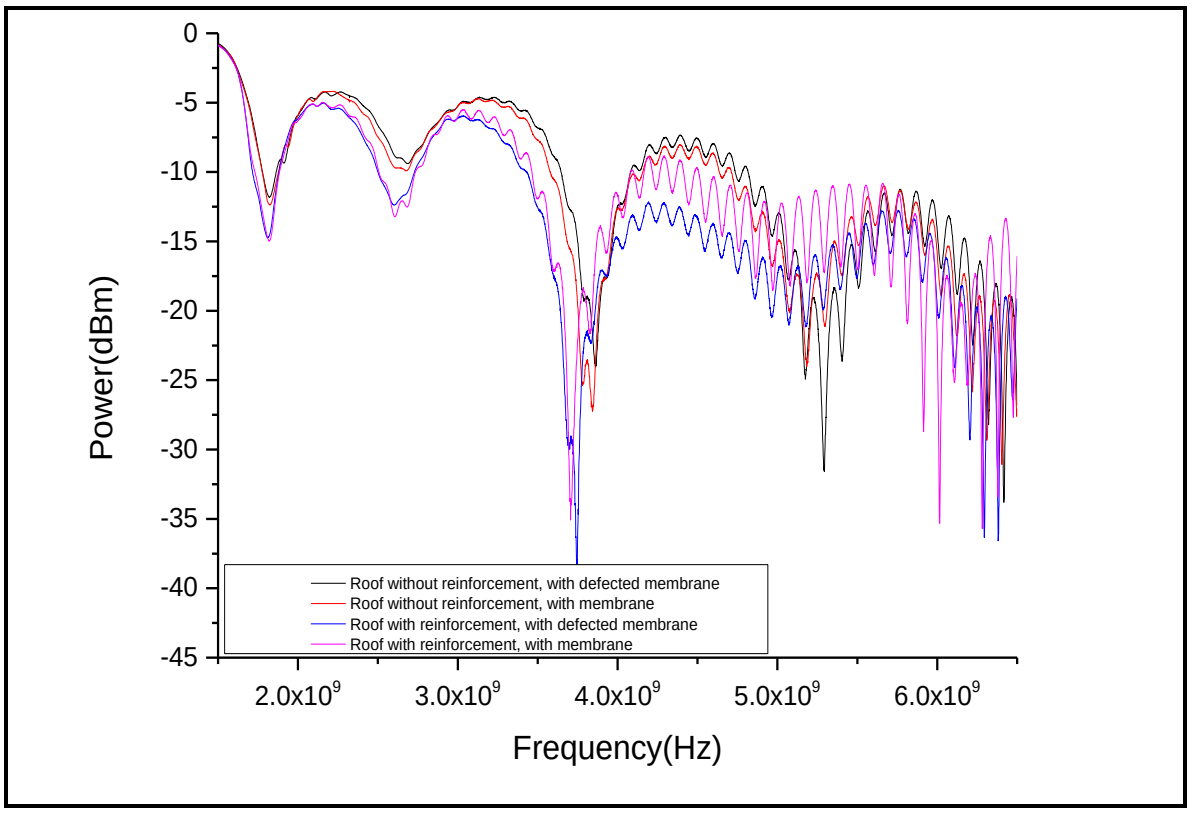

Figure 6.9. Membrane failure on concrete flat roof structure.

6.2.3. Analysis

This experiment was undertaken to detect the changes in microwave spectroscopy when there is waterproof membrane failure. There were concrete roof structures used during this experiment with and without the reinforcement. Results shows there is a frequency and amplitude shift across the measured spectrum. There are two significant peaks at 2.5GHz and between 3.8GHz to 4 GHz. At 2.45GHz there is 2.5dBm difference between structure with reinforcement and without reinforcement. The visible change is owing to steel bars used to increase the strength of the concrete structure which reflects the microwave energy. There is a similar phenomenon at approximately 4GHz where reinforcement bars affect the microwave spectrum. The differences between membrane with and without fault can be identify due to water penetration into the concrete which increase the dielectric properties of the measured surface.

6.2.4. Discussion

The experimental results in section 6.2 shows that EM waves can be used to determinate the membrane damage in the concrete flat roof structure with and without the membrane failure. There are two significant peaks at 2.5GHz and approximately 4GHz which shows the changes in microwave frequency and attenuation.

6.3. Identification of Concrete Reinforcement

This experiment was undertaken to identify the location of the concrete reinforcement bar. Reinforcement steel bar affect the microwave spectroscopy due to steel dielectric properties.

6.3.1. Methodology

Linear traverse was used to monitor the movements of the horn antenna (Figure 6.10). Antenna was mounted 5mm above the roof surface. Special software created to control linear traverse enable to control movement distance. Each measurement was taken at every 1cm. Frequency range during this experiment was between 2GHz to 6GHz.

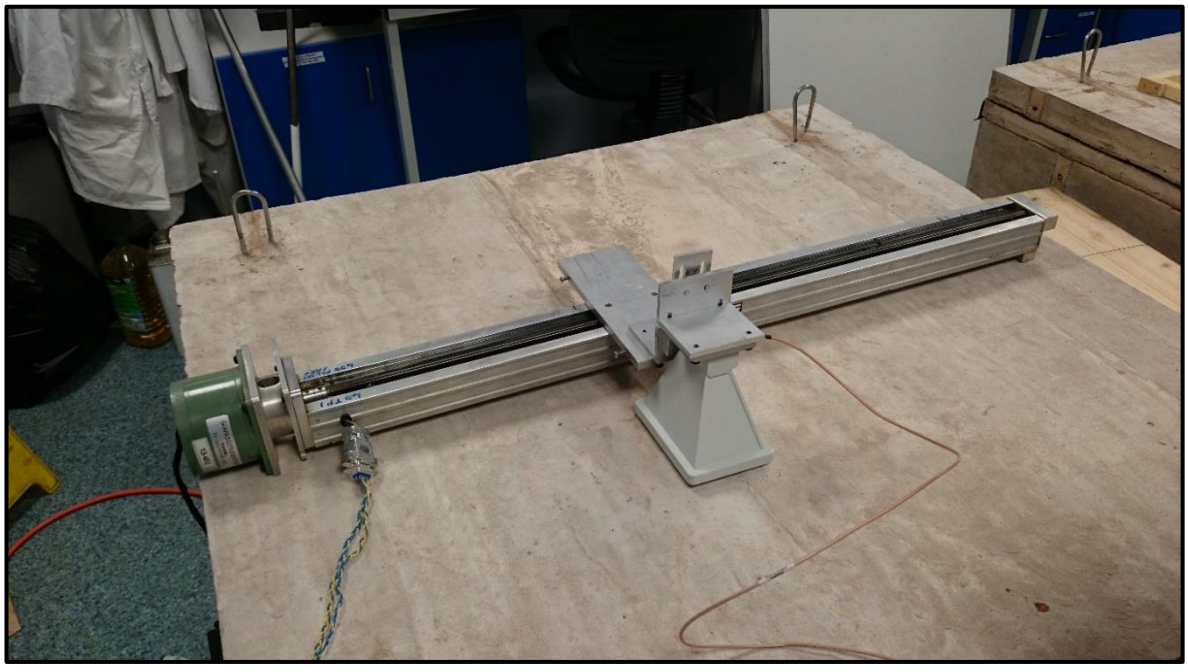

Figure 6.10. Linear Traverse setup.

6.3.2. Results

Most of the concrete structures are reinforced to improve the strength of the construction. It is important to be able to identify the location of the reinforcement bar inside of the concrete structure. The results of the experiment are presented in Figure 6.11. It can be seen that there is a significant amplitude and frequency shift in range between 3.5GHz and 4GHz. This is caused by the dielectric properties of the reinforcement bar which differ from the concrete properties.

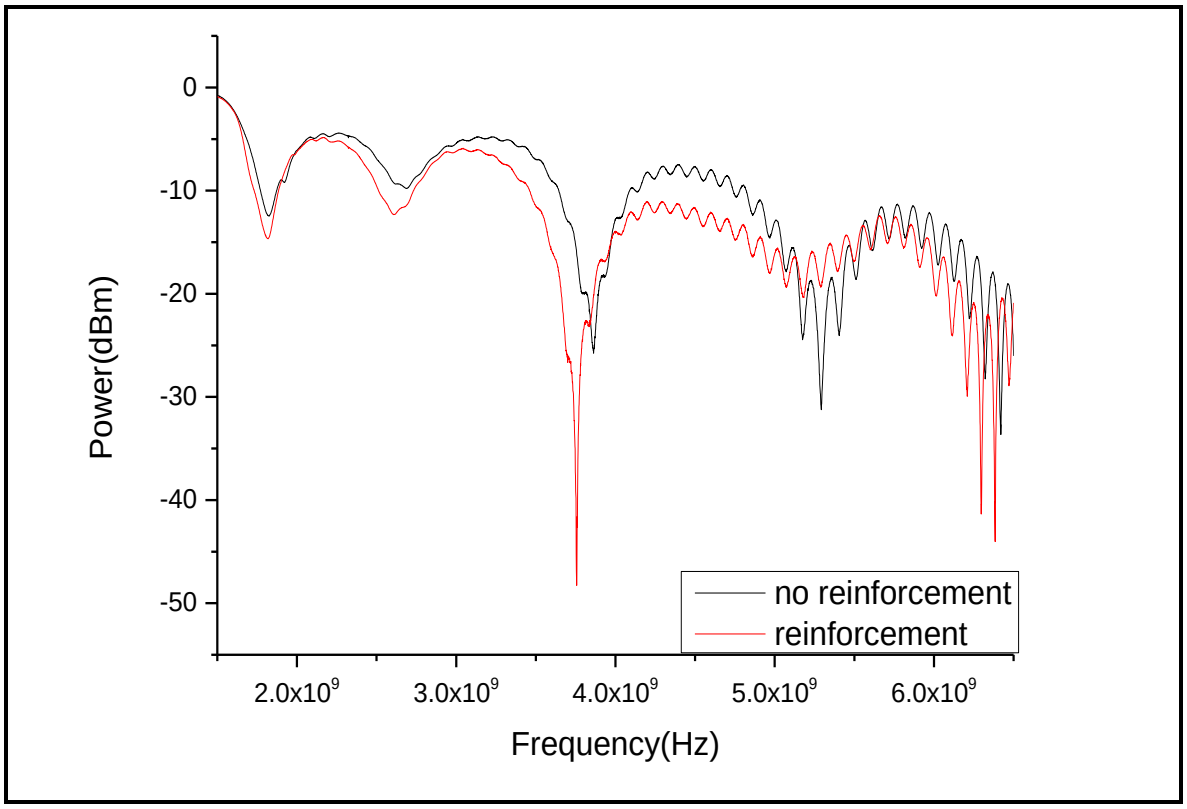

Figure 6.11. Location of Reinforcement in concrete flat roof structure.

6.3.3. Analysis

This experiment was conducted to determine the location of the reinforcement within the concrete flat roof structure. Results in section 6.3.2 shows that there is significant change in EM attenuation and frequency at approximately 4GHz. This change is caused by steel bar and its properties which reflects the microwave spectrum. There is 25dBm difference between two measurements.

6.3.4. Discussion

The experiment shows the possibility to use EM spectrum to determine the location of the reinforcement bars within concrete flat roof structure. The results demonstrated a significant change in the attenuation and frequency of an EM signal when the horn antenna was pointed in the direction of the steel bar, namely decrease of the reflected power by 25dBm and the frequency around 4GHz by 150mHz.

6.4. Summary

In this chapter a sequence of experimental work to detect the concrete flat roof structure defects mainly waterproof membrane failure. Results from section 6.1.2 illustrated that microwave spectroscopy can be used to detect the membrane failure on the concrete paving slab. Results shows that there is a significant change in attenuation of EM signal at frequency between 8GHz to 9.5GHz. The results in section 6.2.2 shows that EM waves can be used to determinate the membrane damage in the concrete flat roof structure with and without the reinforcement. There are two significant peaks at 2.5GHz and approximately 4GHz which shows the changes in microwave frequency and attenuation. The results in section 6.3.2 shows the possibility to use EM spectrum to determine the location of the reinforcement bars within concrete flat roof structure.

Chapter 7 Conclusions and Future Work

7.1 Conclusions

In recent years there was an increase in the need to implement sustainable solutions in building fabrics and structures. To achieve the optimum life span of these structures it is important to monitor parameters such as moisture content, indoor temperature profiles, influence of vibration and material fatigue. Building materials that require a special mixing ratio such as concrete, mortar and membrane layers will be subject to significant effects when exposed to variety of weather changes.

The major part of the work presented in this thesis was to develop a novel non-destructive electromagnetic (EM) wave sensor to determine the moisture content of building fabrics.

As no previous research had been undertaken on moisture content detection using microwave spectroscopy, the first objective was to investigate electromagnetism (EM) and associated sensors to determine if EM waves would propagate through the building materials. This was conducted using a combination of HFSS simulation and laboratory experiment.

Using HFSS it was possible to model the EM sensor and determine that the propagation through building materials was possible. HFSS was also used to determine the distance between measured materials and foreign objects placed behind them. A series of experiments were conducted to validate the HFSS model which showed agreement with both frequency and amplitude between experimental results and the simulation results, and could therefore be used for sensor development.

From the experimental work, it was found that the pyramidal horn antenna offered the most appropriate performance with regards to gain, directivity and penetration depth. The developed sensor was able to sweep frequencies from 2GHz to 12GHz, and this range covered the resonance frequencies which corresponded to a change in moisture content, foreign object detection, types of building materials detection and concrete flat roof defects detection as discussed in Chapters 4, 5 and 6.

Experimental work presented in Chapter 4 was undertaken to identify the location of a foreign objects in real time. The results demonstrated that the senor could be used not only for foreign object location, but also to identify types of foreign object. It was also demonstrated that sensor was working correctly.

The next stage of this project was to identify the moisture content in building fabrics. The experimental work in Chapter 5 shows that the EM sensor can be used to monitor the moisture content in building fabrics. The PLS method was used for the prediction of water content in common building fabrics. The results show the high correlation between calibrated and validated moisture content.

Penetration depth of EM wave sensor through concrete structure was investigated in Chapter 6. It was found that the penetration depth will vary depending the concrete mix ratio and aggregate. Penetration depth of the horn antenna throughout concrete paving slab was equal to 25 cm in frequency range between 2GHz to 6GHz and 20cm throughout standard Malaysian concrete flat roof structure.

EM sensor was used to determine waterproof membrane failure in concrete flat roof structure. The results in Chapter 6 demonstrated that the senor could not only be used for detection of membrane failure but can also identify the location of the reinforcement bars within the concrete flat roof structure in the frequency range between 2GHz and 6GHz.

The next stage of thesis was to implement alternative patch sensors into building fabrics to monitor their performance internally. It was found that there is significant difference within standard concrete mix ratios as well as type of aggregate used. There were two types of patch antennas used that responded at two different resonance frequencies 2,45GHz and 9.7GHz which corresponded to a change in a concrete mix ratio and type of aggregate used.

This thesis has led to a much greater understanding of the EM wave's propagation through building materials. It is noticeable that different types of building materials, different types of foreign objects and defects to waterproof membrane layer have a unique spectrum based on the dielectric properties, size and shape of materials. The development of novel EM wave sensor was a significant approach that could be used to monitor the moisture level in building structures.

7.2 Limitations

Electromagnetic waves are effected by different factors, such as different building materials and foreign objects within the building structures. Therefore, the limitations of this methods are a requirement to create a database with various building materials and foreign objects to avoid false measurements. On the other hand, this limitation can be compensated by building the database with existing building fabrics and foreign objects within the structures.

7.3 Future Work

For future work and development, it will be beneficial to build the database with various building materials and foreign objects within the building structures to improve the reliability of the method. Corrosion of the reinforcement in a concrete reduces the strength of the material, which leads to decrease of the building performance. Therefore, the microwave technology could be investigated to detect the corrosion progress of a reinforcement steel in a concrete structure, which could reduce maintenance costs for different structures. Additional study could be done to determine chloride attacks and carbonation of a concrete. Finally, implementing RFID Tags sensors into selected building fabrics would allow to remotely monitor the performance of the building structure over the years.

References

Afridi, M.A., 2015. Microstrip Patch Antenna − Designing at 2.4 GHz Frequency. *Biological and Chemical Research*, 2015, pp.128–132.

Agilent, 2006. *Basics of Measuring the Dielectric Properties of Materials*, USA.

Allen, W., 1995. The pathology of modern building. *Building Research & Information*, 23(3), pp.139–146.

Al-Sanea, S.A., Zedan, M.F., Al-Ajlan, S.A. & Abdul Hadi, A.S., 2003. Heat Transfer Characteristics and Optimum Insulation Thickness for Cavity Walls. *Journal of Building Physics*, 26(3), pp.285–307.

Ansoft, 2005. *High Frequency Structure Simulator User's Guide*, Pittsburgh.

Bailey, D.M. & Bradford, D., 2005. Membrane and Flashing Defects in Low-Slope Roofing : Causes and Effects on Performance. *Journal of Performance of Constructed Facilities*, 19(3), pp.234–244.

Bakshi, A. & Bakshi, U., 2009. *Electromagnetic Wave Theory* First., India: Technical Publications Pune.

Balanis, C., 2005. *Antenna Theory. Analysis and design* Third., New Jersey: John Wiley & Sons.

Balmus, S., Pascariu, G., Creanga, F., Dumitru, I., Sandu, D.D., Physics, F. & Cuza, A.I., 2006. The cavity perturbation method for the measurement of the relative dielectric permittivity in the microwave range. *Journal of Optoelectronics and advanced materials*, 8(3), pp.971–977.

Bond, A.J., Brooker, O., Harris, A.J., Harrison, T., Moss, R.M., Narayanan, R.S. & Webster, R., 2006. *How to design concrete structures using Eurocode 2*, Surrey: The Concrete Centre.

Brick Southeast, 2006. *Guide to Brick Construction*,

Brimblecombe, P., Grossi, C.M. & Harris, I., 2006. The effect of long-term trends in dampness on historic buildings. *Weather*, 61(10), pp.278–281.

Bucurescu, D. & Bucurescu, I., 2011. Non-destructive measurement of moisture in building materials by compton scatering of gamma rays. , 63(1), pp.61–75.

Burkinshaw, R. & Parrett, M., 2004. *Diagnosing Damp*, Coventry: RICS Books.

Buyukozturk, O., Yu, T.-Y. & Ortega, J.A., 2006. A methodology for determining complex permittivity of construction materials based on transmission-only coherent, wide-bandwidth free-space measurements. *Cement & Concrete Composites*, (28), pp.349–359.

Černý, R., 2009. Time-domain reflectometry method and its application for measuring moisture content in porous materials: A review. *Measurement*, 42(3), pp.329–336.

Chelas Roofing, 2007. Chelas Roofing and Concrete. , p.1. Available at: http://www.chelasroofingandconcrete.com/flat_roofs.html [Accessed August 15, 2015].

Chintakindi, V., Pattnaik, S., Bajpae, O., Devil, S., Sastry, V. & Pradyumna, P., 2007. Parameters Calculations of Rectangular Microstrip Patch Antenna using Particle Swarm Optimization Technique. *Applied Electromagnetics Conference*, pp.1–4.

CIB & RILEM, 1987. New technology roofing, Elastomeric, thermoplastic and polymer-modified bitumen membranes. *Batiment International, Building Research and Practice*, 15(1-6), pp.146–156.

Daniyan, O.., Opara, F.., Okere, B.., Aliyu, N., Ezechi, N., Wali, J., Adejoh, J., Eze, K., Chapi, J., Justus, C. & Adehina, K.., 2014. Horn Antenna Design: The Concepts and Considerations. *International Journal of Emerging Technology and Advanced Engineering*, 4(5), pp.706–708.

Davies, M. & Ye, Z., 2009. A " pad " sensor for measuring the moisture content of building materials. *Building Services Engineering Research and Technology*, 3(30), pp.263–270.

Domone, P. & Illston, J., 2010. *Construction materials, their nature and behaviour* 4th editio., Spon Press.

EcoMech, 2014. EcoMech Insulation Wall. , p.1. Available at: http://www.ecomech.co.uk/ [Accessed April 14, 2015].

European Union, 2004. *Eurocode 2: Design of concrete structures*, Brussels.

Firstcall, 2014. Cavity Wall Insulation. , p.1. Available at: http://www.firstcallhomeassist.co.uk/insulation/cavity-wall-insulation [Accessed April 20, 2016].

Fischer Innovative Solutions, 2012. *Aircrete Booklet*, Oxon.

Fung, C., 2011. *Basic Antenna Theory and Application*, Worcester.

Goh, J.H., Shaw, A., Cullen, J.D., Oliver, M., Vines, M., Al-Shamma'a, A.I. & Brockhurst, M., 2006. EM Waves Sensor For Water Industry Asset Management. , pp.94–100.

Grainger, 2012. Types of Moisture Meters. , pp.1–2. Available at: https://www.grainger.com/content/qt-types-of-moisture-meters-346 [Accessed October 17, 2016].

Gromicko, N. & Shepard, K., 2013. Moisture Meters for Inspectors. , pp.1–2. Available at: http://www.nachi.org/moisture-meters.html [Accessed October 17, 2016].

Gwynne, T., 2010. *Building Control Guidance for Domestic Extensions & Garages*, Coleford.

Halim, A., Harun, S. & Hamid, M., 2012. Diagnosis of Dampness in Conservation of Historic Building. *Jurnal of Design + Built*, 5, pp.1–14.

Hamad, A.J., 2014. Materials, Production, Properties and Application of Aerated Lightweight Concrete: Review. *International Journal of Materials Science and Engineering*, 2(2), pp.152–157.

Hens, H., Janssens, a., Depraetere, W., Carmeliet, J. & Lecompte, J., 2007. Brick Cavity Walls: A Performance Analysis Based on Measurements and Simulations. *Journal of*

Building Physics, 31(2), pp.95–124.

Huang, Y. & Boyle, K., 2008. *Antennas: From Theory to Practice*, Chichester, UK: John Wiley & Sons, Ltd.

HubPages, 2015. How To Plaster Board A Wall Using The Dot & Dab System, Drylining. , pp.1–2. Available at: http://hubpages.com/living/How-To-Plaster-Board-A-Wall-Using-The-Dot-Dab-System [Accessed April 20, 2016].

Imal, J., 2002. Measurement of Moisture Fields in the Bridge Structure of Charles Bridge. *Acta Polytechnica*, 42(3), pp.53–58.

Interior Shapes & Designs, 2013. Brickwork bonds. , p.1. Available at: http://www.interiordesignsandshapes.com/detail.php?id=20). [Accessed April 20, 2016].

Kadir, A., Marsono, B. & Balasbaneh, A.T., 2015. Combinations of building construction material for residential building for the global warming mitigation for Malaysia. *Construction and Building Materials*, 85, pp.100–108.

Karayannis, C.G., Chalioris, C.E., Angeli, G.M., Papadopoulos, N.A., Favvata, M.J. & Providakis, C.P., 2016. Experimental damage evaluation of reinforced concrete steel bars using piezoelectric sensors. *Construction and Building Materials*, 105, pp.227–244.

Kirshin, E., Oreshkin, B., Zhu, G.K., Popović, M. & Coates, M., 2013. Microwave radar and microwave-induced thermoacoustics: dual-modality approach for breast cancer detection. *IEEE transactions on bio-medical engineering*, 60(2), pp.354–60.

Korostynska, O., Mason, A. & Al-Shamma'a, A., 2014. Microwave sensors for the non-invasive monitoring of industrial and medical applications. *Sensor Review*, 34(2), pp.182–191.

Kosmatka, S.H., Kerkhoff, B. & Panarese, W.C., 2003. *Design and Control of Concrete Mixtures* 14th ed., Illinois: Portland Cement Association.

Kus, H., Nygren, K. & Norberg, P., 2004. In-use performance assessment of rendered

autoclaved aerated concrete walls by long-term moisture monitoring. *Building and Environment*, 39(6), pp.677–687.

Lawrence, C., Van der Veen, J. & Arballo, J., 2012. Jet Propulsion Laboratory, California Institute of Technology. , p.1. Available at: http://planck.caltech.edu/epo/epo-cmbDiscovery3.html [Accessed April 20, 2016].

Lo, Y.T., Leung, W.M. & Cui, H.Z., 2005. Roof construction defects of medium-rise buildings in sub-tropical climates. *Structural Survey*, 23(3), pp.203–209.

Lourenço, P.B., Hees, R., Fernandes, F. & Lubelli, B., 2014. Characterization and damage of brick masonry. In A. Costa, M. J. Guedes, & H. Varum, eds. *Structural Rhabilitation of Old Buildings*. Berlin, Heidelberg: Springer Berlin Heidelberg, pp. 109–130.

Maierhofer, C. & Wsstmann, J., 1998. Investigation of Dielectric properties of brick materials as a function of moisture and salt content using a microwave impulse technique at very high frequencies. *Nondestructive Testing and Evaluation International*, 31(4), pp.259–263.

Maksimović, M., Stojanović, G.M., Radovanović, M., Malešev, M., Radonjanin, V., Radosavljević, G. & Smetana, W., 2012. Application of a LTCC sensor for measuring moisture content of building materials. *Construction and Building Materials*, 26(1), pp.327–333.

Manacorda, G., Persico, R. & Scott, H.F., 2015. Design of Advanced GPR Equipment for Civil Engineering Applications. In *Civil Engineering Applications of Groud Penetrating Radar*. pp. 3–8.

Maragoudakis, C.E. & Rede, E., 2009. *Validated Antenna Models for Standard Gain Horn Antennas*, White Sands Missile Range.

Masonry Advisory Council, 2002. *Design Guide for Taller Cavity Walls*, Park Ridge.

McCann, D.. & Forde, M.., 2001. Review of NDT methods in the assessment of concrete and masonry structures. *Nondestructive Testing and Evaluation International*, 34(2), pp.71–84.

McDonald, R., 2013. Algo Centre Mall Collapse. , pp.1–3. Available at: http://failures.wikispaces.com/x-4.0 Collapse [Accessed March 9, 2016].

Minitab, 2016. What is partial least squares regression. , p.1. Available at: http://support.minitab.com/en-us/minitab/17/topic-library/modeling-statistics/regression-and-correlation/partial-least-squares-regression/what-is-partial-least-squares-regression/ [Accessed October 11, 2016].

Moisturemeters, 2010. Moisture Meter Technology. , pp.1–2. Available at: http://www.moisturemeters.com/moisture-meter-technology/ [Accessed April 20, 2016].

Moore, J.F.A., 1992. *Monitoring Building Structures* First., Glasgow: Blackie and Son Ltd.

Munkittrick, D., 2015. Moisture Meters. , pp.1–2. Available at: http://www.popularwoodworking.com/american-woodworker-blog/moisture-meters [Accessed April 20, 2016].

Muradov, M., Cullen, J.D., Abdullah, B., Ateeq, M., Mason, A., Shaw, A. & Al-, A.I., 2014. Real-time monitoring of meat drying process using microwave spectroscopy. *Proceedings of the 8th International Conference on Sensing Technology*, pp.407–411.

Nikolova, N., 2014. Horn Antennas. , pp.1–30. Available at: http://www.ece.mcmaster.ca/faculty/nikolova/antenna_dload/current_lectures/L18_Horns.pdf [Accessed April 20, 2016].

Ong, J.B., You, Z.Y.Z., Mills-Beale, J., Tan, E.L.T.E.L., Pereles, B.D. & Ong, K.G.O.K.G., 2008. A Wireless, Passive Embedded Sensor for Real-Time Monitoring of Water Content in Civil Engineering Materials. *IEEE Sensors Journal*, 8(12), pp.2053–2058.

PCWI International Pty, 2000. *Moisture measurement in buildings*, Cardiff.

Phillipson, M., Baker, P., Davies, M., Ye, Z., Galbraith, G. & McLean, R., 2008. Suitability of time domain reflectometry for monitoring moisture in building materials. *Building Service Engineering Research and Technology*, 29(3), pp.261–272.

Phillipson, M.C., Baker, P.H., Davies, M., Ye, Z., McNaughtan, A., Galbraith, G.H. &

McLean, R.C., 2007. Moisture measurement in building materials: an overview of current methods and new approaches. *Building Service Engineering Research and Technology*, 28(4), pp.303–316.

Poole, I., 2015. Microwave Horn Antenna Theory & Equations. *Antennas and propagation*, pp.1–5. Available at: http://www.radio-electronics.com/info/antennas/horn_antenna/theory.php [Accessed April 20, 2016].

Radosavljevic, G., 2012. Wireless LTCC sensors for monitoring of pressure, temperature and moisture. *Journal of Microelectronics*, 42(4), pp.272–281.

Ramna & Sappal, A.S., 2012. Design and Analysis of Rectangular Microstrip Patch Antenna Using. *International Journal of Advanced Research in Computer and Communication Engineering*, 2(6), pp.51–58.

Ranasinghe, N.D.S.., 2010. Maintainability of reinforced concrete flat roofs in Sri Lanka. *Structural Survey*, 28(4), pp.314–329.

Raut, S.P., Ralegaonkar, R. V. & Mandavgane, S.A., 2011. Development of sustainable construction material using industrial and agricultural solid waste: A review of waste-create bricks. *Construction and Building Materials*, 25(10), pp.4037–4042.

Reci, H., Maï, T.C., Sbartaï, Z.M., Pajewski, L. & Kiri, E., 2016. Non-destructive evaluation of moisture content in wood by using Ground Penetrating Radar. *Geoscientific Instrumentation, Methods and Data Systems Discussions*, (July), pp.1–12. Available at: http://www.geosci-instrum-method-data-syst-discuss.net/gi-2016-24/.

Rodrigo, R., 2010. *Fundamental Parameters of Antennas*, Katubedda.

Roy, A. & Puri, I., 2015. Design and Analysis of X band Pyramidal Horn Antenna Using HFSS . *International Journal of Advanced Research in Eletronics and Communication Engineering*, 4(3), pp.488–493.

Sadia Khandaker, M., Mousume, H., Mubina, F. & Kazi Riaz, U., 2010. *Design and Implementation of a pair of Horn antenna for UIU microwave test setup*. United International University.

Sanders, C.H. & Phillipson, M.C., 2003. UK adaptation strategy and technical measures: the impacts of climate change on buildings. *Building Research & Information*, 31(3), pp.210–221.

Sarwate, V., 1993. *Electromagnetic fields and waves*, India: New Age International.

Scott, A.W., 2005. *Understanding Microwaves*, New York: John Wiley & Sons.

Seward, D., 2009. *Understanding Structures: Analysis, Materials, Design* 4th ed., Basingstoke: Palgrave Macmillan.

Sharma, S., 2014. Design and Analysis of Pyramidal Horn Antenna at 8 GHz Frequency. *International Journal of Advanced Research in Eletronics and Cummunication Engineering*, 3(2), pp.231–234.

Singh, J., Yu, C.W.F. & Jeong Tai Kim, 2010. Building Pathology, Investigation of Sick Buildings -Toxic Moulds. *Indoor and Built Environment*, 19(1), pp.40–47.

Smith, L., 2002. *A tutorial on Principal Components Analysis*,

Smith, R., 2015. Pin vs. Pinless Moisture Meters: Accuracy That Still Stands. , pp.1–2. Available at: http://www.wagnermeters.com/flooring/wood-flooring/pin-moisture-meter/ [Accessed October 17, 2016].

Sorrentino, R. & Bianchi, G., 2010. *Microwave and RF Engineering*, Singapore: John Wiley & Sons.

Stavrou, S. & Saunders, S.R., 2003. Review of constitutive parameters of building materials. *Antennas and Propagation, 2003. (ICAP 2003). Twelfth International Conference on (Conf. Publ. No. 491)*, 1, pp.211–215 vol.1.

Stirling, C., 2011. *Building pathology: moisture conditions within external masonry walls*, Newcastle upon Tyne.

Stojanovic, G., Radovanovic, M., Malesev, M. & Radonjanin, V., 2010. Monitoring of water content in building materials using a wireless passive sensor. *Sensors*, 10(5), pp.4270–4280.

Straube, J.F., 2002. Moisture in buildings. *American Society of Heating, Refrigerating and Air-Conditioning Engineers Journal*, 44(1), pp.15–19.

Stuerga, D., 2006. Microwave – Material Interactions and Dielectric Properties , Key Ingredients for Mastery of Chemical Microwave Processes. In *Microwaves in Organic Synthesis*. pp. 1–61.

Thomas Armstrong LTD, 2016. Concrete Blocks Division. , p.1. Available at: http://www.thomasarmstrong.co.uk/about-us/divisions/concrete-blocks/about/ [Accessed April 20, 2016].

Tontechnik, 2016. Bandpass Filter (BPF) and EQ Filter. , pp.1–2. Available at: http://www.sengpielaudio.com/calculator-bandwidth.htm [Accessed April 20, 2016].

Vijayakumar, K., Wylie, S.R., Cullen, J.D., Wright, C.C. & Ai-Shamma'a, a I., 2009. Non invasive rail track detection system using microwave sensor. *Journal of Physics: Conference Series*, 178(15), pp.1–6.

Vijayakumar, R., Rajasekaran, L. & Ramamurhy, N., 2002. Determing the Moisture content in Limestone Concrete by Gamma Scattering Method: A Feasibility Study. *Non-Destructive Evaluation, National Seminar of Indian Society for Non-Destructive Testing*, (1), pp.1–10.

Virdi, S.S., 2012. *Construction science and materials*, West Sussex: John Wiley & Sons.

Vun, R.Y., Hoover, K., Janowiak, J. & Bhardwaj, M., 2007. Calibration of non-contact ultrasound as an online sensor for wood characterization: Effects of temperature, moisture, and scanning direction. *Applied Physics A Materials Science & Processing*, 90(1), pp.191–196.

Wendling, L., Cullen, J.D., Al-Shamma'a, A. & Shaw, A., 2009. Real Time Monitoring and Detection of Alcohol Using Microwave Sensor Technology. In *Second International Conference on Developments in eSystems Engineering*. Abu Dhabi, pp. 113–116.

Wittmann, F.., Zhang, P., Zhao, T., Lehmann, E. & Vontobel, P., 2008. Neutron Radiography, A Powerful Method for Investigating Water Penetration Into Concrete. *Advances in Civil Engineering Materials*, pp.61–70.

Wormald, R. & Britch, A.L., 1969. Methods of Measuring Moisture Content Applicable to Building Materials. *Building Science*, 3(1), pp.135–145.

Ye, Z., Tirovic, M., Davies, M., Baker, P., Phillipson, M., Galbraith, G. & McLean, R.C., 2007. The optimisation of a thermal dual probe instrument for the measurement of the moisture content of building envelopes. *Building Service Engineering Research and Technology*, 28(4), pp.317–327.

Young, M.E., 2007. Dampness penetration problems in granite buildings in Aberdeen, UK: Causes and remedies. *Construction and Building Materials*, 21(9), pp.1846–1859.

Yunus, M.A.M. & Mukhopadhyay, S.C., 2011. Novel Planar Electromagnetic Sensors for Detection of Nitrates and Contamination in. *IEEE Sensors Journal*, 11(6), pp.1440–1447.

Zhang, H., 2011. *Building Materials in Civil Engineering* First., Cambridge: Woodhead Publishing.

Appendix A

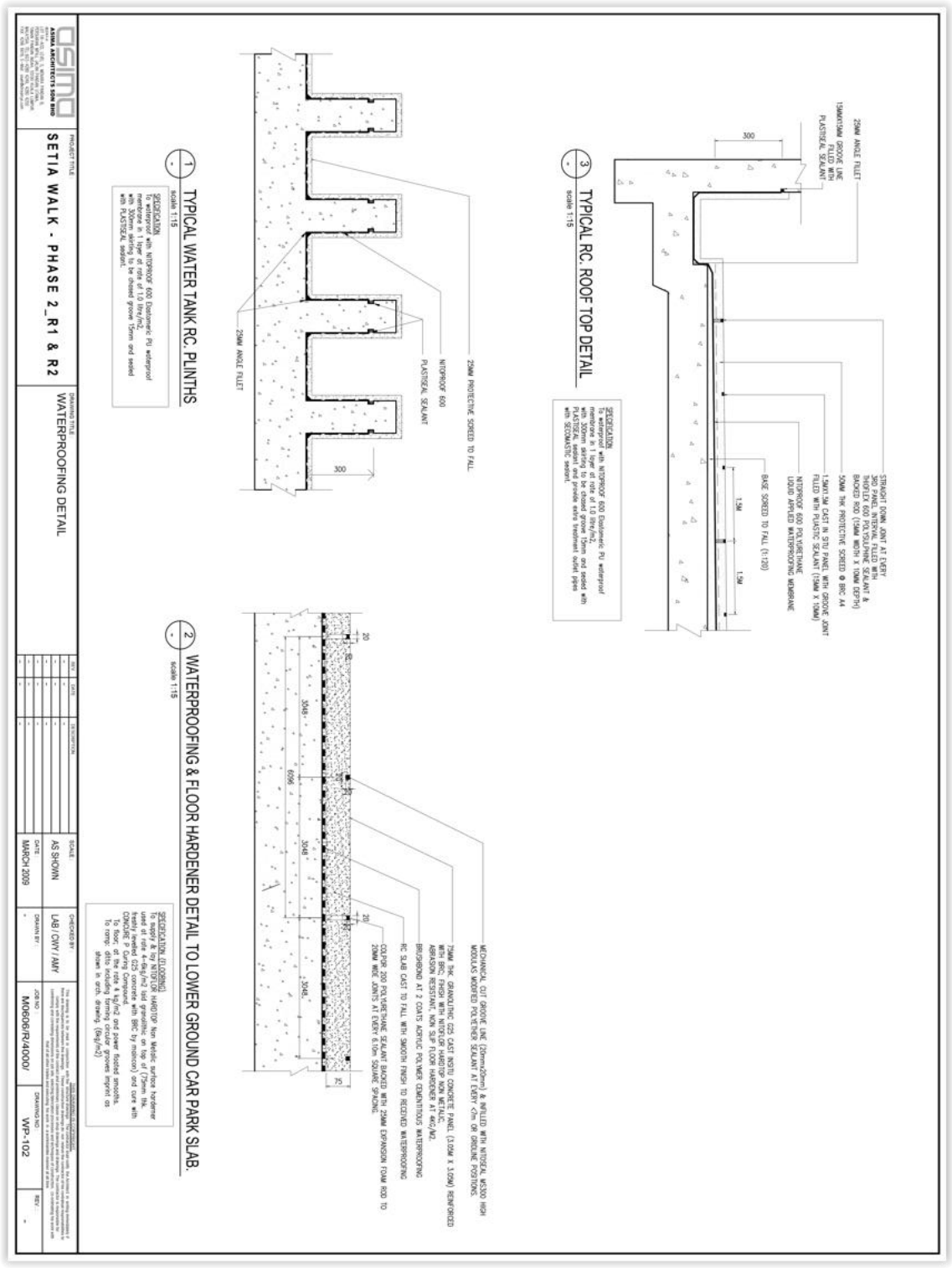

Figure A1. Flat roof structure design common in Malaysia.

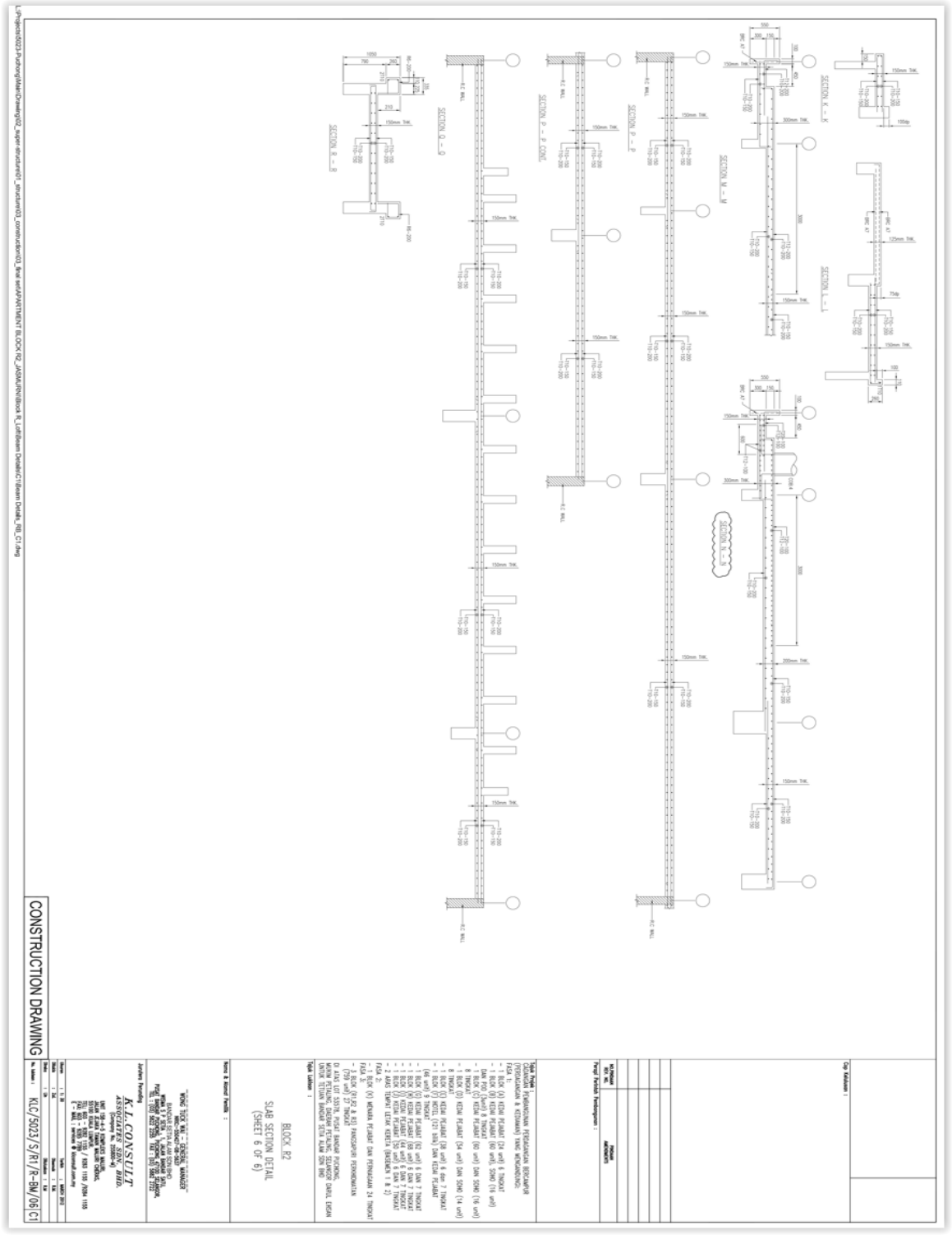

Figure A2. Schematic diagram of reinforcement in concrete flat roof structure used in Malaysia.

Appendix B

ICST Conference- Liverpool 2014

The feasibility of using electromagnetic waves in determining the moisture content of building fabrics and the cause of the water ingress.

P. Kot, A. Shaw, K. O. Jones, J. D. Cullen, A. Mason and A. I. Al-Shamma'a

Built Environment and Sustainable Technologies (BEST) Research Institute
School of Built Environment
Liverpool John Moores University
Liverpool, UK
P.Kot@2009.ljmu.ac.uk
A.Shaw@ljmu.ac.uk

Abstract— **In this paper, the feasibility of using electromagnetic (EM) waves in determining the moisture content of building fabrics and the case of water ingress is experimentally assessed. This paper will concentrate on investigating the propagation of EM waves through typical structures and their interaction with concealed pipework, wiring and timber. All current methods are overviewed and analysed. Novel microwave sensor described in this paper operates in 6 GHz to 12 GHz frequency range using Marconi 6200A microwave test set. Results of experimental tests confirm that microwaves can be used as an alternative non-destructive method for identifying different object behind the walls.**

ICST Conference- New Zealand 2015

The feasibility of electromagnetic waves in determining the moisture content of concrete blocks

P. Kot, A. Shaw, K. O. Jones, J. D. Cullen, A. Mason and A. I. Al-Shamma'a
Built Environment and Sustainable Technologies (BEST) Research Institute
School of Built Environment
Liverpool John Moores University
Liverpool, UK
P.Kot@2009.ljmu.ac.uk
A.Shaw@ljmu.ac.uk

***Abstract*— In some of the tropical countries such as Malaysia, various conditions of temperature and rainfall throughout the year are severe when compared to European countries. Humidity and rainfall throughout the year are likely to affect the durability of material used in buildings. Very high level of rainfall causes significant issues in concrete flat roofs due to membrane failure. This would potentially contribute to the occurrence of severe roof leaks, especially for buildings that use flat roof design solutions. Membrane failure is hard to recognise due to the slow process of water leakage into the surface which most of the time causes dampness and reduces buildings' structural performance. To monitor this condition effectively, non-destructive test methods are required to recognise problems at an early stage to avoid further damages to concrete structure. This paper presents the use of electromagnetic waves for the purpose of monitoring concrete blocks' moisture level which will be highlighted. This study experimentally investigated the propagation of EM waves through the concrete blocks and their interaction with water. The novel microwave sensor described in the paper operates in the 2GHz to 6GHz frequency range using a Vector Network Analyser. Results of experimental tests confirmed that microwaves could be used as an alternative non-destructive method for identifying water ingress into the concrete blocks.**

Construction & Building Materials, Elsevier 2015

The Application of Electromagnetic Waves in Monitoring Water Infiltration on Concrete Flat Roof: The Case of Malaysia

P. Kot[1], A.S. Ali[2], A. Shaw[1], M. Riley[1] and A. Alias[2]

[1]Built Environment and Sustainable Technologies (BEST) Research Institute, School of Built Environment, Liverpool John Moores University, Liverpool, UK

Email: P.Kot@2009.ljmu.ac.uk

[2]Center for Construction, Building and Urban Studies (CeBUS), Faculty of Built Environment, University of Malaya, Kuala Lumpur, Malaysia

Email: asafab@um.edu.my

Abstract

Roof leakages of high-rise buildings involving concrete flat roof design in tropical countries continue to be a serious problem. Currently, exiting methods of detecting potential leaks are mostly destructive to the building material. Although the method of detecting a defect using non-destructive measurement exists, current methods such as infrared thermography, metal detector and humidity meter have varying constraints in their application. This paper describes the potential use of microwave technology as an effective non-destructive tool to monitor and investigate leakage of concrete flat roof due to failure of membrane layer. This study was performed experimentally on flat room structures built for laboratory use and according to Malaysian flat roof concrete proportions standards. Experiments performed utilized a sensor equipped with essential parameters that enable control to sensor angle, temperature and distance between object and sensor structure and designed to enable numerous measurements in real time. The study determined that microwave technology can be used to identify moisture content in concrete flat roof by analysing properties of the concrete roof and water. This proves to be an effective non-destructive method of determining leakage problems in concrete flat roof in real time before the defects become critical.

International Journal of Civil Engineering, 2015

The feasibility of using electromagnetic waves in determining membrane failure of concrete flat roof

P. Kot[1], A. Shaw[1], M. Riley[1], A. Cotgrave[1] and A.S. Ali [2*]

[1]Built Environment and Sustainable Technologies
(BEST) Research Institute
School of Built Environment
Liverpool John Moores University
Liverpool, UK

P.Kot@2009.ljmu.ac.uk
A.Shaw@ljmu.ac.uk
[2] Center for Construction, Building and Urban Studies
(CeBUS)
Faculty of Built Environment
University of Malaya
Kuala Lumpur, Malaysia
asafab@um.edu.my
*corresponding author

Abstract
Concrete flat roof defects such as water leakage present a significant and common problem in large building, particularly in tropical countries, where rainfall is high. To monitor this condition, effective non-destructive test methods are required to detect problems at an early stage, especially hidden defect within the concrete roof, which are critical. This paper presents the potential use of electromagnetic (EM) waves for determining possible leakage of the concrete flat roof as a result of failure of the waterproof membrane layer. This study was assessed, experimentally by investigation of the propagation of EM waves through the roof and their interaction with water. Novel Microwave sensors described in the paper operates in the 6 GHz to 12 GHz frequency range using a Marconi 6200A microwave test set. A range of existing current methods were overviewed and analysed. Results of experimental tests confirmed that microwaves could be used as an alternative non-destructive method for identifying water ingress caused by membrane failure into the concrete roof surface.

Keywords: Horn Antenna; Electromagnetic waves; Microwaves; Sensor; Concrete Flat Roof; Membrane

IEEE Sensors Journal 2016 (Submitted)

P. Kot, A. Shaw, K.O. Jones, M. Ateeq, A.S. Ali, A. Mason and M. Riley

The Feasibility of Electromagnetic Waves in determining the moisture content of concrete

***Abstract*— This work concerns the use of an electromagnetic (EM) wave sensor to determine the moisture content of concrete building materials which require a special mixing ratio. Building fabrics such as concrete, mortar and membrane layers are subject to significant effects when exposed to weathering which affects the overall performance of buildings. This work demonstrates the use of an EM wave sensor to monitor a structure in real-time to determine its moisture content. The sensor is shown to operate at two frequency ranges; 2GHz to 6GHz and 6GHz to 12GHz at a power of 0dB. Different concrete mixes have been made within a laboratory environment to determine the levels of moisture content. Results of the linear best fit at 3.75 GHz over 24 hours weight loss, gives R2 = 0.97 which is an accurate result for the correlation between S21 parameter and moisture loss in the concrete sample.**